TECHNISCHE UNIVERSITÄT MÜNCHEN
Lehrstuhl für Entwicklungsgenetik

Dissecting the role of CRH and CRH-R1 in Alzheimer´s disease

Kristin Lerche

Vollständiger Abdruck der von der Fakultät Wissenschaftszentrum Weihenstephan für Ernährung, Landnutzung und Umwelt der Technischen Universität München zur Erlangung des akademischen Grades eines

Doktors der Naturwissenschaften

genehmigten Dissertation.

Vorsitzende:	Univ.-Prof. A. Schnieke, Ph.D.
Prüfer der Dissertation:	1. Univ.-Prof. Dr. W. Wurst
	2. Univ.-Prof. Dr. K. Schneitz

Die Dissertation wurde am 23.02.2012 bei der Technischen Universität München eingereicht und durch die Fakultät Wissenschaftszentrum Weihenstephan für Ernährung, Landnutzung und Umwelt am 17.09.2012 angenommen.

Table of contents

List of figures

Abbreviations

AICD	APP intracellular domain
APP	amyloid precursor protein
Aß	amyloid ß
BBB	blood brain barrier
BSA	bovine serum albumin
cAMP	cyclic adenosine monophosphate
cDNA	copy DNA
CeA	central Amygdala
CNS	central nervous system
CRH	corticotropin-releasing hormone
CRH-R	CRH-receptor
CTX	cortex
DaLi	dark/light box
DEPC	diethylpyrocarbonate
DMEM	Dulbecco´s modified essential medium
EDTA	ethylenediaminetetraacetic acid
ELISA	enzyme linked immuno-sorbent assay
EPM	elevated Plus Maze
EtOH	ethanol
FCS	fetal calf serum
fEPSP	field excitatory postsynaptic potential
FST	forced swim test
GC	glucocorticoid
GR	glucocorticoid receptor
GWAS	genome wide association studies
hAPP	human APP
HIP	Hippocampus
HPA	hypothalalmic-pituitary-adrenocortical
IFN	interferon
IL	Interleukin
KO, ko	CRH-R1KO
LDLR	low-density lipoprotein receptor
LTD	long-term depression

LTP	long-term potentiation
MAPK	mitogen-activated protein kinases
MeOH	methanol
MR	mineralcorticoid-receptor
NFT	neurofibrillary tangle
NMDA	N-methyl-D-aspartate
o.n.	over night
OD	optical density
OF	open field
OR	spontaneous object recognition
PCR	polymerase chain reaction
PDGF	plateled-derived growth factor
PFC	prefrontal cortex
PHF	paired helical filament
PPF	paired-pulse facilitation
PVC	poylvinylchloride
PVN	paraventricular nucleus
qRT-PCR	quantitative real-time polymerase chain reaction
RNA	ribonucleic acid
ROI	reactive oxygen intermediates
ROS	reactive oxygen species
RT	room temperature
sAPP	soluble APP
SDS	sodium dodecyl slfate
SEM	standard error of the means
SNPs	single nucleotide polymorphisms
TAE	tris acetate EDTA
TEA	tiethanolamine
tg	arcAß transgenic
tgcoe	arcAß mice with CRH overexpression
tgko	arcAß mice with CRH-R1KO
Tris	trisaminomethane
WCM	water cross maze
wt	wild-type

Please note that all units defined by the International System of units (SI) are not considered in the list of abbreviations.

Abstract

Alzheimer´s disesase (AD) is the most common neurodegenerative disorder with increasing prevalence. Alterations of the corticotropin-releasing hormone (CRH) system in AD patients have been reported and along these lines, chronic stress and hyperactivity of the hypothalamic-pituitary-adrenal (HPA) axis have been shown to increase amyloid ß (Aβ) production. Moreover, there is evidence that CRH can directly interfere with amyloid precursor protein (APP) processing.

To shed light on the involvement of the CRH system in AD-related processes *in vivo*, we bred mice overexpressing human APP (arcAβ mice, Knobloch et al. 2007a) to i) conventional CRH-R1 knockout (KO) mice (Timpl et al. 1998) and ii) conditional CRH-overexpressing mice CRH-COE^{CNS} (Lu et al., 2008). In the F2 generation of either line, mice of four different genotypes were obtained: i) transgenic arcAß (tg), transgenic arcAß CRH-R1KO (tgko), CRH-R1KO (ko), wild-type (wt) and ii) transgenic arcAß (tg), transgenic arcAß CRH-COE^{CNS} (tgcoe), CRH-COE^{CNS} (coe) and wild-type (wt) mice, which have been subjected to comprehensive phenotyping involving behavioral analyses, electrophysiology, neuropathology and APP processing.

Our data provide insight into the involvement of the CRH system and the HPA axis in the onset and progression of AD: we observed impaired object recognition (OR) memory in tg mice at the age of four months, which was restored by CRH-R1 deficiency (tgko mice). Furthermore, all tg mice (tg, tgko, tgcoe) of 8 months and older exhibited deteriorated spatial memory in the water cross maze (WCM) task. In addition, tgko mice tended to apply striatum-mediated egocentric learning strategies and exhibited less cognitive flexibility compared to tg mice. Mice overexpressing CRH (coe, tgcoe) were characterized by an aroused phenotype and showed impaired OR memory most likely related to attention deficits. Compared to tg mice, Aß levels in hippocampal and cortical tissue of tgko mice were reduced as was the hippocampal plaque load. In tgcoe mice these findings were reversed. Astrocytes and microglia were equally infiltrating Aß plaques in all APP transgenic mice, implying that there was no direct impact of CRH-R1 loss or CRH overexpression on the inflammatory response.

Taken together, this study points towards a role of the CRH/CRH-R1 system and the HPA axis in the pathophysiology of AD in arcAß mice. The loss of CRH-R1 alleviates some aspects of the disease while overexpression of CRH has to some extent rather detrimental effects on AD pathologies.

Zusammenfassung

Morbus Alzheimer ist die am häufigsten auftretende neurodegenerative Erkrankung mit steigender Prävalenz. Bei Alzheimer Patienten wurden Veränderungen des Corticotropin-releasing Hormon (CRH)-Systems festgestellt und es wurde gezeigt, dass chronischer Stress sowie eine Überaktivität der Hypothalamus-Hypophysen-Nebennieren (HHN)-Achse die Amyloid ß (Aß) Produktion steigern können. Des Weiteren gibt es Hinweise, dass CRH direkt an der Prozessierung des Amyloid Prekursor Proteins (APP) beteiligt ist.

Um den Einfluss des CRH Systems im Morbus Alzheimer zu beleuchten, haben wir eine APP-überexprimierende Mauslinie (arcAβ, Knobloch et al. 2007a) mit i) konventionellen CRH-R1 knockout (KO) Mäusen (Timpl et al., 1998) und ii) konditionalen CRH-überexprimierenden Mäusen (Lu et al., 2008) verpaart. In der zweiten Generation der jeweiligen Linie wurden Mäuse mit vier verschiedenen Genotypen erhalten: i) arcAß (transgen, tg), arcAß CRH-R1KO (tgko), CRH-R1KO (ko), Wild-typ (wt) and ii) arcAß (tg), arcAß CRH-COE^{CNS} (tgcoe), CRH-COE^{CNS} (coe) and Wild-typ (wt). Diese wurden umfassend hinsichtlich Verhalten, Elektrophysiologie, Neuropathologie und APP Prozessierung phänotypisiert.

Unsere Ergebnisse deuten auf eine Rolle des CRH-Systems sowie der HHN-Achse im Rahmen der Morbus Alzheimer Pathogenese hin: wir haben ein beeinträchtigtes Erinnerungsvermögen im Test für Objekterkennung (object recognition, OR) bei tg Mäusen im Alter von 4 Monaten beobachtet, das durch die Deletion des CRH-R1 (tgko) wiederhergestellt wurde. Außerdem wiesen alle transgenen Mäuse (tg, tgko, tgcoe) ab dem Alter von 8 Monaten eine beeinträchtigte räumliche Erinnerung im Water cross maze (WCM) test auf. Darüber hinaus tendierten tgko Mäuse zu einer Striatum-basierten egozentrischen Lern-Strategie und wiesen eine reduzierte kognitive Flexibilität im Vergleich zu tg Mäusen auf. CRH-überexprimierende Mäuse (coe, tgcoe) zeichneten sich durch einen hyperaktiven Phänotyp aus und zeigten eine beeinträchtigte Leistung im OR Test, die vermutlich auf ein Aufmerksamkeitsdefizit zurückzuführen ist.

Im Vergleich zu tg Mäusen waren die Aß Spiegel in hippokampalem und kortikalem Gewebe in tgko Mäusen reduziert, ebenso wie die hippokampale Aß Plaque-Belastung. In tgcoe Mäusen verhielten sich diese Befunde entgegengesetzt. Astrozyten und Mikroglia infiltrierten in allen APP transgenen Mäusen gleichermaßen Aß Plaques, was darauf hindeuted, dass weder die Deletion des CRH-R1 noch die Überexpression von CRH einen direkten Einfluss auf die neuroinflammatorische Antwort haben.

Zusammengefasst deutet diese Studie auf eine Rolle des CRH-/CRH-R1-Systems und der HHN-Achse in der Pathophysiologie des Morbus Alzheimers in arcAß Mäusen hin. Der Verlust des CRH-R1 verbessert einige Symptome der Erkrankung während die Überexpression von CRH sich zum Teil eher nachteilig auf den Krankheitsverlauf auswirkt.

1. Introduction

1.1. Neurodegenerative diseases

Neurodegenerative diseases such as Alzheimer´s disease (AD), Parkinson´s disease (PD), Huntington´s disease (HD) and Amyotrophic lateral sclerosis (ALS) involve atrophy of affected central or peripheral structures of the nervous system (Bossy-Wetzel et al., 2004).
In AD, the most common neurodegenerative disorder, the brain is characterized by the loss of hippocampal and cortical neurons as well as assemblies of amyloid ß (Aß) and tau protein. PD is the most common neurodegenerative movement disorder, with the prevalence rising from one percent of the population older than 60 years up to four percent in those over 80 years (de Lau and Breteler, 2006). The clinical picture of PD is predicated on the selective degeneration of dopaminergic neurons in the substantia nigra pars compacta. Also, brains of PD patients exhibit misfolded protein inclusions, so called Lewy bodies (Jankovic, 2008). In HD, a toxic gain of function of the huntingtin protein caused by expanded CAG repeats of the Huntingtin gene induces loss of neurons in the striatum and cerebral cortex. HD follows an autosomal dominant pattern of inheritance, affecting 1 in 10000 individuals (Walker, 2007). The brain of ALS subjects is hallmarked by a decline of motor neurons, leading to muscle atrophy and respiratory failure.
Although the etiology of most neurodegenerative diseases remains unclear, they show common pathologic characteristics e.g. loss of neurons in affected brain regions, accumulation of misfolded proteins, reactive oxygen and nitrogen species, excitotoxicity, mitochondrial injury, calcium dysregulation, and death-receptor activation (Bossy-Wetzel et al., 2004;Bredesen et al., 2006).

1.2. Alzheimer´s disease (AD)

Dementia is the most common neurodegenerative disease affecting about 36 million people worldwide (Ferri et al., 2005). Aging is the primary risk factor, thus, due to the aging population, the prevalence of dementia is increasing with doubling of patients every twenty years (Zhu and Sano, 2006). AD accounts for up to 70 % of all cases and is therefore the most common cause of dementia (Fratiglioni et al., 1999). About 100 years after the first description of the disease by Alois Alzheimer, the genesis is still poorly understood.

1.2.1. Clinical presentation

DSM-IV (Diagnostic and Statistical Manual of Mental Diseases fourth edition) designates following criteria for diagnosis of AD in patients:

1) Memory impairment (recently learned facts)
2) At least one of the following cognitive disturbances:
   - Aphasia (language disturbance)
   - Apraxia (impaired ability to carry out motor activities)
   - Agnosia (failure to recognize familiar objects despite sensory function)
   - Disturbance in executive functioning (i.e., planning).

The cognitive deficits in Criteria 1) and 2) each cause significant impairment in social or occupational functioning and represent a significant decline from a previous level of functioning and the course is characterized by gradual onset and continuing cognitive decline. Furthermore, the disturbance is not better accounted for by another neuropsychiatric disorder (e.g. Major Depressive Disorder).

1.2.2. Therapeutic strategies

Due to the unknown genesis of AD no causal treatment strategy is available. Thus, the available medications constitute no cure, but rather alleviate symptoms to a minor degree. Currently, two classes of medication are indicated to treat the cognitive decline: acetylcholinesterase inhibitors (Tacrine, Rivastigmine, Galantamine and Donepezil) and the N-methyl-D-aspartate (NMDA) antagonist memantine (Vardy et al., 2005). Research on drugs to halt or reverse the disease mainly focuses on reduction of amyloid ß (Aß) by immunotherapeutic strategies (Fu et al., 2010). In this context, active Aß vaccination with synthetic Aβ peptides or fragments aims in the stimulation of the cellular and humoral immune responses of the host to generate anti-Aß antibodies. For passive immunization, injected Aß-specific antibodies directly target harmful Aß proteins. An initial clinical trial of an active Aß vaccine in humans was halted due to autoreactive T-cell responses which caused meningoencephalitis in 6 % of the vaccinated patients (Nitsch and Hock, 2008). Therefore, current and future immunotherapeutic approaches are challenged by the improvement of safety and tolerability of the vaccines (Nitsch and Hock, 2008).

1.2.3. Genetics

Most cases of AD are not hereditary. However, there is a small subset of cases that have an early age of onset (< 65 years). Ten percent of these cases are among the familial Alzheimer´s disease (FAD), also termed early onset AD and are based on autosomal

dominant mutations, which have been found in three genes: amyloid precursor protein (APP), presenilin 1 (PSEN 1) and PSEN 2 (Ballard et al., 2011). In the APP gene 20 pathogenic mutations have been identified, most often labeled by the place of identification, e.g. V717I ´London mutation´, V717F ´Indiana mutation´, K670D/M671L ´Swedish mutation´, E693G ´Arctic mutation´. Most FAD cases are caused by mutations in PSEN 1 and 2, of which already 130 mutations have been identified. Presenilins are components of the proteolytic γ-secretase complex, which is essential for directing the amyloid ß (Aß) generation (LaFerla et al., 2007). For the late onset AD, mutations in the APP, PSEN1 and PSEN2 genes account for less than 1 % of cases (Tol et al., 1999). Besides Aß plaques neurofibrillar tangles consisting of the microtubule-associated protein tau (MAPT) are the pathologic characteristic of AD and are even supposed to aggravate one another (Fath et al., 2002;Busciglio et al., 1995;Ittner et al., 2010). However, mutations in the MAPT gene encoding tau do not result in AD but are related to frontotemporal dementia and parkinsonism linked to chromosome 17 (FTDP-17), which is characterized by personality changes, cognitive decline and extrapyramidal symptoms (Goedert and Spillantini, 2000).

The APOE gene is the strongest genetic risk factor for late onset AD, especially the E4 allele, which is contributing to 50 % of cases (Kim et al., 2009). Recently, genome wide association studies (GWAS) revealed several additional risk genes associated with AD: CLU, CR1 and PICALM are supposed to affect the development of senile plaques (Kok et al., 2011). Furthermore, single nucleotide polymorphisms (SNPs) were found in the genes EFNA5, CAND1, MAGI2, ARSB and PRUNE2, which are involved in protein degradation, apoptosis and neuronal survival and are thus affecting hippocampal atrophy in AD subjects (Potkin et al., 2009).

Besides aging, possible risk factors for AD are sex (females have a higher incidence to develop AD), a lack of sex hormones, smoking, low degree of education and cardiovascular disorders (Bao et al., 2008).

1.2.4. Neuropathology

The most distinctive neuropathological hallmarks of AD include amyloid ß (Aß) plaques and neurofibrillary tangles (NFT). The post-mortem AD brain is characterized by a massive neuronal cell and synapse loss (Gotz and Ittner, 2008;Selkoe, 2002). The damage in the brain is accompanied by microglial activation and neuroinflammation (Lee et al., 2010). Furthermore, in AD subjects the cholinergic neurotransmission is reduced, exemplified by reduced levels of acetylcholine and activity of choline acetyltransferase (Francis et al., 1999). Some evidence suggests reactive oxygen species (ROS) to crucially contribute to the progression of AD by oxidative molecular damage of tissue and apoptosis signaling (Patten

et al., 2010). Besides ROS, reactive nitrogen species involving mitochondrial dysfunction are similarily associated with the AD pathology (Patten et al., 2010). Along these lines, vascular risk factors may contribute to the progression of the disease: capillary degeneration caused by endothelial nitric oxide supports the ongoing degenerative changes in the AD brain (Mohandas et al., 2009). Furthermore, oligomeric Aß can incorporate into membranes of neurons, form cation sensitive ion channels and thus cause abnormal increase in calcium levels, which in turn can drive the production of ROS and cytokines (Kawahara et al., 2009). It becomes clear that various events occur concomitantly and are interconnected (Mohandas et al., 2009).

1.2.4.1. Amyloid precursor protein processing and amyloid ß

The amyloid precursor protein (APP) is a membrane-spanning glycoprotein existing in humans in three major isoforms consisting of 695, 751 or 770 amino acids. Neurons most abundantly synthesize APP 695 (Pleckaityte, 2010;Priller et al., 2006). In its physiological role it is thought to contribute to signaling of neurons (Neve et al., 2001) and inhibition of synapses (Priller et al., 2006).

Amyloid ß (Aß) is derived by proteolytic cleavage from APP (Figure 1). Cleavage by α-secretase (ADAM 10) generates soluble sAPPα (non-amyloidogenic pathway); ß-secretase (beta-site amyloid precursor protein-cleaving enzyme 1 = BACE1) generates sAPPβ (amyloidogenic pathway). Additional cleavage of either membrane standing remnant C83 or C99 (ß-stub) by γ-secretase forms P3 or Aß, with $Aß_{40}$ being the more common and $Aß_{42}$ the more fibrillogenic and neurotoxic species. Gamma-secretase activity depends on 4 molecules: presenilin, nicastrin, anterior pharynx-defective 1 (APH1) and presenilin enhancer 2 (PEN2) (Gotz and Ittner, 2008). Presuming normal conditions, 90 % of total Aß accounts for $Aß_{40}$, which only slowly converts to insoluble assemblies, whereas the fibrillogenic $Aß_{42}$ amounts to 10 %. Aß monomers assemble to toxic oligomers which are thought to trigger synaptic degeneration and neuronal loss and thus are suspected of being primarily responsible for the clinical picture of AD such as cognitive impairment (Kawahara et al., 2009;Lord et al., 2009;Pleckaityte, 2010;Rowan et al., 2005). Finally, by accumulating more Aß, protofibrils deposit as plaques. A senile plaque is composed of Aß, activated microglia, astrocytes and degenerating neurons (El Khoury J. et al., 2007).

The activity of Aß generating secretases, which are membrane-spanning proteins, depends on the local lipid environment (Grosgen et al., 2010). For example, cholesterol is required for BACE1 activity and depletion of cholesterol has been demonstrated to inhibit the amyloidogenic pathway (Grimm et al., 2011). Furthermore, cholesterol is enriched in Aß plaques (Panchal et al., 2010). In addition, several members of the low-density lipoprotein

receptor (LDLR) family, e.g. sorLA/LR11, can interact with APP and regulate its processing (Marzolo and Bu, 2009). SorLA/LR11 acts as a sorting receptor that prevents Aß generation by interaction with APP and BACE1. Consistently, expression of sorLA/LR11 is significantly reduced in AD brains. But not only APP processing is influenced by the lipid metabolism, APP and APP processing products have also been shown to modulate lipid homeostasis (Grimm et al., 2011).

A recent study identified the extracellular amino-terminal fragment of APP (N-APP) to be a ligand for death receptor 6 (DR6), which is expressed by developing neurons and essential for axonal pruning and cell body death. Activation of DR6 triggers a neuronal self-destruction pathway, involving degeneration of cell bodies via caspase 3 and axons via caspase 6 (Nikolaev et al., 2009).

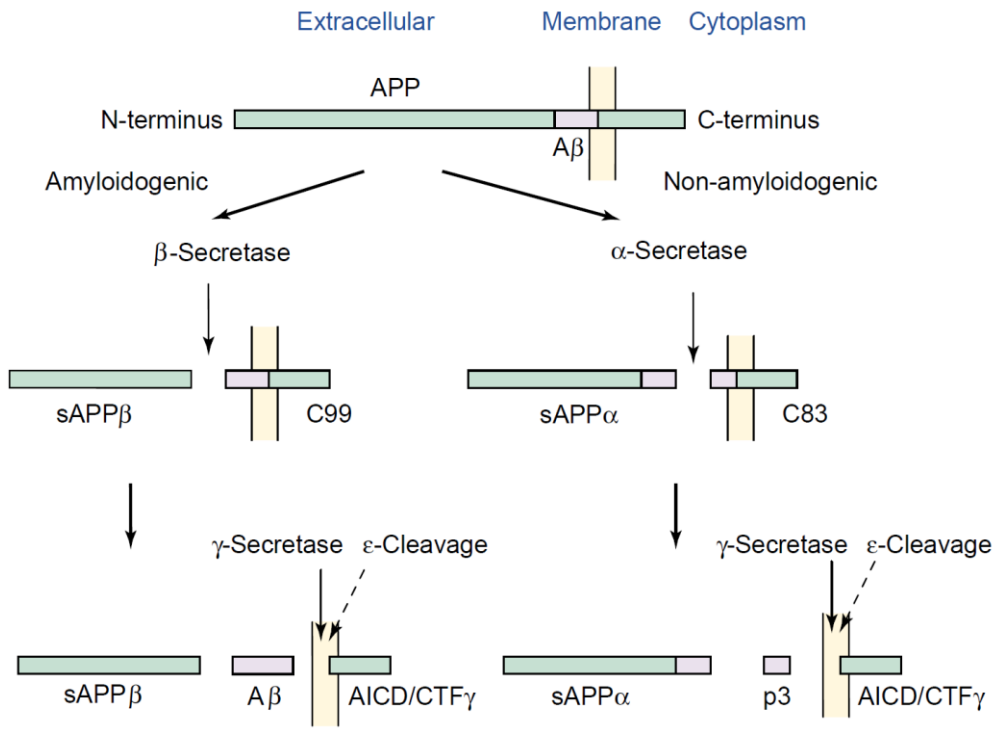

Figure 1. APP processing pathways. Amyloid ß (Aß) is derived by cleavage of APP by ß- and γ-secretase (amyloidogenic pathway). Within this cleavage pathway also a membrane standing stub/C-terminal fragment (C99) and soluble APPß (sAPPß) are generated. Cleavage of APP by α-secretase yields sAPPα and C83 and consecutively, cleavage by γ-secretase, P3 (non-amyloidogenic pathway). Cleavage of either C-terminal fragment (C83 and C99) by γ-secretase results in the membrane bound stub CTFγ or by additional cleavage at the ε-site in the release of the APP intracellular domain (AICD) into the cytoplasm. Adapted with permission from Vardy et al. (2005).

1.2.4.2. Tau pathology

Tau is a phosphoprotein essential for stabilizing microtubules, axonal transport and structural support. Alternative splicing of tau RNA results in humans in six tau isoforms (352-441 amino acids) differing in the presence of either three or four peptide repeats of 31 or 32 residues in the carboxy-terminal region and absence or presence of one or two inserts in the N-terminal part (Buee et al., 2000) (Figure 2).

Splicing of isoforms and the phosphorylation state of tau are strongly modified during development. At embryonic stages only one tau isoform is expressed, by contrast, all six isoforms are present in the mature brain (Buee et al., 2000). Due to the ratio of kinases and phosphatases, phosphorylation of tau is on its highest level during embryogenesis and early development when differentiation and plasticity of neurons is accordingly high (Hanger et al., 2009).

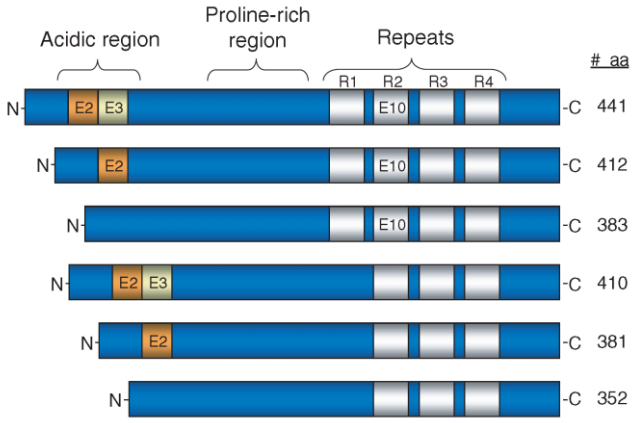

Figure 2. Schematic drawing of the six tau isoforms found in the human brain. The isoforms differ in the number of amino acids (# aa), presence of three or four peptide repeats and absence or presence of inserts in the N-terminal region. Adapted with permission from Johnson and Stoothoff (2004).

Due to its numerous serine and threonine residues tau is a substrate of many kinases such as GSK-3ß and Cdk5. In AD brains hyperphoshphorylation (phosphorylation to a higher, pathological degree) occurs at 20-30 potential phosphorylation sites (Geschwind, 2003).

In its phosphorylated state tau is detached, whereas in its dephosphorylated state it is bound to microtubules. In AD tau is hyperphosphorylated and in consequence is constantly detached from microtubeles which therewith are lacking stability and cannot maintain their functions (Figure 3). Detached tau can be phosphorylated at additional sites or cleaved by caspases and therefore gains increased propensity to oligomerize, forms intracellular

aggregates and finally deposits as fibrils and tangles, which have proven to be cytotoxic (Fath et al., 2002) (Figure 3).

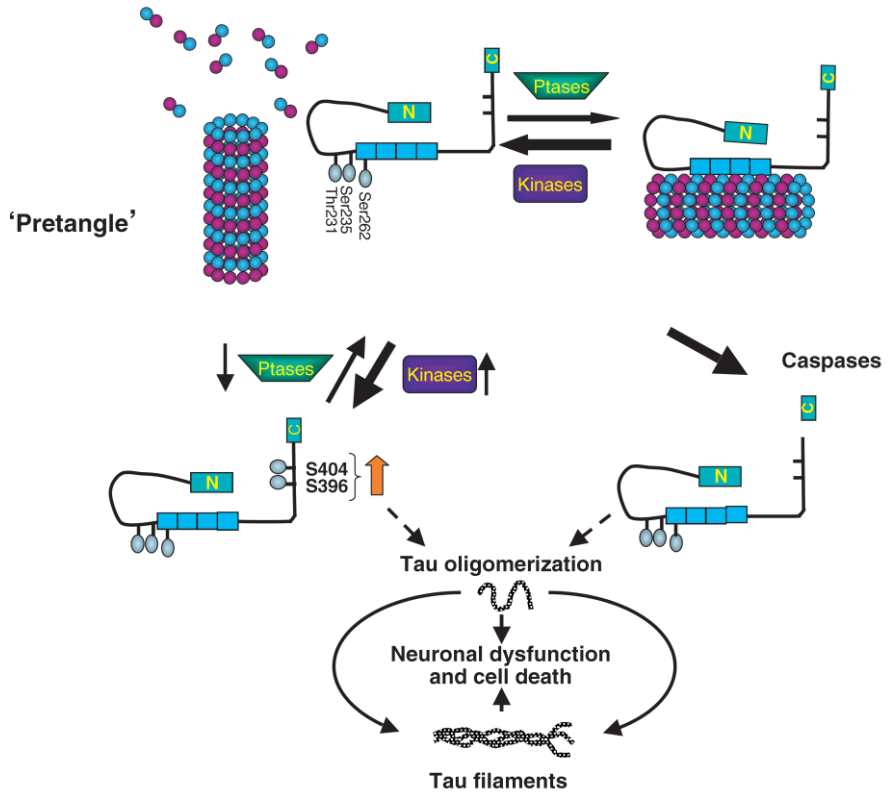

Figure 3. Tau phosphorylation and oligomerization. After phosphorylation tau loses the ability to bind to microtubules which consequently forfeit their integrity. Detached tau can be phosphorylated at additional sites or cleaved by caspases and therefore gains increased propensity to oligomerize with subsequent deposition of tau filaments. Adapted with permission from Johnson and Stoothoff (2004).

1.2.4.3. Linking amyloid ß to tau pathology

Originally, the amyloid cascade hypothesis (Hardy and Higgins, 1992) proposed Aß deposition to trigger neuronal dysfunction and cell death in the brain and to subsequently challenge tau tangle formation. Although there is emerging evidence illuminating a possible interaction of Aß and tau, the linkage still remains unclear. Some evidence from animal models suggest that tau kinases such as GSK-3ß and Cdk5 are also involved in APP processing and Aß deposition (Geschwind, 2003). Furthermore, it has been demonstrated that $Aß_{42}$ increases neurofibrillary tangles and activates GSK-3ß, which together with the previous statement indicates a vicious circle (Geschwind, 2003). Injection of Aß fibrils has shown to increase neurofibrillary tangle pathology in mice that express mutant human tau (Gotz et al., 2001). In transgenic mice exhibiting Aß and tau pathology (triple transgenic mice

(3xTg), see 1.2.5 Genetic mouse models of AD) reduction of Aß depostits by Aß immunotherapy subsequently reduced tau phosphorylation via the proteasome (Oddo et al., 2004). Aß fibrils can induce tau phosphorylation in rat hippocampal neurons (Busciglio et al., 1995), more specifically fibrillar Aß has been shown to induce progressive and sustained activation of the mitogen-activated protein kinase (MAPK) (Rapoport and Ferreira, 2000). Recent evidence suggests that Aß may drive tau pathology not only by activating specific kinases but also by inhibition of tau degradation via the proteasome. (Blurton-Jones and LaFerla, 2006;Tseng et al., 2008). Tau seems to be essential for Aß-induced neurotoxicity and may link the cytotoxic effect of Aß to neurodegeneration (Rapoport et al., 2002). Accordingly, in tau knockout mice Aß plaque load did not differ, whereas the excitotoxicity decreased, implying that Aß toxicity is mediated via tau (Ittner et al., 2010). Reduction of endogenous tau rescued behavioral deficits in APP transgenic mice without altering Aß levels and protected both APP transgenic and non-transgenic mice against Aß induced excitotoxicity (Roberson et al., 2007).

1.2.4.4. Inflammation

In the brain of AD subjects the neuroinflammatory response, comprising microglial activation and cytokine expression, is enhanced (El Khoury J. and Luster, 2008). Also, systemic inflammatory events measured in AD patients could be correlated to the cognitive decline (Holmes et al., 2009).

After disturbances in the brain microglia are the first cells responding by activation through transformation. Neurotransmitter receptors on microglia lead to specific reactions such as the initiation of an inflammatory cascade or acquisition of a neuroprotective phenotype (Pocock and Kettenmann, 2007). Activated microglia accumulate around Aß plaques and in some instances ingest intracellular deposits of Aß (El Khoury J. and Luster, 2008). The absence of early microglial clustering leads to a decreased Aß clearance and increased mortality (El Khoury J. et al., 2007). On the one hand microglia secrete proteolytic enzymes that degrade Aß and express receptors promoting the phagocytosis of Aß, thus conferring a rather neuroprotective and disease alleviating role (Rodriguez et al., 2010). On the other hand microglia release neurotoxins such as reactive oxygen intermediates (ROIs) (Parvathenani et al., 2003) and pro-inflammatory cytokines such as IL-1ß, IFNγ and TNF and hence may also cause neuroinflammation and neurodegeneration in the brain (Delarasse et al., 2011). In this respect, a growing body of evidence assumes moderate activation of microglia to be advantageous for the progression of AD, whereas strong activation might have opposite effects by reduced capacity of Aß clearance, release of pro-inflammatory cytokines and accompanying neuronal damage (Johnston et al., 2011) (Figure 4).

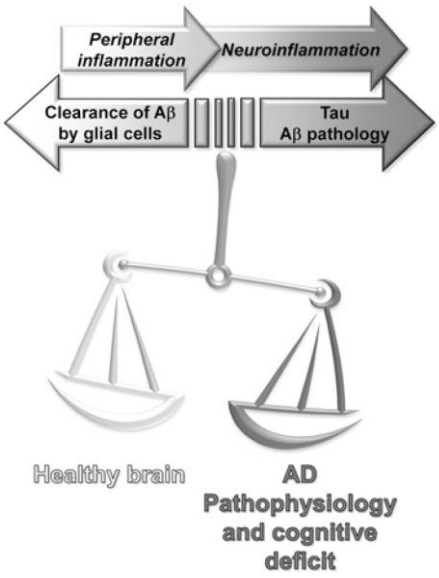

Figure 4. Ambiguous role of the neuroinflammatory response in AD. The overall outcome of beneficial factors (arrows pointing left) and detrimental factors (arrows pointing right) of inflammatory events in the progression of AD. Adapted with permission from Johnston et al. (2011).

The role of cytokines is ambiguous: the pro-inflammatory cytokine IL-1 has been shown to contribute to AD pathophysiology in patients (Griffin and Mrak, 2002). However, mice deficient for the IL-1 receptor showed increased susceptibility to intra-hippocampal injections of Aß (Craft et al., 2005). This ambivalence was reflected in electrophysiological measurements: physiological levels of IL-1 were required to maintain long-term-potentiation (LTP), whereas high levels were detrimental in this regard (Yirmiya and Goshen, 2011). Similarily, IFNγ and IL-6 are accused to play both a beneficial and detrimental role in AD (Johnston et al., 2011). Accompanying the massive cytokine release and therewith increased permeability of the BBB, infiltration of peripheral bone marrow-derived cells can be observed at the sites of Aß deposition and inflammation where they, as a mechanism of inflammatory response, phagocytose Aß plaques (Butovsky et al., 2007). At initial stages of AD the number of resting microglia increases as if in preparation for the ensuing activation in an attempt to fight the extracellular Aß load (Rodriguez et al., 2010). In an APP mouse model with impaired microglia accumulation, Aß clearance was decreased and therewith Aß levels increased more than two fold (El Khoury J. et al., 2007). An increase in the density of resting microglia precedes both plaque formation and activation of microglia by extracellular Aß accumulation. In principle, AD transgenic models do not reflect all features of the human AD (see 1.2.5 Genetic mouse models of AD) and probably fail to correctly model inflammation as an overall result from the neurodegeneration in the brain.

1.2.5. Genetic mouse models of AD

In the past two decades, several transgenic mouse models mimicking a particular aspect of human AD pathology have been generated. In this respect transgenic mouse models based on FAD mutations (see 1.2.3 Genetics), in particular models resulting in increased Aß deposition, are widely used and found broad acceptance in the field for modeling AD *in vivo* (Duyckaerts et al., 2008). One of the three isoforms of hAPP (695, 751, 770 amino acids) combined with mutations mentioned earlier, e.g. the Swedish mutation or Arctic mutation driven by promoters like Thy-1 for neuron-specific expression or hamster prion protein (PrP) promoter including expression in extraneuronal tissue were used to generate transgenic mice expressing human APP (hAPP). Due to their robust Aß pathology good representative models are the Tg2576, APP23, Tg CRND8 and the arcAß mouse line (see Table 1).

AD mouse model	mutation	promoter	Aß pathology
Tg2576 (Hsiao et al., 1996)	hAPP 695 Swedish	PrP	diffuse Aß deposition at 9-11 months
APP23 (Sturchler-Pierrat et al., 1997)	hAPP 751 Swedish	Thy-1.2	diffuse and congophilic Aß deposition from 6 months
Tg CRND8 (Chishti et al., 2001)	hAPP 695 Indiana and Swedish	PrP	Aß plaque formation at 3 months
$PS1_{M146L}$ (Duff et al., 1996)	PS1 M146L	PDGFß2	increased $Aß_{42}$ levels
PSAPP (Langui et al., 2004)	(Tg2576 x PS1 M146L)	PrP, PDGFß2	diffuse Aß deposition at 6 months
$APP_{SL}PS1_{M146L}$ (Blanchard et al., 2003)	hAPP 751 London and Swedish PS1 M146L	Thy-1 HMG-CoA reductase	intracellular Aß accumulation at 2 months, Aß plaques at 3 months
Triple transgenic (3xTg) (Oddo et al., 2003)	APP, Swedish PS1 M146L P301L	Thy-1.2	intracellular Aß accumulation at 3 months, Aß plaques at 6 months, NFT at 12 months

Table 1. Selection of transgenic AD mouse models expressing human APP.

Besides, overexpression of mutant forms of hAPP, affecting the APP processing pathway by mutating ß- and γ-secretases has been explored as an alternative approach. Mice deficient for BACE-1 (ß-secretase) do not produce Aß (Luo et al., 2001). Transgenic mice expressing single FAD PS1 or PS mutations do not develop Aß plaques, but show increased levels of Aß (Duyckaerts et al., 2008). This might be explained by the fact that PS1 and PS2 knockout mice compared to APP transgenic mice exhibit lower levels of $Aß_{42}$, which constitutes the toxic form of Aß prone to form aggregates. However, combined expression of PS1 and hAPP enhances Aß pathology (Elder et al., 2010).

The mouse models mentioned above center on Aß pahthology but are lacking tau pathology. Mouse and human tau protein are physiologically different and the expression of wild-type human tau in the mouse brain does not result in tau aggregation and therewith paired helical filaments (PHF) and neurofibrillary tangles (NFT) (Duyckaerts et al., 2008). However, mutated versions of the tau protein, e.g. P301L, V337M or P301S, are directing the formation of NFTs (Duyckaerts et al., 2008). To study the interaction between the accumulation of Aß and tau, transgenic mice representing both mutated tau and altered APP processing were established (see Table 1).

Despite enormous achievements in mimicking AD in mouse models, none of the models can fully reproduce the complex aspects of the human disease but allow for investigation of certain aspects of AD pathology.

1.3. The CRH system and the HPA axis

The neuropeptide corticotropin-releasing hormone (CRH) is the central regulator of the hypothalamic-pituitary-adrenal (HPA) axis and a neuromodulator acting throughout the brain (Vale et al., 1981). CRH binds with high affinity to the CRH receptor type 1 (CRH-R1) and with lower affinity to CRH-R2. CRH receptors are G-protein-coupled transmembrane receptors with distinct expression patterns in the brain (Deussing and Wurst, 2005). CRH-R1 is highly expressed in the neocortex, hippocampus, cerebellum and sensory relay structures, whereas CRH-R2 is located in subcortical structures, particularly in the lateral septal nuclei, choroid plexus and various hypothalamic nuclei (Chalmers et al., 1995). In contrast to the CRH-R1, CRH-R2 is also expressed in peripheral tissue, foremost in the cardiac and skeletal muscle (Chalmers et al., 1995). By binding to CRH-R1, CRH activates G_s proteins and subsequently the cAMP/protein kinase A pathway (Grammatopoulos and Chrousos, 2002). Thereby CRH is involved in regulating sleep, libido and appetite. Elevated levels of CRH or its exogenous administration can induce psychomotor symptoms and anxiety (Lehnert et al., 1998;Swaab et al., 2003). In addition, memory, learning and synaptic plasticity have been shown to be influenced by the CRH/CRH-R1 system (Gallagher et al., 2008).

The highest density of CRH-containing neurons is found in the paraventricular nucleus (PVN) of the hypothalamus (Van Pett et al., 2000) where CRH is released in the course of the circadian regulation of the HPA axis and in response to stress. The HPA axis is a key neuroendocrine system involved in orchestrating the organisms stress response, regulated by complex direct influences and feedback interactions (Figure 5): from the PVN, CRH-expressing neurons project to the portal capillary zone of the median eminence and subsequently, CRH is transported to the anterior pituitary. Here, CRH triggers the release of adrenocorticotropic hormone (ACTH), which by binding to ACTH receptors in the adrenal cortex finally induces the synthesis and release of glucocorticoids (GCs; cortisol in humans, corticosterone in rodents). Inhibition of the HPA axis is mediated by negative feedback of GCs by binding to GC receptors (GRs) in the pituitary, PVN and in the hippocampus (Herman and Cullinan, 1997). GRs in the prefrontal cortex (PFC) also contribute to the negative feedback (Mizoguchi et al., 2004). Moreover, GRs are located in multiple brain regions such as hippocampus, PFC, amygdala and locus coeruleus, where they are involved in stress relevant effects on memory and cognition (Quirarte et al., 1997;Roozendaal, 2002;Fuchs et al., 2004). Besides the stress response, GCs regulate gluconeogenesis, lipolysis, proteolysis, blood pressure and insulin resistance and are necessary for facilitating memory processes (Sotiropoulos et al., 2008b;Sandi, 2011). Aside from the GR, GCs act on mineralcorticoid-receptors (MRs) which are restricted in their distribution to the lateral septum and the hippocampus. Moreover, GCs have a 6- to 10-fold higher affinity to the MR than to the GR (Reul and de Kloet, 1985). Consequently, MRs are occupied constantly with endogenous GCs (> 90 %), whereas GRs only get occupied when GCs in the plasma increase, which is the case after stress or during the circadian peak (Reul and de Kloet, 1985). With respect to HPA axis regulation, both GR and MR are involved in regaining homeostasis after stressful challenges: the MR density in the hippocampus is rapidly increasing after acute experience of stress and binding of GCs exerts inhibitory control of the HPA axis apart from GR (Reul et al., 2000). In general, the function of GRs and MRs on cellular level differs: GRs are rather implicated in maintaining homeostasis and information storage, whereas MRs control structure and excitability of networks (de Kloet et al., 2005).

Several studies observed an age-related activation of CRH neurons and the HPA axis, which could be due to a decline of the hippocampus during aging and the accompanying reduced sensitivity of the HPA axis to negative feedback of GCs (Goncharova and Lapin, 2002;Bao et al., 2008;Raadsheer et al., 1994b). Thus, cortisol levels in the cerebrospinal fluid (CSF) and in the plasma are found to progressively increase during aging. In male C57BL/6 mice aged 3, 9 and 16 months the circadian pattern of corticosterone showed age-related changes: the peak of corticosterone secretion at the end of the light phase/beginning of the dark phase

was at its highest level in mice at 3 months of age, whereas mice aged 9 months reached peak corticosterone concentrations about 2 hours earlier and the lowest levels of GCs were observed in 16 months aged mice. However, the total levels of corticosterone were rather equal (Dalm et al., 2005). Furthermore, in this study, CRH levels remained constant, but MR and GR mRNA expression in the hippocampus decreased starting at the age of 6 months.

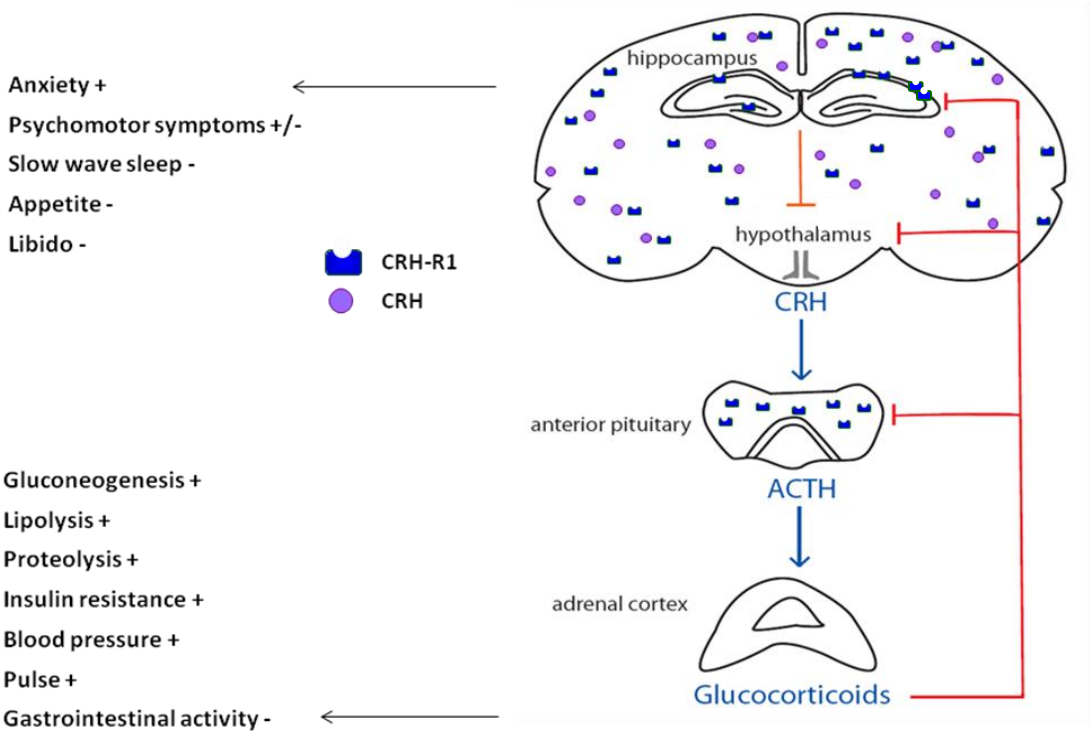

Figure 5. CRH/CRH-R1 system in the brain and the HPA axis. CRH binds to CRH-R1 throughout the brain and thereby affects anxiety, psychomotor symptoms, sleep and appetite (excess of CRH promotes (+) or attenuates (-) listed properties above). By binding to CRH-R1 in the pituitary, CRH triggers the activation of the HPA axis, which by the release of glucocorticoids, is mediating the body´s stress response and modulates among others gluconeogenesis, lipolysis and blood pressure.

1.3.1. The CRH system and the HPA axis – gain- and loss-of-function mouse models

Genetically engineered mice modeling alterations of the CRH system and the HPA axis have been established and are widely used tools to study the manifold functions of these systems. Two conventional CRH-R1 knockout (KO) mouse lines have been created, which exhibit reduced anxiety-related behavior (Smith et al., 1998;Timpl et al., 1998). Due to complete loss

of CRH-R1 the HPA axis also is disrupted, which is reflected by a chronic deficit in plasma corticosterone. Other loss of function approaches are conditional CRH-R1KO lines with spatially restricted disruption of CRH-R1 signaling, e.g. $Crhr1^{Camk2aCre}$ mutants in which the CRH-R1 is knocked out in the anterior forebrain including limbic brain structures (Muller et al., 2003). $Crhr1^{Camk2aCre}$ mutants showed reduced anxiety-related behavior, however, due to CRH-R1 expression in the pituitary normal HPA axis function under basal conditions (Muller et al., 2003). Refojo and colleagues demonstrated the role of CRH-R1 in anxiety-like behavior to be dependent on the neuronal circuit: CRH-R1 deletion in forebrain glutamatergic neurons reduced anxiety, whereas CRH-R1 deficiency in midbrain dopaminergic neurons increased anxiety-like behavior (Refojo et al., 2011).

Gain-of-function approaches are represented by CRH-overexpressing mouse lines, e.g. restricted to the central nervous system (CNS) in $CRH\text{-}COE^{CNS}$ mice (Lu et al., 2008). $CRH\text{-}COE^{CNS}$ mice showed increased active stress-coping behavior and stress-induced hypersecretion of corticosterone (Lu et al., 2008).

1.4. Dysregulated CRH system versus stress effects in AD

In AD patients and transgenic rodent models of AD several alterations of the CRH system, the HPA axis and GC regulation have been observed. On the one hand, CRH-immunoreactivity in the cortex of dement patients was found to be reduced (Davis et al., 1999;Bissette et al., 1985). On the other hand, increased numbers of CRH-producing neurons in the paravantricular nucleus of AD patients have been reported to lead to hyperactivation of the HPA axis (Raadsheer et al., 1994a;Raadsheer et al., 1995). In general, the degree of HPA axis hyperactivity has been shown to correlate with the severity of cognitive impairment and hippocampal atrophy (Gurevich et al., 1990;Lupien et al., 1998).

Along these lines, many AD patients exhibit elevated cortisol levels (Rothman and Mattson, 2010;Davis et al., 1986;Csernansky et al., 2006;Rasmuson et al., 2001;Lee et al., 2009;Jeong et al., 2006;Kulstad et al., 2005), which are a consequence of the disturbed feedback control of the HPA axis and are linked to impaired memory function (Lupien and McEwen, 1997;Lupien et al., 1998). Basal and stress-induced corticosterone levels are also elevated in several transgenic rodent models of AD, where they have been demonstrated to exacerbate cognitive deficits (Pedersen et al., 2006;Pedersen et al., 1999;Touma et al., 2004;Green et al., 2006;Dong et al., 2008;Carroll et al., 2011).

Chronic stress and increased GC levels can reduce hippocampal dendritic complexity and promote hippocampal cell death (Csernansky et al., 2006). Concomitant to hippocampal atrophy, GRs in the hippocampus are downregulated and thus, the negative feedback of the hippocampus to the hypothalamus is impaired contributing to HPA axis hyerpactivity.

Generation and deposition of amyloid ß (Aß), the most prominent neuropathological hallmark of AD, also has been shown to be influenced by mediators of the HPA axis. In particular GCs and chronic stress have been found to have detrimental effects in this regard (Catania et al., 2009;Sotiropoulos et al., 2008a;Sotiropoulos et al., 2011;Lee et al., 2009). Stress/GCs have also been found to trigger pathologic tau hyperphosphorylation (Sotiropoulos et al., 2011) and to potentiate Aß-induced tau pathology (Sotiropoulos et al., 2008a). Recently, stress induced tau phosphorylation has been shown to be mediated via the CRH-R1 (Rissman et al., 2007;Carroll et al., 2011), indicating a direct role of CRH apart from GCs. Also the Aß increase in the interstitial fluid after acute stress has been demonstrated to be CRH dependent (Kang et al., 2007a).

The glucocorticoid hypothesis (Sapolsky et al., 1986) explains the HPA axis hyperactivity in the context of AD (Figure 6): Aß deposits and increased GC-levels damage hippocampal neurons. Thus, the inhibitory tone on the hypothalamus is disturbed, resulting in a hyperactivated HPA axis with increased levels of CRH and GCs (Roozendaal et al., 2001). High GC levels promote Aß generation and further damage the hippocampus. Aggravated hippocampal damage could amplify the HPA axis dysregulation and ongoing hippocampal destruction. Ultimately, a detrimental feed-forward loop exacerbating AD pathology via disinhibition of HPA axis and GC production is initiated (Kulstad et al., 2005;Breyhan et al., 2009;Nuntagij et al., 2009;Rothman and Mattson, 2010).

Besides the above described rather detrimental effects of CRH in the context of AD, some publications demonstrated neuroprotective effects of CRH *in vitro*. Bayatti and Behl (2005) reported neuroprotective capacities of CRH via stimulation of CRH-R1. These involve inactivation of the tau-kinases GSK3ß and Cdk5 and enhanced secretion of non-amyloidogenic sAPPα. Bayatti et al. observed that pretreatment of cells with CRH can attenuate Aß mediated toxicity in primary hippocampal neurons (Bayatti et al., 2003). Similar findings regarding the neuroprotective effects of CRH against Aß toxicity were explained by stabilization of the cellular calcium homeostasis. In contrast, higher CRH-concentrations may cause insults due to increased Ca^{2+}-influx (Pedersen et al., 2001). Also Facci and colleagues supported the neuroprotective effect of CRH via cAMP-dependent signaling pathways (Facci et al., 2003). Finally, Lezoulch and colleagues demonstrated that neuroprotective effects of CRH via CRH-R1 are associated with an increase of non amyloidogenic sAPP and suppression of NFκB (Lezoualc'h et al., 2000).

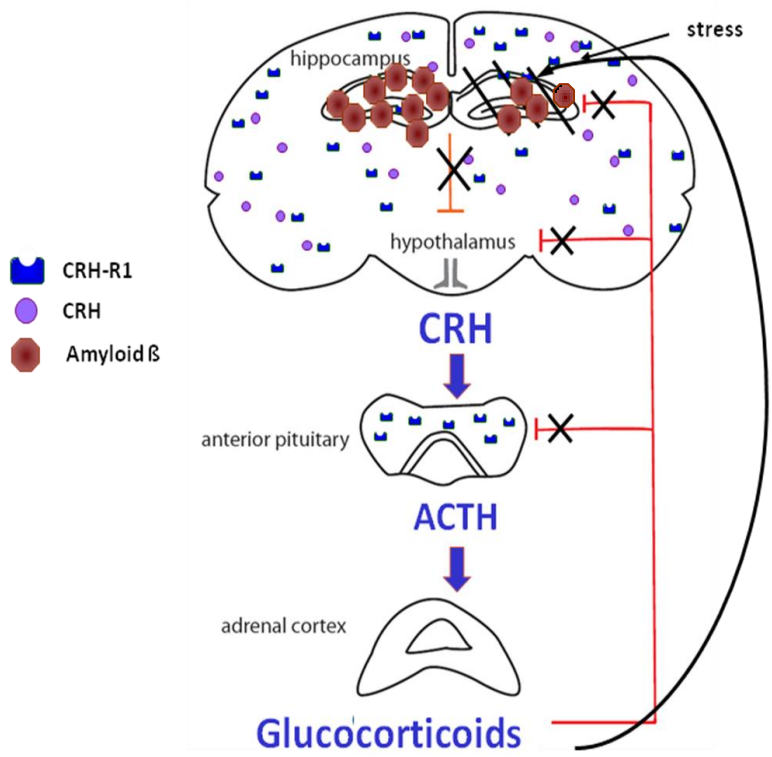

Figure 6. A feed-forward loop is exacerbating AD pathology: The glucocorticoid hypothesis. Elevated GC-levels, Aß deposits and stress induce hippocampal atrophy. Thus, the inhibitory effect on the hypothalamus is not provided anymore, the HPA axis is hyperactivated, levels of CRH and GC increase further. High GC levels promote Aß generation and further damage to the hippocampus completing a vicious cycle.

1.4.1. Linking neurodegeneration to mood disorders

The prevalence of major depression in AD patients is 20-25 % (Ballard and Waite, 2006;Lyketsos and Olin, 2002;Lyketsos et al., 2002;Starkstein et al., 2005). From the clinical point of view, depression and dementia share common symptoms such as impairment in attention and working memory, alteration in sleep patterns and reduction of social and occupational function (Steffens and Potter, 2008). These and some further attending ills of either disease like mood swings, irritability, anhedonia, psychomotor agitation/retardation, appetite loss and worthlessness are at least partly to be ascribed to the CRH system. Early cognitive impairment may induce depressive symptoms in AD patients and thus depression may be seen as an early symptom of dementia (Byers and Yaffe, 2011). Also in depressed patients altered regulation of the CRH system and the HPA axis can be detected: Stress has shown to be a risk factor for the disease (Mizoguchi et al., 2000). In some depressed subjects the HPA axis is hyperactivated (Raadsheer et al., 1995;McEwen, 1998;Modell et al., 1997) and thus GC levels are increased (Gold et al., 1995;Gold et al., 2002;Gold and

Chrousos, 2002;de Kloet et al., 2005). Along these lines, CRH-immunoreactive neurons are increased in number (Raadsheer et al., 1994a;Raadsheer et al., 1994c;Gold and Chrousos, 2002;Swaab et al., 2005).

GC levels in humans have been demonstrated to negatively correlate with hippocampal volume and positively with age-related cognitive decline (Lupien et al., 1998;Starkman et al., 2001;Starkman et al., 2003). Since GCs themselves do neither produce Aß plaques nor massive cell death as seen in AD patients, elevated GC levels in AD patients might rather be the result than the cause of the ongoing neurodegeneration (Swaab et al., 2005;Bao et al., 2008). However, stress via GCs can induce cell signaling events that culminate in mood and also cognitive disorders (Sotiropoulos et al., 2008b). Stress/elevated GC levels might induce a set of molecular and cellular pathways that, in turn, initiate a series of mutually enhancing malfunctions (Sotiropoulos et al., 2008b).

In AD and major depression volume reduction in the hippocampus and prefrontal cortex (PFC) has been observed (Braak and Braak, 1991;Sheline et al., 1996). Both structures are crucial for feedback regulation of the HPA axis (Herman and Cullinan, 1997) and are indispensible for memory and learning capabilities (see 1.5 Memory and learning). Neuroinflammation as a defence strategy against neuronal damage and dysregulation in the brain is advocating intact brain function in AD as well as in depression (Yu et al., 2003;Bonotis et al., 2008;Hewett et al., 1994).

The overlay of symptoms and neuropathological features, supported by the comorbidity data indicate a link between AD and depression which may be directed at least to some extent via the CRH system.

1.5. Memory and learning

This section aims to elaborate on the different memory and learning systems in the brain. In general it can be discriminated between sensory, short-term and long-term memory. Sensory memory corresponds to the memory after perceiving an object only for millseconds up to one second (Winkler and Cowan, 2005). Short-term memory involves the range of seconds and subordinates working memory, which is the abililty to hold information in the mind in order to perform complex tasks such as reasoning (Baddeley, 2003). Long-term memory can be divided into declarative (explicit) and procedural (implicit) memories, both will be explained in detail below. In addition, there are diverse cognitive qualities such as cognitive flexibility and attention which have to be incorporated in surveying complex diseases like AD.

1.5.1. Declarative memory

Declarative memory is also termed explicit memory, since information is explicitly stored and consciously recalled. This conscious memory for facts and events is acquirable with relatively few exposures to the material to be learned (Winters et al., 2008). The hippocampus is essential for declarative learning, consolidation and long-term storage of information, in particular for the spatial learning, e.g. learning that the goal is in the same position relative to the surrounding. Spatial learning is also termed allocentric or place learning. In rodents, this paradigm can be recalled in diverse maze-apparatuses based on Tolman´s wooden cross-maze (Tolman et al., 1946). In the eighties Morris and colleagues developed a behavioral procedure to analyse spatial navigation in rodents by requiring the mouse to search for a hidden platform in opaque water (Morris et al., 1982). To present the so called Morris water maze is the gold standard for testing cognition in mice and rats.

Another form of declarative memory is spontaneous object recognition (OR) memory that is the tendency to recognize and prefer a novel object, which is dependent on temporal lobe areas, in particular the perirhinal cortex (PRh) (Bussey et al., 2000). Aggleton and Brown (1999) provided evidence that PRh-lesioned rats have impaired OR memory and that also the hippocampus contributes to the performance of the task, probably to combine spatial or contextual information with the specific object information processed by the PRh.

1.5.2. Procedural memory

Procedural memory bases upon unconscious assessing of previous experiences involving executive functions and movement pathways, thus termed implicit memory. Procedural memory is principally mediated by the striatum. The striatum, also termed corpus striatum, striate nucleus or caudate putamen, is the largest component of the basal ganglia. It gets input from the cerebral cortex and projects to other parts of the basal ganglia (Squire and Zola, 1996;Cohen et al., 1997).

In humans the striatum is activated by stimuli associated with reward, but also by aversive, novel, unexpected or intense stimuli. Procedural striatum-dependent learning is also termed egocentric, response or habit learning.

1.5.3. Cognitive flexibility

The ability to react to situations different from previous already known situations and patterns is termed cognitive flexibility. Cognitive flexibility mainly depends on the prefrontal cortex (PFC) (Sotiropoulos et al., 2011), but there is considerable evidence that also synapses to the basal ganglia and the hippocampus are supposed to contribute (Cerqueira et al.,

2007;Ragozzino et al., 2002). In animal models, cognitive flexibility and herewith PFC functionality can be reflected by revearsal learning tasks.
Temporary inactivation or lesions of the medial prefrontal cortex and orbital prefrontal cortex both produce behavioral flexibility impairments by increasing perseverative responses (Eichenbaum et al., 1983;Ragozzino et al., 1999;Dias and Aggleton, 2000). Interestingly, both of these prefrontal cortex areas project to the medial striatum (Berendse et al., 1992). The neuromorphological effects of chronic stress in the PFC are mediated by GCs and have been shown to be correlated to PFC volume and thus behavioral flexibility (Cerqueira et al., 2005;Cerqueira et al., 2007).

1.5.4. The role of acetylcholine in learning and memory

Growing evidence supports acetylcholine as a central modulator of learning and memory. The release of this neurotransmitter is used to track activation of memory systems (McIntyre et al., 2003b). For example, levels of acetylcholine in the hippocampus or the striatum predicted the strategy of solving a place or response version of a four-arm plus-shaped maze: rats initially used the hippocampal dominated place-solution; whereas later in the training they changed to procedural learning. Accordingly, acetylcholine was first released in the hippocampus, later in the striatum (Chang and Gold, 2003b). Consistent with these findings, the ratio of acetylcholine in the hippocampus vs. the striatum was correlated to the choice of task solution in place or response versions of food-rewarded mazes: the higher the ratio, the more rats were prone to apply the place-solution and vice versa (Pych et al., 2005).
Moreover, other learning paradigms also appear to rely on cholinergic transmission: acetylcholine release in the amygdala positively correlated with performance of spontaneous alternation (McIntyre et al., 2003a). Acetylcholine also has been shown to influence synaptic plasticity within the PRh (Massey et al., 2001). Here, blocking of muscarinic receptors by scopolamine induced deficits in object recognition memory (Warburton et al., 2003). In the orbital prefrontal cortex acetylcholine is involved in aspects of reversal learning which reflects cognitive flexibility. A functional role is ascribed to the central nicotinic receptor in the context of attention-deficit/hyperactivity disorders (Rezvani and Levin, 2001). Also attention processes during the recall in working memory tasks are subscribed to the central nicotinic receptor (Maviel and Durkin, 2003). In general, the role of muscarinic and nicotinic receptors in the context of learning and memory remains to be elucidated (Deiana et al., 2011).
The oldest hypothesis for the cause of AD proposes that deterioration of cognition is due to the loss of cholingergic neurons and thus due to the decline of cholinergic neurotransmission in the brain (Davies and Maloney, 1976;Drachman and Leavitt, 1974). Therefore, therapeutic treatment largely concentrates on increasing levels of acetylcholine. Today, it is evident that

the cholinergic deficit does not directly cause symptoms of AD, but is indirectly contributing to the genesis of the disease e.g. by diminishing attention processes (Francis et al., 1999).

1.5.5. Dysfunction of cognitive systems

In general, dysfunction in an anatomical memory system abolishes specific memory operations but leaves other forms of acquisition intact. Cognitive systems such as hippocampus-dependent spatial learning and response learning mediated by the striatum (Packard et al., 1989) can function in parallel (Packard and McGaugh, 1996) but can also interact competitively or synergistically (Kim and Ragozzino, 2005). Previous studies showed that suppression of one system affects learning by another, e.g. depressing the hippocampal function has been shown to enhance striatum-dependent procedural responding in rats (Middei et al., 2004). Chang and Gold (2003a) observed that intra-hippocampal injections of lidocaine retarded acquisition of place learning but enhanced acquisition of response learning. Furthermore, memory rules can change from their first association to those that take place when the task is mastered (Rossato et al., 2006). Along these lines, the PFC is implicated in strategy switching: in rodents strategy switching between place and response learning is impaired by medial PFC (mPFC) inactivation (Ragozzino et al., 1999;Rich and Shapiro, 2007) and mPFC neuronal activity predicts switching between hippocampus- and caudate-dependent memory strategies (Rich and Shapiro, 2009). Growing evidence claims the PFC – basal ganglia circuitry to play a critical role in facilitating learning shifts (Block et al., 2007).The dissociation in error patterns following medial striatal and prefrontal cortex inactivation suggests that these interconnected areas play complimentary roles as part of a larger neural system to enable the shifting of strategies under changing environmental demands (Ragozzino and Choi, 2004).

2. Objective of this study

Previous data strongly suggest a role of the CRH system/HPA axis in the onset and progression of AD. The objective of this study was to directly elucidate the impact of CRH, the CRH-R1 and glucocorticoids (GCs) in this context.

To this end, a transgenic AD mouse model, the arcAß mouse line (Knobloch et al., 2007a), was chosen. The first aim of this study was to investigate the regulation of the CRH system and the HPA axis in arcAß mice at different ages.

The second aim was to introduce specific alterations of the CRH system into the arcAß mouse line by generating double-transgenic mouse lines:
I) a loss-of-function approach by abolishing CRH-R1 signaling and
II) a gain-of-function approach by overexpressing CRH.
Therefore, arcAß mice were bred to I) conventional CRH-R1 knockout (KO) mice (Timpl et al., 1998) to obtain arcAß CRH-R1KO mice and (II) conditional CRH overexpressing (CRH-COE) mice with a CNS-restricted CRH overexpression (CRH-COE^{CNS}) (Lu et al., 2008) to generate arcAß CRH-COE^{CNS} mice.
The final goal of this thesis was to analyze the onset and course of AD symptoms and pathology in the gain- and loss-of-function mouse models described above. Therefore, mice of different genotypes of arcAß CRH-R1KO and arcAß CRH-COE^{CNS} were subjected to comprehensive phenotyping involving emotional behavior, cognition and learning abilities, electrophysiology, biochemical analyses of Aß levels and APP processing and neuropathological analyses of Aß plaque formation as well as neuroinflammation at different ages.

3. Material and Methods

3.1. Material

3.1.1. Buffers and solutions

All chemicals and solutions were purchased from Sigma-Aldrich, Munich, Germany or Carl Roth, Karlsruhe, Germany, if not mentioned otherwise.

3.1.1.1. Buffers for agarose gel electrophoresis

1 x Tris acetate EDTA (TAE) buffer

4.84g Tris(hydroxylmethyl)-aminomethane (TRIS)
1.142 ml Acetic acid
20 ml 0.05 M Ethylendiaminetetraacetate (EDTA), pH 8.0
800 ml H_2O_{bidest}
adjust pH to 8.3 with acetic acid
ad 1 l H_2O_{bidest}

6 x DNA loading buffer (orange)

1g Orange G
10 ml 2 M TRIS/HCL, pH 7.5
150 ml Glycerol
ad 1 l H_2O_{bidest}

3.1.1.2. Solutions for *in situ* hybridization (ISH)

H_2O-DEPC

1 ml Diethylpyrocarbonate (DEPC) (Sigma-Aldrich)
ad 1 l H_2O_{bidest}
2 x autoclave

10 x Phosphate buffered saline (PBS)

1.37 M NaCl
27 mM KCl
200 mM Na_2HPO_4 x 12 H_2O (Merck, Darmstadt, Germany)
20 mM KH_2PO_4 (Merck)
pH 7.4

add 1 ml DEPC/l, ad H_2O_{bidest}
incubate over night (o.n.), 2 x autoclave

20 % Paraformaldehyde (PFA)

20% w/v	Paraformaldehyde

in 1 x PBS-DEPC
pH 7.4

10 x Triethanolamine (TEA)

1.0 M	TEA

pH 8.0
add 1 ml DEPC/l, ad H_2O_{bidest}
incubate o.n., 2 x autoclave

20 x Standard saline citrate (SSC)

3 M	NaCl
300 mM	Sodium citrate

pH 7.4
add 1 ml DEPC/l, ad H_2O_{bidest}
incubate o.n., 2 x autoclave

Hybridization mix (hybmix)

50 ml	Formamide
1 ml	2 M TRIS/HCl, pH 8.0
1.775 g	NaCl
1 ml	0.5 M EDTA, pH 8.0
10 g	Dextran sulphate
0.02 g	Ficoll 400
0.02 g	Polyvinylpyrrolidone 40 (PVP40)
0.02 g	Bovine serum albumin (BSA)
5 ml	tRNA (10 mg/ml, Roche Diagnostics GmbH, Mannheim, Germany)
1 ml	carrier DNA (salmon sperm, 10 mg/ml, Sigma-Aldrich)
4 ml	5 M dithiothreitol (DTT, Roche)

store as 1 to 5 ml aliquots at -80°C

Hybridization chamber fluid

250 ml Formamide

50 ml 20 x SSC

200 ml H_2O_{bidest}

5 M DTT/DEPC

7.715 g DTT

4 ml H_2O-DEPC

shake falcon tube until the powder is nearly solved

ad 10 l H_2O-DEPC

5 x NTE

146.1 g NaCl

50 ml 1 M TRIS/HCl, pH 8.0

50 ml 0.5 M EDTA, pH 8.0

add 1 ml DEPC/l, ad 1 l H_2O_{bidest}

incubate o.n., autoclave

3 M NH_4OAc

3.0 M Ammonium acetate (NH_4OAc)

ad H_2O_{bidest}

Alcohol (dehydration)-solutions

alcohol conc.	**vol. of EtOH 100 % (ml)**	**vol. of 3 M NH4OAc (ml)**	**vol. of $H2O_{bidest}$ (ml)**
30 % EtOH/ NH_4OAc	150	50	300
50 % EtOH/ NH_4OAc	250	50	200
70 % EtOH/ NH_4OAc	350	50	100
96 % EtOH	480 + 20 ml H_2O_{dest}		
100 % EtOH	500		

Cresyl violet staining solution

2.5 g Cresyl violet (Merck)

0.102 g Na-acetate

1.55 ml Acetic acid

ad 500 ml H_2O_{bidest}

pH 3.5

filtrate

3.1.1.3. Solutions for generation of lysates (ELISA and Western blotting)

Diethylamine (DEA) buffer

0.2%	Diethylamine
50 mM	NaCl

ad H_2O_{bidest}

pH 10

Neutralisation buffer

0.5 M	TRIS/HCl

ad H_2O_{bidest}

pH 6.8

STEN buffer

150 mM	NaCl
100 mM	TRIS/HCl
1 mM	EDTA
1.2 %	NP-40

Guanidine-HCl buffer 5 M pH 8

5.0 M	Guanidinium/HCl
50 mM	TRIS/HCl

ad H_2O_{bidest}

pH 8

Citrate buffer

15-20 mM	Na-citrate
1 mM	EDTA

ad H_2O_{bidest}

pH 6.4

3.1.1.4. Solutions for Western blotting (WB)

10 x TBS

200 mM TRIS/HCl

1.35 M NaCl

ad H_2O_{bidest}

pH 7.6

TBS/T

100 ml 10 x TBS

1 ml Tween20 (BioRad)

ad 1 l H_2O_{bidest}

Blocking solution and solution for antibodies

0.2 % I-Block (Applied Biosystems)

0.1 % Tween-20

ad 1 x PBS

pH 7.4

Lämmli 4x

40 % Glycerol (v/v)

0.25 M TRIS/HCl

8 % SDS

0.008 % Bromphenoleblue

ad H_2O_{bidest}

add 7.5 % ß-mercapto-EtOH prior to use.

Running buffer (acrylamide gels)

25 mM TRIS/HCl

190 mM Glycine

0.1 % Sodium dodecyl sulfate (SDS)

ad H_2O_{bidest}

Running buffer (Tricine gradient gels)

0.1 M TRIS/HCl

0.1 M Tricine

0.1 % SDS

ad H_2O_{bidest}

Transfer buffer

25 mM	TRIS/HCl
190 mM	Glycine (Sigma-Aldrich)
ad 800ml	H_2O_{bidest}
200 ml	MeOH

3.1.1.5. Solutions for immunohistochemistry (IHC)

Blocking solution

5 %	BSA
0.1 %	Triton

Solution for antibodies

5 %	BSA
0.01 %	Triton

3.1.1.6. Solutions for electrophysiology

Ringer solution

124 mM	NaCl
3 mM	KCl
26 mM	$NaHCO_3$
2 mM	$CaCl_2$
1 mM	$MgSO_4$
10 mM	D-glucose
1.25 mM	NaH_2PO_4

bubbled with a 95 % O_2/5 % CO_2 mixture

pH 7.3.

3.1.2. Oligonucleotides for genotyping

name of primer	**primer sequence (5´→ 3´)**	**amplicon [bp]**	**detection of:**
Prp-sense hAPPdn	CAGAACTGAACCATTTCAACCGAGC TCAGTGGGTACCTCCAGCGCCCGAG	180	huAPP mt

Ctsq-up Ctsq-dn	ACAAGGTCTGTGAATCATGC TTACAATGTGGATTTTGTGGG	1098	Cathepsin Q, DNA control
Cre-fwd Cre-rev	GATCGCTGCCAGGATATACG AATCGCCATCTTCCAGCAG	574	Cre-recombinase
R1GT1 R1GT2 R1GT3B	TCACCTAAGTCCAGCTGAGGA GTGCTGTCCATCTGACGAGA GGGGCCCTGGTAGATGTAGT	697 (wt): R1-GT1/ R1GT3B 496 (mt): R1-GT1/ R1GT2	CRH-R1
ROSA1 ROSA5 ROSA6 ROSA7	AAAGTCGCTCTGAGTTGTTAT TAGAGCTGGTTCGTGGTGTG GCTGCATAAAACCCCAGATG GGGGAACTTCCTGACTAGGG	398 (wt): ROSA1+ROSA6 646 (mt): ROSA1+ROSA7 505 (del): ROSA1+ROSA5	ROSA26 locus of CRH-COE^{CNS} mice

3.1.3. Oligonucleotides for qRT-PCR

name of primer	**primer sequence (5´→ 3´)**	**amplicon [bp]**	**melting temperature [°C]**
GAPDH	CCATCACCATCTTCCAGGAGCGAG GATGGCATGGACTGTGGTCATGAG	326	67
CRH-R1	GGTGTGCCTTTCCCCATCATT CAACATGTAGGTGATGCCCAG	278	57

3.1.4. mRNA probes for ISH

name	**antisense**	**sense**	**vector**	**GenBank acc. no.**	**insert size [bp]**	**complem. region [bp]**
CRH-R1	T7	T3	pBluescript II SK	NM_007762	702	1728-2428
CRH	T7	Sp6	pCRII-TOPO	AY128673	263	2114-2370
hAPP 695	Sp6	T7	pCRII-TOPO	NM_201414	711	3973-4684

3.1.5. Antibodies and stainings

specificity	denotation	company	appli-cation	concentration
Human amyloid ß	A2275-75B	Biomol, Hamburg, Germany, (A2275-75B)	IHC	1:500
Poly-N-acetyl lactosamine (resting microglia)	Tomato lectin (*Lycopersicon esculentum*), FITC conjugated	Sigma-Aldrich, Munich, Germany, (L401)	IHC	1:500
Ionized calcium-binding adaptor molecule 1 (resting and activated microglia)	Iba-1	Wako Chemicals, Neuss, Germany, (019-19741)	IHC	1:1000
Glial fibrillary acidic protein (astrocytes)	GFAP	DakoCytomation, Glostrup, Denmark, (Z 0334)	IHC	1:1000
1-16 of amyloid ß, αAPPs	6E10	Signet, Sacramento, California, (SIG-39320)	IHC WB	IHC: 1:500 WB: 1:1000
1-16 of amyloid ß, αAPPs	2D8	provided by E. Kremer (Shirotani et al., 2007)	WB	WB: 1:1000
total APP	22C11	Chemicon, Temecula, California, (MAB348)	WB	1:1000
αAPPs	Aß rodent	Signet, Sacramento, California	WB	1:1000
ßAPPs	192wt	Elan Pharmaceuticals, Dublin, Ireland	WB	1 µg/ml
Human APP	5315	Steiner et al., NCB2(2000)848	WB	1:1000
α-secretase (ADAM10)	Anti-ADAM10 (735-749)	Calbiochem, Darmstadt, Germany	WB	1:1000
ß-secretase (BACE1)	BACE1	ProSci, Poway, California	WB	1:1000
ß-secretase (BACE1)	3D5	provided by Robert Vassar	WB	1:1000

Immunohistochemistry (IHC), Western blotting (WB)

3.1.6. Cell lines

AtT-20

Cell type mouse pituitary tumor

Origin cloned in 1966 by G. Sato; the mouse pituitary tumor was originally established in LAF1 mice (Furth et al., 1955)

Reference (Buonassisi et al., 1962)

HT22

Cell type mouse hippocampus

Origin subclone of HT4 (Morimoto and Koshland, Jr., 1990), selected for its sensitivity to glutamate toxicity

Reference (Li et al., 1997)

HT22C2 and HT22C3 are HT22 cells which are stably transfected with CRH-R1.

3.1.7. Media and solutions for cell culture

3.1.7.1. Media

Growth medium

500 ml	Dulbecco´s modified eagle medium phenolred free (DMEM, Invitrogen)
50 ml	Fetal calf serum (FCS, Invitrogen)
10 ml	Penicillin/streptocmycin (5000 U/ml, Invitrogen)

Freezing medium

90 %	FCS
10 %	Dimethylsulfoxide (DMSO, Sigma-Aldrich)

3.1.7.2. Solutions for cell culture

CRH (H-2435, Bachem, Bubendorf, Switzerland): 200 µM in sterile 0.01 M acetic acid

Amyloid ß (H-1192, Bachem, Bubendorf, Switzerland) 2 mg/µl (=1.886 µM) in sterile H_2O

MTT (Thiazolyl Blue Tetrazolium Bromide, Sigma-Aldrich): 5 mg/ml in sterile H_2O

All stored aliquoted at -20°C.

3.1.8. Animals

arcAß mice

As an Alzheimer´s disease mouse model we used arcAß transgenic mice which express human APP 695 carrying both the Swedish (K670N; M671L) (Swe) and the Arctic (E693G) (Arc) mutation in a single construct under the control of the prion protein promoter (Knobloch et al., 2007a) (Figure 7).

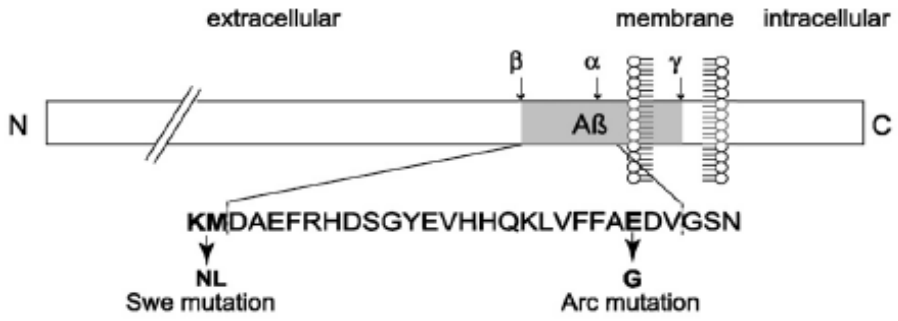

Figure 7. APP transgene in arcAß mice. The human APP 695 transgene in arcAß mice contains the Swedish (Swe) and Arctic (Arc) mutation within the Aß sequence (Knobloch et al., 2007a).

Due to the known expression pattern of the PrP-promotor, the construct is not only expressed in brain, but also in extraneuronal tissues including heart, lung and muscle. Nevertheless, Aß was detected only in brain and sciatic nerve, implying that the generation or accumulation of Aß occurs preferentially in neuronal tissues (Knobloch et al., 2007a).
Intracellular deposits predate extracellular Aß deposition in this mouse model.
The Arc mutation alters aggregation properties of Aß by accelerating the formation of protofibrils (Nilsberth et al., 2001). The Swe mutation increases the activity of BACE (ß-secretase) (Knobloch et al., 2007a).

CRH-R1KO mice

The role of CRH-R1 was dissected by using conventional CRH-R1 knockout (KO) mice (Timpl et al., 1998). In these mice a 3.1-kb fragment of *Crhr1* encoding the transmembrane regions 5, 6 and 7, including the G-protein coupling domain and the intracellular cytoplasmatic tail, were deleted. Translation of the remaining first exons would lead to a truncated version of the protein, incapable of any function.

CRH-COE^{CNS} mice

In order to study the role of the CRH system, CRH-overexpressing (CRH-COE) mice with a CNS-restricted CRH overexpression (CRH-COE^{CNS}) (Lu et al., 2008) were used.

CRH-COE^{CNS} mice carry a CRH-expression unit within the ROSA26 locus, which can be activated via cre recombinase. CRH expression in the entire CNS was attained by breeding to Nes-cre mice (Tronche et al., 1999).

3.2. Methods

3.2.1. Preparation and analysis of nucleic acids

3.2.1.1. DNA preparation from mouse tail tissue

For genotyping PCRs of transgenic mice, tail tissue was digested in 100 µl 50 mM NaOH for 30 min at 99°C followed by a neutralization step using 30 µl 1M Tris-HCl (pH 7.0) and stored at 4°C.1-2 µl of the tail lysates were used as PCR template.

3.2.1.2. Agarose gel electrophoresis

For DNA agarose gel electrophoresis agarose (Invitrogen) was boiled in 1 x TAE buffer with the agarose concentration depending on the size of DNA fragment to be seperated. For fragments between 100 and 1000 bp 2% agarose gels were chosen. For bigger fragments 0.8-1% agarose gels were applied. 0.1 µg/ml ethidiumbromide (Carl Roth) was added to boiled and liquid agarose in 1 x TAE which was poured into a gel electrophoresis chamber (PeqLab). DNA or RNA samples mixed with 1/6 of 6 x DNA loading buffer were loaded. As size marker the smart ladder (Eurogentec, Brussels, Belgium) was used. Electrophoresis was carried out with 80-140 V for 1-2 h. The DNA fragments were detected with UV light and documented using a gel documentation system (Biometra, Göttingen, Germany).

3.2.2. Polymerase chain reaction (PCR)

3.2.2.1. Standard PCR

To amplify DNA for genotyping of transgenic mice, polymerase chain reactions were performed using the Thermoprime Plus DNA polymerase (ABgene, Hamburg, Germany) as follows:

1-2 µl	genomic DNA/ tail lysate
5 µl	10 x reaction buffer IV (ABgene)
3 µl	25 mM $MgCl_2$ (ABgene)
1 µl	dNTPs (dATP, dTTP, dCTP and dGTP, 10 mM each, Roche Applied Science)
3 µl	10 µM primer fwd
3 µl	10 µM primer rev
0.5 µl	Thermoprime Plus DNA polymerase (5 U/µl, ABgene)
ad 50µl	H_2O_{bidest}

PCR was carried out in a PCR machine (GeneAmp PCR System 9700, Applied Biosystems) with the following temperature settings:

programme	**cycles**	**temperature**	**hold**
preincubation	1	94°C	5 min
amplification: denaturation annealing elongation	33	 94°C x°C 72°C	 30 sec 30 sec y sec
	1	72°C 8°C	5 min ∞

Annealing temperature (x) and elongation time (y) were adjusted according to the melting temperature of the primers and the amplicon size.

3.2.2.2. Reverse transcription (RT) PCR

First strand cDNA synthesis from RNA was performed using the SuperScript II Reverse Transcriptase Kit (Invitrogen, Karlsruhe, Germany) according to the provided protocol. 500-1000 ng of total RNA was incubated together with 0.5 µg/µl oligo d(T) primers (Invitrogen) in a total volume of 11 µl (H_2O) at 65°C for 5 min and subsequently chilled on ice. Per sample 8 µl of RT-mastermix were added and tubes were incubated at 40°C for 2 min.

RT-mastermix

4 µl	5 x buffer (Invitrogen)
2 µl	0.1 M DTT (Invitrogen)
1 µl	10 mM dNTPs
1µl	RNase inhibitor (40 U/µl; Roche)

Afterwards, samples were incubated with 1 µl SuperScript II at 42°C for 1 h followed by 70°C for 15 min to inactivate the enzyme. 1 µl RNase H (Invitrogen) was added to digest the RNA template at 37°C for 20 min. RNase H activity was stopped by incubation at 70°C for 15 min and cDNA was stored at -20°C.

3.2.2.3. Quantitative real-time PCR (qRT-PCR)

Real-time PCR was carried out with the QuantiFast SYBR Green PCR Kit (Qiagen, Hilden, Germany) according to the manufacturer`s protocol in the Lightcycler 2.0 System (Roche). Mastermix was prepared as follows:

5.0 µl QuantiFast SYBR Green PCR Mix (Qiagen, Hilden, Germany)
1.0 µl primer forward (10 µM)
1.0 µl primer reverse (10 µM)
1.0 µl H_2O_{bidest}

8 µl mastermix were pipetted in each capillary which was fixed in the LightCycler carousel, 2 µl DNA (1/10 diluted) were added and capillaries were closed immediately. Following programme was applied:

programme	**cycles**	**target [°C]**	**hold [sec]**	**slope [°C/s]**	**sec target**	**step size**	**step delay**	**acquisition mode**
Preincubation	1	95	5 min	20	0	0	0	none
Amplification	40							
Denaturation		95	10	20	0	0	0	none
Annealing		60	30					none
Elongation		72	y	20	0	0	0	single
Melting Curve	1	95	0	20	0	0	0	none
		50	10	20	0	0	0	none
		95	0	0.1	0	0	0	continuous
Cooling	1	42	30	20	0	0	0	none

Relative gene expression was determined by the $2^{-\Delta\Delta CT}$ method (Livak and Schmittgen, 2001), using the real PCR efficiency calculated from an external standard curve, normalized to the housekeeping genes Hprt and Gapdh and related to the data of control experiments.

3.2.3. Plasma corticosterone analysis

Two weeks before the experiment mice were left undisturbed with a 12:12 h light:dark schedule (lights on at 7:00 a.m.). Blood sampling was performed in the morning (7:30-9:30 a.m.) under light isoflurane anesthesia. For evaluation of the endocrine response to stress, blood samples were collected immediately after 10-min restraint stress, for which the animals were placed in a 50-ml conical tube with bottom removed. 100-300 µl blood was taken retrobulbar, collected in ice-cold EDTA-coated tubes and centrifuged (10000 g, 4°C). Plasma

(supernatant) was transferred in 96 well plates and stored at -80°C until measurment of corticosterone concentrations in duplicate by ^{125}I-Radioimmunoassay (RIA-Kit, ICN Biomedicals, Frankfurt/Main, Germany).

3.2.4. Tissue preparation

Mice were anaesthetized with isoflurane (Forene, Abbott, Wiesbaden, Germany), sacrificed by decapitation and brains were carefully removed. For *in situ* hybridization brains were immediately shock-frozen on dry ice and stored at -80°C until cutting with a cryostat, for immunohistochemistry brains were either frozen or post-fixed in 4% PFA for 48 h, transferred into 25% Sucrose in PBS and stored at 4°C until processing. In terms of analyses of Aß levels by ELISA, cortex and hippocampus were dissected from one hemisphere, shock-frozen on dry ice and stored at -80°C until lysis.

3.2.5. *In situ* hybridization (ISH)

For quantitative *in situ* hybridization 20-µm sections of arcAß brains and wt littermates were cut using a cryostat and mounted side by side on SuperFrost Plus slides (Menzel GmbH, Braunschweig, Germany) allowing parallel comparison of hybridisation signals within one slide. *In situ* hybridization using ^{35}S-labeld cRNA probes was performed according to a modified version of a previously described procedure (Dagerlind et al., 1992). Briefly, specific riboprobes were generated by PCR applying T7 and T3 or SP6 primers using plasmids containing respective cDNAs as templates. Radiolabeled antisense cRNA probes were generated from the PCR products by *in vitro* transcription with ^{35}S-UTP using T7 and T3 or SP6 RNA polymerase. Hybridization was performed o.n. with a probe concentration of 3.5 to 7 million counts per slide. Quantification of mRNA signals was conducted by ImageJ (http://rsb.info.nih.gov/ij/).

3.2.5.1. Radioactive labeling of probes

Probes were amplified using the following PCR reaction:

2 µl	plasmid DNA template (20-100 ng)
3 µl	25 mM $MgCl_2$ solution (ABgene)
5 µl	10 x reaction buffer IV (ABgene)
1 µl	10 mM dNTPs (Roche)
0.5 µl	Thermoprime plus DNA polymerase (5 U/µl, ABgene)
3 µl	10 µM Primer forward
3 µl	10 µM Primer reverse
add 50 µl	H_2O_{bidest}

PCR programme:

programme	**cycles**	**temperature**	**hold**
preincubation	1	94°C	2 min
amplification: denaturation annealing elongation	35	 94°C 67°C 72°C	 30 sec 30 sec 40 sec
	1	72°C 8°C	5 min ∞

To prevent RNA degradation all precautions were taken to avoid RNase activity.

The *in vitro* transcription was pipetted as follows (mastermix for approximately 10 slides):

1.5 µl PCR product (200 ng)
13.5 µl H_2O-DEPC
3 µl 10 x transcription buffer (Roche)
3 µl NTP-mix (rATP/rCTP/rGTP 10mM, Roche)
1 µl 0.5 M DTT
1 µl RNasin (RNAse-inhibitor, 40 U/µl, Roche)
6 µl ^{35}S-thio-rUTP (12.5 mCi/mM, 1250 Ci/mmol, Amersham)
1 µl T7 or sp6 RNA polymerase (20 U/µl, Roche)

The reaction samples were gently mixed. Afterwards, samples were incubated at 37°C for 3 hours in total; after 1 h another 0.5 µl of RNA polymerase was added.
To destroy the DNA template, 2 µl RNase-free DNase I (10 U/µl, Roche) were added and samples were incubated for 15 min at 37°C.

3.2.5.2. Purification of riboprobes

For purification of riboprobes the RNeasy Mini Kit (Qiagen) was used according to the manufacturer´s protocol. RNA was diluted in 100 µl RNase-free water and 1 µl of the probe was measured in 2 ml scintillation fluid (Zinsser Analytic, Frankfurt, Germany) in a beta-counter (LS 6000 IC, Beckmann Coulter). For *in situ* hybridization 35000 to 70000 cmp/µl and 90 µl/slide (7 million/slide) were required.

3.2.5.3. Pre-treatment of cryo-slides

Slides were taken out of the -20°C freezer and warmed up and dried for at least 1 h at room temperature (RT). For pre-treatment the following protocol was applied:

action	**duration**	**chemical**	**comments**
1. fix	10 min	4 % PFA/PBS	ice-cold (4°C)
2. rinse	3 x 5 min	PBS/DEPC	
3.	10 min	0.1 M triethanolamine-HCl (TEA) (pH 8.0) 200 ml	add 600 µl acetic anhydride (Sigma-Aldrich) to rapidly rotating stirring bar of TEA
4. rinse	2 x 5 min	2 x SSC/DEPC	
5. dehydrate	1 min	60 % EtOH/DEPC	
6.	1 min	75 % EtOH/DEPC	
7.	1 min	95 % EtOH/DEPC	
8.	1 min	100 % EtOH	
9.	1 min	$CHCl_3$	
10.	1 min	100 % EtOH	
11.	1 min	95 % EtOH/DEPC	
12. air dry (dust free)			

3.2.5.4. Hybridization

An appropriate amount of hybridization mix (hybmix) containing the riboprobe of interest was prepared. 90 to 100 µl hybmix and 3.5 to 7 million counts per slide were required.

The hybridization mix containing the probe was heated to 90°C for 2 min and snap cooled on ice. The solution was pipetted onto the slides and coverslips were carefully mounted, avoiding air bubbles in between. The slides were carefully placed into a hybridization chamber containing hybridization chamber fluid to prevent drying out of the hybmix and the chamber was sealed with adhesive tape. The slides were incubated in an oven (Memmert, Schwabach, Germany) at 55-68°C o.n. (up to 20 h).

3.2.5.5. Washing

After hybridization the coverslips were carefully removed and the following protocol was applied:

action	duration	temperature	chemical	comments
1.	4 x 5 min	RT	4 x SSC	
2.	20 min	37°C	NTE (20 µg/ml RNaseA)	add 500 µl RNaseA (10 mg/ml, Sigma-Aldrich) to 250 ml of NTE
3.	2 x 5 min	RT	2 x SSC/1 mM DTT	50 µl of 5 M DTT/250 ml
4.	10 min	RT	1 x SSC/1 mM DTT	50 µl of 5 M DTT/250 ml
5.	10 min	RT	0.5 x SSC/1 mM DTT	50 µl of 5 M DTT/250 ml
6.	2 x 30 min	64°C	0.1 x SSC/1 mM DTT	50 µl of 5 M DTT/250 ml
7.	2 x 10 min	RT	0.1 x SSC	
8.	1 min	RT	30 % EtOH in 300 mM NH_4OAc	
9.	1 min	RT	50 % EtOH in 300 mM NH_4OAc	
10.	1 min	RT	70 % EtOH in 300 mM NH_4OAc	
11.	1 min	RT	95 % EtOH	
12.	2 x 1 min	RT	100 % EtOH	
13. air dry (dust free)				

3.2.5.6. Autoradiography

Dried *in situ* sections were exposed to a special high performance X-ray (BioMax MR from Kodak) for one to seven days.

3.2.5.7. Quantification of relative expression

Expression of mRNAs in different brain areas was quantified by measuring the OD on scanned ISH films using ImageJ.

3.2.6. Extraction and quantification of secreted Aß and APP processing forms

3.2.6.1. Enzyme Linked Immuno-Sorbent Assay (ELISA)

For determination of $Aß_{40}$ and $Aß_{42}$ levels hippocampus and cortex were homogenized in 1 ml Diethylamine (DEA) buffer. After initial centrifugation at 5000 rpm (5 min, 4°C) the resulting DEA fraction was ultra-centrifuged (TLA55 Rotor, Beckman Optima Max-E Ultracentifuge) at 55000 rpm (30 min, 4°C) and stored at -80°C (soluble fraction) for analysis of secreted Aß and APPs after neutralisation with 10 % neutralisation buffer. Pellets from the initial centrifugation step were homogenized in STEN buffer and centrifuged at 5000 rpm (5 min, 4°C). The postnuclear fraction was subjected to ultracentrifugation 55000 rpm (30 min, 4°C). The insoluble material in the pellet was dispersed by shaking in 500 µl guanidine-HCl buffer 5 M pH 8.0 (1.5 h, 4°C), followed by ultra-centrifuging at 55000 rpm (30 min, 4°C). For determination of the guanidinium-HCl soluble Aß (insoluble fraction) the supernatant was collected thereafter and stored at -80°C. All buffers were substituted with 1 x protease-inhibitor cocktail (Sigma-Aldrich, P2714) and 200 µM phenanthroline (Sigma-Aldrich). Aß soluble and insoluble fractions were quantified by sandwich immunoassay using the Meso Scale Discovery Triplex Assay according to Page et al. (Page et al., 2008). The corresponding concentrations of Aß peptides were calculated using the Meso Scale Discovery Discovery Workbench software. Ratios of each Aß species as a percentage of total Aß ($Aß_{38}$, $Aß_{40}$, and $Aß_{42}$) were calculated, and graphs were plotted using the GraphPad Prism software.

3.2.6.2. SDS polyacrylamide gel electrohoresis and Western blotting

To analyze products and enzymes of the APP processing, such as APP, total APPs, αAPPs, βAPPs and Aß, BACE and ADAM, different lysis fractions of brain tissue were prepared.

Diethylamine (DEA): Determination of sAPP

One hemisphere or combined tissue of hippocampus and cortex were homogenized in 1 ml DEA buffer. After initial centrifugation at 5000 rpm (5 min, 4°C) the resulting DEA fraction was ultra-centrifuged (TLA55 Rotor, Beckman Optima Max-E Ultracentifuge) at 55000 rpm (30 min, 4°C) and stored at -80°C (soluble fraction) for analysis of secreted Aß and APPs after neutralisation with 10 % neutralisation buffer. Buffer was substituted with 1 x protease-inhibitor cocktail (Sigma-Aldrich, P2714) and 200 µM phenanthroline (Sigma-Aldrich).

2 % SDS: Determination of APP, β-stubs, Aβ

Pellets from the initial centrifugation step (DEA) were resuspended in 1 ml 2 % SDS buffer (pipetting, shaking RT 10 min) and centrifuged at 5000 rpm (10 min, 4°C). The postnuclear fraction was subjected to ultracentrifugation 55000 rpm (30 min, 4°C). Supernatant constitutes the SDS-fraction. Buffer was substituted with 1 x protease-inhibitor cocktail (Sigma-Aldrich, P2714) and 200 µM phenanthroline (Sigma-Aldrich).

70 % Formic acid (FA): Determination of Aβ

The insoluble material in the pellets after 2 % SDS treatment was dispersed by shaking in 1 ml 70 % FA for 10 min at RT, followed by ultra-centrifuging at 55000 rpm (30 min, 4°C). For determination of the FA soluble Aß (insoluble fraction) supernatant was transferred in 20-fold volume of 1 M Tris pH 9.5 and stored at -80°C.

Membrane preparation: Determination of β-stubs, γ-secretase, endogenous APP, BACE

The resulting pellet of the DEA fraction was subjected to resuspension in 1 ml Citrate buffer, which due to its hypoton properties leads to an explosion of cells and exposition of membrane proteins. Therefore, open tubes were shock-frozen in liquid N_2 or on dry ice for less than 1 min and thawed on ice thereafter. After centrifugion at 5000 rpm (10 min, 4°C), the soluble fraction was collected, enriched with 40 % Glycerol (Sigma-Aldrich) and subjected to ultracentrifugation 55000 rpm (60 min, 4°C). The pellet was homogenized with 190 µl Citrate buffer, followed by 10 µl 20 % Triton, mixed immediately by pipetting, incubated 10 min on ice and ultracentrifugated at 55000 rpm (30 min, 4°C). Supernatant was collected and stored at -80°C for analyses of membrane proteins.

Protein concentration was determined based on reaction of bicinchoninic acid (BCA) with Cu^{2+} (Smith et al., 1985) by a commercially available kit (Pierce BCA Protein Assay Kit, Thermo Scientific, Rockford, USA). Before loading of 10-20 µg protein into the gel, ¼ volume Lämmli 4x was added and the sample was boiled (95°C, 5 min). To examine levels of APP in brain lysates and of the soluble shed ectodomain αAPPs, βAPPs and total APPs DEA fractions were electrophoresed on 8 % acrylamide gels using running buffer (100-130 V, 2.5 h) and transferred to Immobilon polyvinylidene difluoride (PVDF) membranes (Millipore, Bedford, MA) by the use of transfer buffer (18 V, 4°C, o.n.). Here, PageRuler Prestained Protein Ladder (Fermentas) was used for predication of molecular weight. For determination of Aß, fractions were electrophoresed on gradient gels (Novex 10-20 % Tricine Gels, Invitrogen), followed by transfer to nitrocellulose membranes (Pore size: 0.45 µm, Whatman Protran, Kent, UK). As a ladder for gradient gels See Blue Plus 2 (Invitrogen) was used. To

enhance Aß signal, nitrocellulose membranes were boiled in PBS for 5 min after blotting. Western blotting was initiated with blocking for 1 h in blocking solution to minimize unspecific protein binding. Thereafter, primary antibodies diluted in the blocking solution were incubated o.n. at 4°C. After washing in 1 x TBS, membranes were incubated with respective HRP-conjugated secondary antibodies (Promega) for 2 h at room temperature, followed by development with chemiluminescence (ECL, Amersham Biosciences) and exposure to X-ray films (Fuji).

3.2.7. Immunohistochemistry (IHC)

Immunohistochemistry (IHC) was applied to visualize Aß plaques, microglia and astrocytes. Therefore slices were generated from frozen brains by cutting with a cryostat or from brains post-fixed in 4 % PFA followed by 25 % Sucrose which were cut by a vibratome. Briefly, after fixation with 4 % PFA for 10 min, followed by blocking of non-specific binding with 5 % BSA for 1 h at RT, the primary antibody was incubated o.n. at 4°C. Aß plaque staining included an additional incubation step in 70 % FA for 15 min at RT after the fixation step. For immunostaining of microglia and astrocytes antibodies Iba-1 (1:1000; Wako Chemicals) and GFAP (1:000; DakoCytomation) were used. Co-staining of Aß plaques was conducted with either 6E10 (1:500; Signet) or A2275-75B (1:500; Biomol). After washing off of unbound first antibody with PBS, slices were incubated for 1 h with respective fluorescently labelled secondary antibodies. In case of microglia staining with tomato lectin (1:250; FITC-conjugated, Sigma-Aldrich), the incubation step with a secondary antibody was omitted. After final PBS washing slices were mounted with DAPI (Vector Labs, Burlington, Canada).

3.2.8. Aß plaque quantification

Plaque burden was assessed using a polyclonal antibody against N-terminal human Aß (A2275-75B, Biomol, Hamburg, Germany). For prefrontal cortex (PFC) 3-4 coronal sections per animal were chosen from bregma +2.22 to +1.78 mm, for hippocampus 3 sections from bregma -1.70 to -2.06 mm according to stereotaxic atlas (Paxinos and Franklin, 2001). All sections were cut from frozen brains by cryostat. Briefly, after fixation with 4 % PFA for 10 min, followed by 70 % FA for 15 min and blocking of non-specific binding with 5 % BSA for 1 h at RT, the primary antibody was incubated o.n. at 4°C. The secondary antibody (Alexa anti-rabbit 594) was incubated for 1 h at RT. Slices which needed to be compared among each other, were processed likewise.

Images were acquired with a Zeiss microscope (Axioplan 2) with a Zeiss camera system (AxioCam MRc5). To enhance contrast, photomicrographs were equally processed using

Adobe Photoshop CS2 (Adobe Systems). Thereafter, analysis of plaque number, plaque size and area occupied with plaques was conducted by ImageJ.

3.2.9. Electrophysiology

Animals were deeply anesthetized with isoflurane and decapitated. The brain was rapidly removed, and slices were prepared in ice-cold Ringer solution using a vibroslicer (HM 650 V, Microm International, Walldorf, Germany). All slices were placed in a holding chamber for at least 60 min at 34°C and were then transferred to a superfusing chamber for extracellular recordings. The flow rate of the Ringer solution, bubbled with a 95 % O_2 – 5 % CO_2 mixture, through the chamber was 1.5 ml/min. Field excitatory postsynaptic potentials (fEPSPs) were recorded extracellularly and evoked by test stimuli (0.066 Hz, 4–5 V, 20 ms) delivered via a bipolar tungsten electrode insulated to the tip (tip diameter 50 µm). All experiments were performed at room temperature.

3.2.9.1. Preparation of perirhinal cortex slices

For preparation of perirhinal cortex slices, a midsagittal section was made, and the rostral part of one hemisphere was cut at 45° to the dorsoventral axis (Cho et al., 2000). The cerebellum was removed from the brain with a further caudal cut along the dorsoventral axis. Slices (350 µm) of perirhinal cortex were taken in the region –2.5 mm to -4 mm rostral from bregma. fEPSP were recorded from layers II/III from directly below the rhinal sulcus (area 35). A stimulation electrode was placed in layer II/III on the temporal side (0.5 mm) of the recording electrode (area 36, Cho et al., 2000). Stimuli (1 ms duration) were delivered to the stimulation electrode at 0.1 Hz. Input/Output curves were produced with stimulation intensities from 1 V to 20 V, in steps of 0.5 V. For monitoring baseline synaptic transmission before LTP or LTD induction, fEPSPs were reduced to 50 – 60 % of the maximum amplitude and recorded for at least 30 minutes, or until responses were stable (less than 20 % amplitude change over 30 min). For LTP induction, 4 stimulus trains were delivered at 0.066 Hz. Each train comprised 10 bursts at 0.5 Hz, and each burst contained 4 stimuli (1 ms) at 100 Hz. For LTD induction, 900 stimulus pairs (1 ms each, 20 ms inter-stimulus interval) were delivered at 2 Hz. Subsequently, fEPSPs elicited by 0.066 Hz stimulation were recorded for further 60 min. Before completion of the experiment, 10 paired pulses were delivered at 0.5 Hz, 5 pairs with an interval of 20 ms and 5 pairs with an interval of 30 ms.

3.2.9.2. Preparation of hippocampal slices

Sagittal hippocampal slices (350 mM thick) were obtained and fEPSPs at synapses between Schaffer-collaterals and CA1 pyramidal cells were recorded extracellularly in the stratum

lucidum of the CA1 region. The stimulation electrode was placed in the Schaffer collateral-commissural pathway. For the induction of LTP in the CA1 region, high-frequency stimulation (HFS) of 1 x 100 Hz / 100 pulses, conditioning pulses were delivered. Basal synaptic transmission was investigated by the mean of an Input/Output relationship. The amplitudes of the fEPSPs were compared in response to a series of five fixed amplitude values of incoming action potentials, known as fibre volley (50, 100, 150, 200, 300, 400 µV). The fEPSP slope was plotted together for each corresponding value of the fibre volley. Paired-pulse stimulation (PPF) was tested at interstimulus intervals (ISI) from 20 ms to 300 ms.
The recordings were amplified, filtered (3 kHz), and digitized (9 kHz) using a laboratory interface board (ITC-16, Instrutech Corp., NY, USA) and stored to disk on a Power Macintosh G3 computer with the acquisition programme Pulse (version 8.5, Heka electronic GmbH, Lambrecht, Germany). Data were analyzed offline with the analysis programme IgorPro v. 6 (Wavemetrics, Lake Oswego, OR, USA) software. Measurements of the amplitude of the fEPSP were taken and were normalized with respect to the 30-min control period before tetanic stimulation.

3.2.10. Cell culture

3.2.10.1. Maintaining cells

To avoid bacteria, funghi or yeast contamination every cell culture work was done under sterile conditions in a sterile hood (Heraeus Instruments, Hanau, Germany). Cells were grown at 37°C with 5 % CO_2 in a sterile incubator (Heraeus). Every second day cells were split or medium was refreshed.

Unfreezing of cells

A frozen vial of cells was thawed quickly at 37°C in a waterbath (GFL, Burgwedel, Germany) suspended in 10 ml of prewarmed growth medium and centrifuged at 1200 rpm for 4 min (Universal 30F centrifuge, Hettich, Tuttlingen, Germany). The cell pellet was resuspended gently in 3 ml growth medium and cells were split on a 10 cm plate containing a total of 10 ml growth medium. Cells were incubated in the incubator up to a confluency of 70-90 %.

Splitting of cells

Medium was removed from the plates and cells were washed with 10 ml prewarmed PBS (Invitrogen). 1 ml Trypsin/EDTA (Invitrogen) was added and plates were incubated for about 5 min at 37°C until cells were detached. To stop the reaction 8 ml growth medium was added and cell suspension was centrifuged at 1200 rpm for 4 min. The cell pellet was resuspended

in 5-10 ml growth medium by pipetting up and down several times to break any cell aggregates. An appropriate amount of the cells (1/3 – 1/10) was plated immediately on new dishes containing growth medium. The dishes were swirled to ensure an equal distribution in the medium.

Freezing of cells

To obtain stocks of used cell lines freshly thawed cells were passaged and amplified at least twice and then refrozen. Therefore one 10 cm dish with about 80 % confluency was trypsinized and centrifuged. Cells were resuspended in 3 ml of freezing medium and aliquoted in 3 cryo vials (Nalgene, Roskilde, Denmark). The vials were cooled down slowly over night to -70°C using an isopropanol-filled freezing container (Nalgene). Afterwards cell vials were stored in liquid nitrogen.

Counting of cells

For determination of cell number a Neubauer chamber (Carl Roth) was used. One chamber of this hemocytometer consists of nine squares with the dimension of 1 x 1 mm and a total volume over each square of 10^{-4} ml. After trypsination cells were resuspended in growth medium and 10 µl of the suspension were pipetted in the chamber in order to count cells in the single squares. The mean value (m) of two counted squares was used to calculate the cell number: cells/ml = m x 10000.

3.2.10.2. Treatment of cells

18000-20000 cells in 200 µl growth medium supplemented with 2 % FCS were seeded per well on 48-well plates. Initially, different concentrations (10-500 nM) of CRH (stock solution in glacial acetic acid) were added. As a control treatment every well obtained the same amount of glacial acetic acid to rule out effects of the chemical. After 24 h, cells were treated with $Aß_{25-35}$ (10-40 µM). On day three cell survival was determined by a MTT assay (Thiazolyl Blue Tetrazolium Bromide, Sigma-Aldrich), a photometric assay to measure reduction ability of mitochondria. Yellow MTT is reduced to a purple formazan and absorbance at 560 nm can be used for quantification of cell survival in the colored solution. Briefly, 1/5 volume of MTT (5 mg/ml) was added to the well. After incubation of 4 hrs at 37°C, media was removed carefully to not suck formazan aggregates. 300 µl DMSO was added and the plate was shaken light protected at RT for 15 min. Afterwards, absorbance at 560 nm was determined in a plate reader (Tecan, Männedorf, Switzerland).

3.2.11. Animal housing and breeding

Mice were housed at three to five animals per cage and acclimated to standard laboratory conditions (light-dark cycle: 12:12 h, lights on at 7 a.m.; temperature: 21 ± 1°C; relative humidity: 50 ± 10 %) with food and water *ad libitum*. All animal breedings and experiments were conducted in accordance with the Guide for the Care and Use of Laboratory Animals of the Government of Bavaria.

In the breedings of arcAß CRH-R1KO mice, pregnant females received drinking water supplemented with corticosterone (20 µg/ml) during pregnancy until weaning. In this way, early mortality caused by CRH-R1KO as a result of pulmonary dysplasia could be prevented (Smith et al., 1998). For setting up the solution, 200 mg corticosterone (Sigma-Aldrich) was solved in 5 ml 100% EtOH (agitation, 50°C, 5 min) and filled up with tap water ad 1 l.

All newborn pups were genotyped according to the indicated protocol (3.2.2.1 Standard PCR; 3.1.2 Oligonucleotides for genotyping).

3.2.12. Behavioral testing

In all experiments male mice were used, singly housed two weeks prior to the experiment and acclimated to standard laboratory conditions (light-dark cycle: 12:12 h, lights on at 7 a.m.; temperature: 22 ± 1°C; relative humidity: 55 ± 5 %) with food and water *ad libitum*. All animal experiments were conducted in accordance with the Guide for the Care and Use of Laboratory Animals of the Government of Bavaria, Germany.
Following the habituation period and three days before starting of behavioral experiments, animals underwent a general health check, including fur and general physical conditions as well as bodyweight analysis to ensure that behavioral findings are not confounded by the health condition of mice. Behavioral testing started with the assessment of basal emotionality, followed by assessment of cognition. Test performances in the open field, elevated plus-maze, dark/light box and Y-maze-task were recorded and analyzed using the ANY-maze software (Stoelting Co., Wood Dale, IL). Test apparatuses were cleaned with water and EtOH 70 % before each trial.

3.2.12.1. Open field (OF)

The open field test (OF) was used to characterize locomotor activity in a novel environment. Testing was performed in circular OF arenas (diameter 58 cm, light grey) evenly unaversive illuminated at low light conditions (10-15 lux) in order to minimize anxiety effects on locomotion. At the beginning of each test, the mouse was placed at the outer boundary,

facing the wall. Parameters of interest were total distance travelled and time of inner zone exploration.

3.2.12.2. Elevated plus maze (EPM)

The elevated plus maze test (EPM) was used to assess anxiety-related behavior. The apparatus was made of grey PVC and consisted of a plus-shaped platform with four intersecting arms, elevated 37 cm above the floor. Two opposing open (30 x 5 cm, 15-20 lux) and closed arms (30 x 5 x 15 cm, 8-10 lux) were connected by a central zone (5 x 5 cm). Animals were placed in the center of the apparatus facing the closed arm and were allowed to freely explore the maze for 5 min. Parameters of interest included open and closed arm time and open arm entries.

3.2.12.3. Dark/light box (DaLi)

The dark/light box test (DaLi) was used to assess anxiety-related behavior. The test box consists of black and white PVC and is divided into two compartments, connected by a tunnel (4 x 7 x 10 cm). The white compartment (30 x 20 x 25 cm) was brightly illuminatd by cold light with an intensity of 680-700 lux; light intensity in the dark compartment (15 x 20 x 25 cm) was < 5 lux. Each animal was placed in the dark compartment of the test apparatus, facing the bright lit compartment. During the 5 min test, the time spent in each compartment (dark, tunnel and lit compartment), the latency until the first full entry (four paw criterion) and the number of full entries into the lit compartment were assessed.

3.2.12.4. Forced swim test (FST)

The FST was used to assess stress-coping/depression-like behavior. Each animal was gently placed into a glass beaker (diameter 12 cm, height 24 cm) filled with water (temperature 24 ± 1°C) to a height of 12 cm and behavior during a 6 min test period was recorded. The parameters floating (immobility except small movements to keep balance), swimming and struggling (vigorous attempts to escape) were recorded using the ANYmaze software and scored throughout the 6 min test period by a trained observer.

3.2.12.5. Y-maze

Spontaneous alternation rate was assessed using a Y-shaped grey PVC maze, with 40 x 20 x 10 cm arm sizes. At the end of each arm a different symbol shaped by adhesive tape was attached (triangle, quadrat, line). At the beginning, each mouse was placed in the centre of the maze, facing one wall angle. During 5 min sessions, the sequences of arm entries were recorded; alternation was defined as successive entries into the three arms, in

overlapping triplet sets. Percent alternation was calculated as the ratio of actual to possible alternations (defined as the total number of arm entries−2) x 100 %.

3.2.12.6. Water cross maze (WCM)

The water cross maze (WCM) was used to assess spatial and response learning, cognitive flexibility and strategy shifting depending on the training protocol.

Apparatus

The WCM was established by the research group of Carsten Wotjak at the institute (unpublished), based on Tolman´s work (Tolman et al., 1946). It was made from 1 cm thick clear acrylic glass to allow for visual orientation via distant extra-maze cues in the experimental room. Each of the four arms was 10 cm wide, 50 cm deep and 30 cm in height. Arms were clockwise labelled North, East, South and West. A clear acrylic glass shield of fitting dimensions blocked the entrance into one arm completely, rendering the WCM a functional T-maze during the single runs.

A submerged platform (8 x 8 x 10 cm) was positioned at various locations inside the maze at the end of the arms. The maze was filled with fresh tap water at 23°C up to 11.5 cm level each day before testing. A metal grid (9 x 9 cm) was used to remove the animal from the maze. The testing room was dimly illuminated (15-20 lux). The room contained several distant visual cues e.g. a sink, cupboard and door.

General procedure

Animals were gently inserted into the water at the starting position described for the particular protocol, facing the wall. The experimenter remained standing motionless behind the current start arm during the trial. Parameters of the run were recorded and the animal was placed back into its home cage, which was subsequently put under infrared light to dry and warm up the animal. After each run, the walls of the maze were wiped dry, and the water was stirred between the four arms every three runs in order to avoid urine and pheromones influence on swimming paths. Animal faeces were removed by a metal strainer. Animals were tested in groups of six, resulting in an intertrial interval of about 10 min for the individual animal. Six runs a day for each mouse were conducted.

Learning protocols

Spatial learning protocol

This protocol enforced spatial learning via allocentric navigation. During five consecutive days the platform was constantly located in the West arm while starting of the mice

alternated between South and North in a pseudorandom manner (Figure 8A). To perform accurately, mice needed to orientate spatially.

Free-choice protocol

In this protocol a response-egocentric strategy was enforced during the first training week (5 days) by unchanged platform location and starting position. The same body turn needed to be applied for accurate performance. In the second week the starting arm still remained unchanged, whereas the platform was located in the opposite arm (Figure 8B). Accurancy in the second week gave evidence about cognitive flexibility.

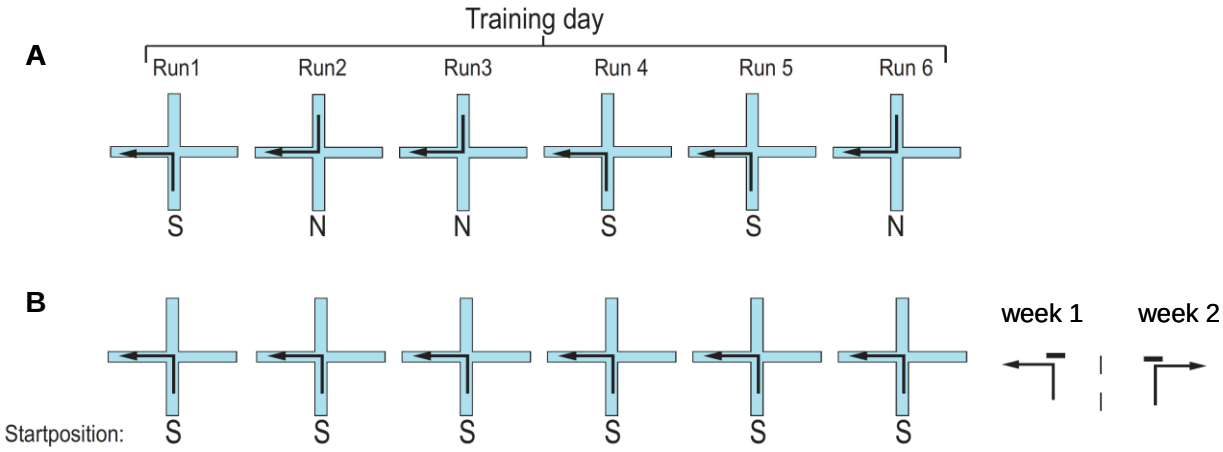

Figure 8. Training protocols in the WCM. (A) In the spatial paradigm 6 runs a day were performed according to a definite scheme which was not foreseeable for the mice. Every other day, starting positions varied (SNNSSN to NSSNNS). The platform was always located in the West arm. (B) In the free-choice protocol starting and platform location remained unchanged during the first week, whereas in the second week the platform was located in the opposite arm.

Performance indicators

Accuracy indicates the success or failure of the mouse to swim the correct path to the platform. Specifically, the mouse is accurate if it does not enter other arms than the goal arm (platform arm), but enters the goal arm directly and climbs onto the platform within 31 s. In this case, the run is given the value 1 (=accurate), otherwise 0 (= not accurate). The sum of correct runs is divided by the total number of runs and the percentage calculated (sum of correct runs/6*100). Given the natural tendeny of mice to explore, one error is permitted, which than manifests in an accuracy of 83.3 % as the bottom threshold for a mouse to be

considered accurate. **Number of accurate learners** indicates the percentage of animals of a particular group performing accurately.

For the spatial protocol the parameter **side bias** indicates animals which adopt a strategy that allows them to solve the maze task. Mice have a high side bias if they tend to apply the same body turn and thus always swim in one direction e.g. always turn left irrespective of the starting location. For calculation of the side bias of one animal, the sum of correct runs from the South arm is subtracted from those of the North arm. The absolute value of the result represents the side bias. The minimum score is 0, the maximum is 3 (= animal completely biased, correct performance of the spatial task only from one starting position). An animal with a score higher than two is considered biased. The **number of biased learners** is calculated accordingly.

3.2.12.7. Spontaneous object recognition (OR)

Spontaneous object recognition (OR) was conducted as previously described for rats (Winters et al., 2004;Forwood et al., 2005) using a Y-shaped apparatus adapted for mice. The Y-apparatus had high, homogenous white walls constructed from Perspex to prevent the mouse from looking out into the room, thereby maximizing attention to the stimuli. One arm was used as the start arm, and the other two arms were used to display the objects (randomly shaped junk objects, dimensions approximately 10 x 4 x 4 cm). All walls were 30 cm high, and each arm was 16 cm in length and 8 cm wide. A lamp illuminated the apparatus, and a white shelf, 50 cm from the top of the apparatus, created a ceiling on which a video camera was mounted to record trials.

All mice were habituated in two consecutive daily sessions in which they were placed in the start arm and left to explore the empty Y-apparatus for 5 min. After habituation, each animal received two test sessions, separated by a minimum of 24 h. Each test session consisted of a sample phase and a choice phase. In the sample phase, two identical objects A were placed at the end of each arm. The animal was placed in the start arm and left to explore the apparatus for 5 min, before it was returned to the home cage for 1 h. The following choice phase was procedurally identical to the sample phase. However, one arm now contained a new copy of the same object A, displayed in the sample phase, and the other arm contained a novel object B. A different object pair was used for each trial for a given animal, and the order of exposure to object pairs as well as the designated sample and novel objects for each pair were counterbalanced within and across groups.

The time spent exploring the objects was assessed from video recordings of the sample and choice phases. Data were collected by scoring exploratory bouts using a personal computer running a programme written in Visual Basic 6.0 (Microsoft). Times where an animal climbed

or sat on an object were not counted. For the choice trials exploration ratio was calculated (% exploration = novel object exploration time / total object exploration time x 100 %). The mean exploration score across the two test sessions was calculated for each animal.

3.2.13. Statistical analysis

Data output and statistical analysis were performed with the computer programme GraphPad Prism 5.0. All results are shown as means ± standard error of the mean (SEM). Differences were considered significant at $p < 0.05$. To examine performance in the WCM task Two-way repeated measures ANOVA was employed. For analysis of 4 groups in the OR task, Y-maze and the electrophysiology, One-way ANOVA was conducted. ELISA and PPF data was analyzed with Two-way ANOVA. The appropriate post-hoc test was performed after acceptance of significant p-values. Analysis of behavior results such as OF, EPM, DaLi, FST and plaque burden was conducted with Student´s t-test.

4. Results

4.1. Neuroprotective effects of CRH *in vitro*

Several studies reported neuroprotective actions of CRH via CRH-R1 in the context of Aß-mediated toxicity in *in vitro* models (Bayatti et al., 2003;Facci et al., 2003;Lezoualc'h et al., 2000).

We examined the neuroprotective effects of CRH pretreatment against Aß toxicity in AtT20 cells, HT22 cells and two HT22 cell lines stably transfected with CRH-R1 (HT22 C2, HT22 C3). CRH-R1 expression levels in those four cell lines were determined by qRT-PCR (Figure 9), normalized to the house keeping gene HPRT. Compared to the endogenous CRH-R1 expression level in AtT20 cells, HT22 cells do not express the CRH-R1, whereas HT22 C2 cells express about 400 times and HT22 C3 cells about 10 times more CRH-R1.

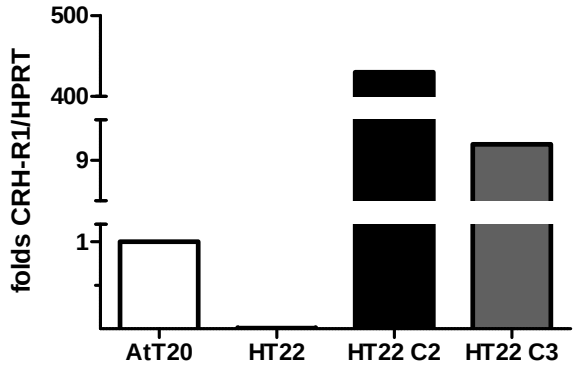

Figure 9. CRH-R1 expression level analysis. CRH-R1 expression in AtT20 cells (endogenous, normalized to 1), HT22 cells, stably CRH-R1 transfected HT22 C2 and HT22 C3 cells was quantified by qRT-PCR.

Different concentrations of CRH (10-500 nM) and $Aß_{25-35}$ (10-40 µM) were used. The $Aß_{25-35}$ fragment is a naturally occurring proteolytic by-product that retains the toxicity of its larger better-known counterpart $Aß_{1-40}$ (Wei et al., 2010a). The $Aß_{25-35}$ fragment aggregates immediately upon dissolution and exerts its toxicity immediately in a highly reproducible manner (Behl, 1997;Behl, 1997).

Cell survival was measured by the photometric MTT assay (Thiazolyl Blue Tetrazolium Bromide). We observed neuroprotective effects of CRH pretreatment against Aß toxicity which depended on the amount of CRH-R1 and the CRH concentration. In HT22 cells, which do not express CRH-R1, CRH pretreatment had rather detrimental effects on cell survival, measured by the MTT assay. In AtT20 cells, which endogenously express CRH-R1, survival curves after CRH treatment and without treatment did not differ, whereas in HT22 C3 cells

pretreated with 500 nM CRH cell survival was elevated (not significant) at Aß concentration of 10-40 µM. In HT22 C2 cells, which overexpress more than 400-fold of CRH-R1, cell survival after CRH treatment was clearly increased at all concentrations of CRH and Aß. This effect was significant following 500 nM CRH in combination with 20 µM Aß. Apparently, CRH can exert neuroprotective effects against Aß treatment in cells carrying the CRH-R1, an effect which depends on the concentration of CRH. The more CRH-R1 and CRH are available, the higher the cell survival and thus the neuroprotective effect of CRH against Aß mediated toxicity.

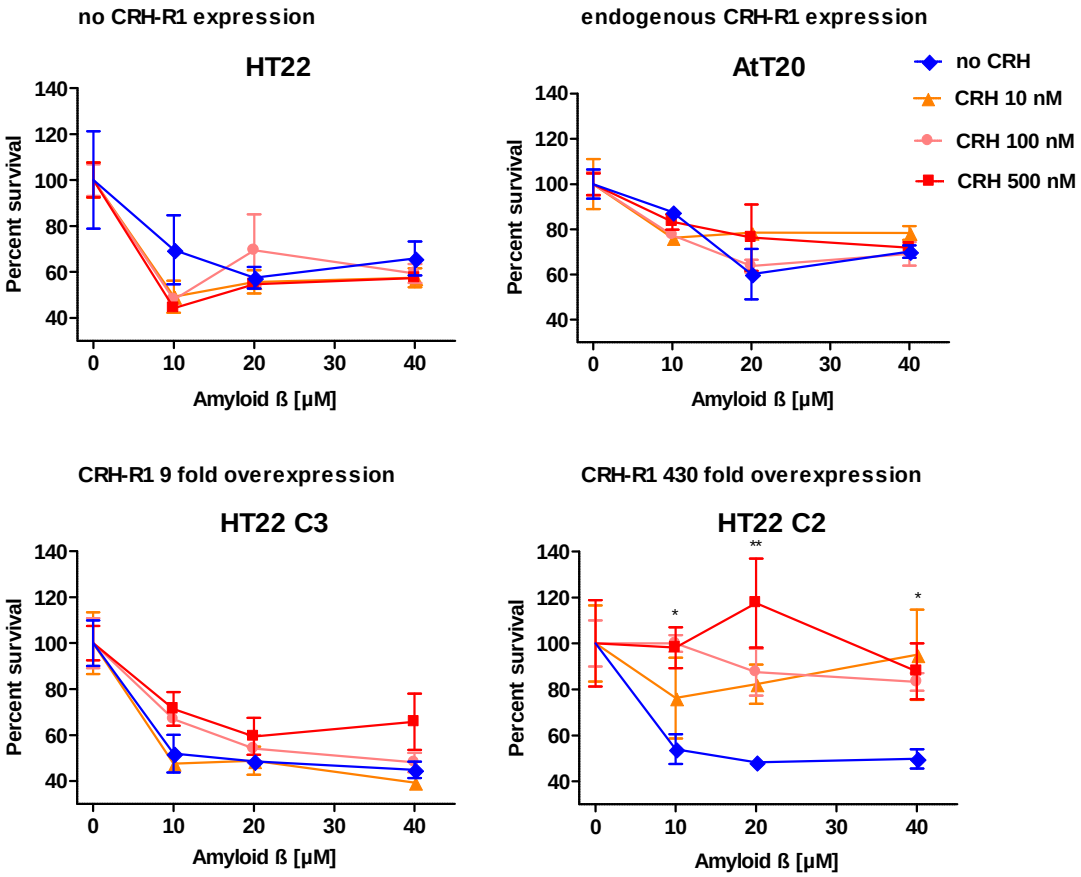

Figure 10. CRH prevents Aß mediated toxicity dependent on its concentration and CRH-R1 expression level. HT22, AtT20, HT22 C2 and HT22 C3 cells were treated with Aß 10-20 µM for 24 h after treatment of 0-500 nM CRH. Cell survival was determined by MTT assay. Significances in HT22 C2 cells with Aß 10 µM: CRH 100 nM vs. no CRH *; Aß 20 µM: CRH 500 nM vs. no CRH **. Values of each CRH concentration are normalized to the respective cell survival rate without Aß. Data are presented as mean ± SEM. n=3; * $p < 0.05$, ** $p < 0.01$ statistical significance, Two-way repeated measures ANOVA, Bonferroni posttests.

4.2. Basal characterization of arcAß mice

ArcAß mice were generated previously and had been analyzed with respect to locomotion, anxiety and cognition at the age of 3, 6 and 9 months (Knobloch et al., 2007a). Nevertheless, we subjected arcAß mice bred in our animal facility to a battery of tests assessing basal emotionality prior to comprehensive cognitive testing. Furthermore, APP overexpression and processing were characterized and the functionality of the HPA axis and the status of the CRH/CRH-R1 system with respect to expression levels were determined in arcAß mice.

4.2.1. APP processing in arcAß mice

ArcAß mice overexpress human APP (hAPP) 695 carrying both the Swedish (K670N; M671L) and the Arctic (E693G) mutation in a single construct under the control of the prion protein promoter (Knobloch et al., 2007a). The Arctic mutation renders Aß monomers more prone to assemble to oligomers (Nilsberth et al., 2001), the Swedish mutation increases the cleavage by the ß-secretase (Knobloch et al., 2007a). Overexpression of hAPP 695 mRNA in arcAß mice versus wt mice is illustrated in Figure 11.

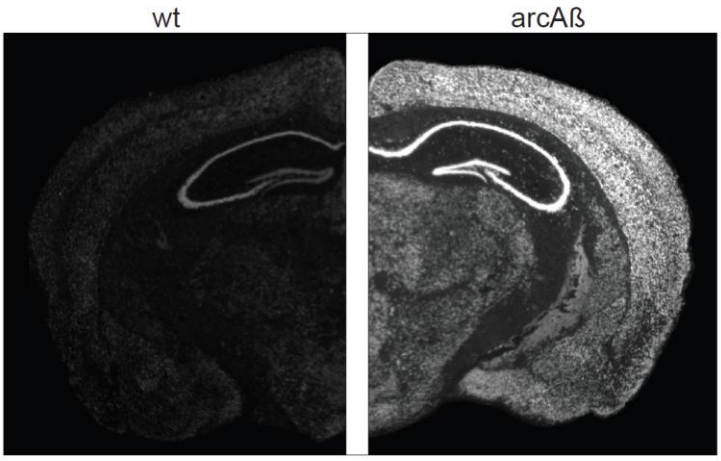

Figure 11. ArcAß mice overexpress human APP (hAPP) 695. Analysis of hAPP mRNA expression in arcAß mice (right) compared to wt mice (left) was conducted using ISH probe APP 695 which is specific for hAPP 695. This probe partly detects endogenous mouse APP.

For visualization of products and intermediates of the APP processing pathway by Western blotting, a three-step-extraction protocol for brain tissue was established (see 3.2.6.2 SDS polyacrylamide gel electrohoresis and Western blotting). In the Diethylamine (DEA) fraction soluble proteins such as sAPP and Aß monomers were detected. The SDS fraction

contained membrane standing ß-stubs and APP as well as Aß oligomers. Finally, the formic acid fraction comprised dispersed Aß from Aß assemblies and plaques. Fractions were electrophoresed on gradient gels and Western blotting was performed with antibody 6E10 against amino acids 1-16 of the Aß protein (Figure 12).

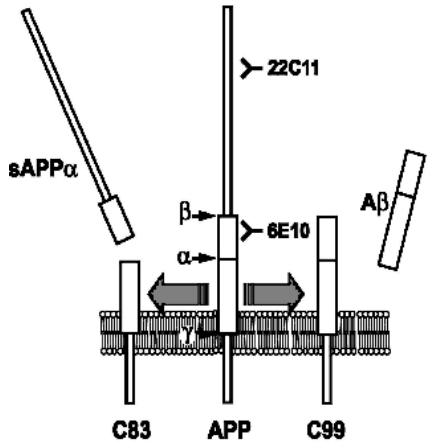

Figure 12. Specific binding of APP antibodies 6E10 and 22C11.
6E10 detects amino acids 1-16 of the Aß-terminus and thus can also detect sAPPα in soluble fractions. 22C11 binds to the N-terminal region of APP and therefore detects APP and in the soluble fraction total sAPP.

In cerebral hemispheres of arcAß mice aged 5-8 months increased levels of APP were detected in all three fractions (DEA, SDS, FA) in comparison to wt mice (Figure 13). After cleavage of APP by ß-secretase, ß-stubs remain in the membrane and were detected in the SDS fraction. Aß monomers were weakly detected in the DEA fraction. Mice aged 8 months showed increased Aß in the SDS fraction compared to younger animals and insoluble Aß also began to accumulate at this age (FA fraction).

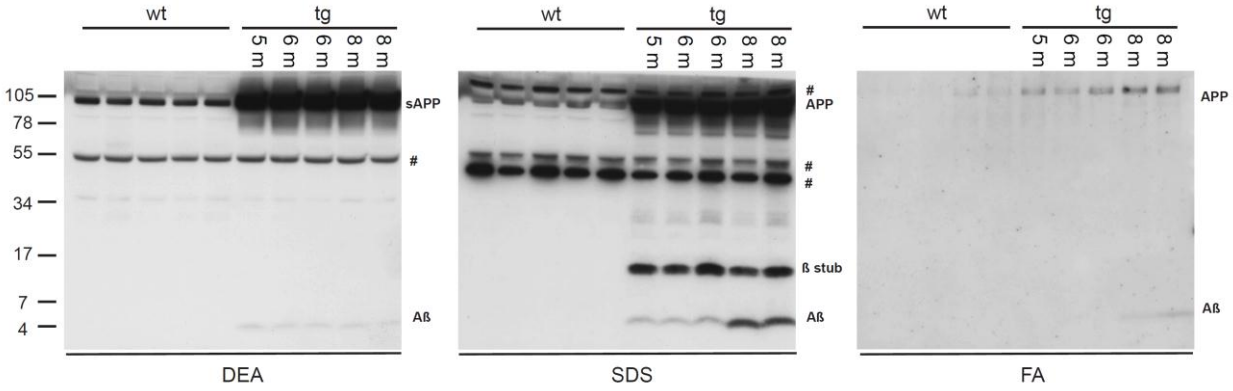

Figure 13. Visualization of APP processing in arcAß (tg) mice. Cerebral hemispheres of wt mice and tg mice aged 5-8 months (m) were processed using an extraction protocol providing three fractions: Diethylamine (DEA) for soluble proteins (sAPP), SDS for Aß oligomers and rather insoluble proteins (ß-stub, APP), and formic acid (FA) for insoluble Aß. # indicates unspecific bands. Protein sizes are depicted in kDa.

4.2.2. Assessment of bodyweight in arcAß mice

In general transgenic (tg) mice were indistinguishable from their wild-type (wt) littermates with respect to their general health state at the age of 4, 8 and 12 months.

Bodyweight in both tg and wt mice increased from 4 to 8 months of age and slightly decreased at 12 months of age with tg mice showing significantly reduced bodyweight compared to wt mice (Figure 14).

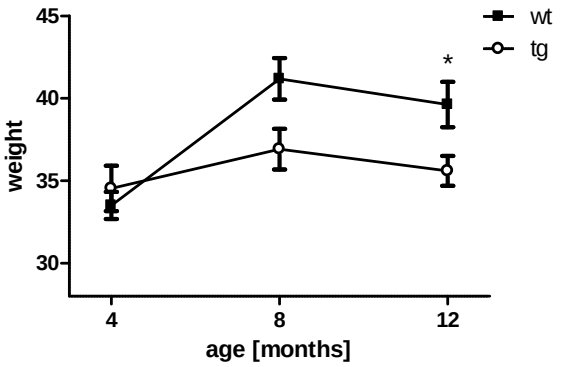

Figure 14. The bodyweight of arcAß (tg) mice is reduced at 12 months of age compared to their wild-type (wt) littermates. At 4 and 8 months of age no significant alterations of bodyweight between tg and wt mice were detectable. Data are presented as means ± SEM; n=11-13; * $p < 0.05$, Student´s t-test.

4.2.3. HPA axis functionality in arcAß mice

Alterations in the HPA axis are common in a number of transgenic rodent models of AD, as indicated by elevated levels of corticosterone, compare e.g. Tg CRND8 (Touma et al., 2004), Tg2576 (Lee et al., 2009;Dong et al., 2008) and 3xTg mice (Green et al., 2006). To asesss HPA axis activity in arcAß mice we determined plasma corticosterone levels under basal conditions and in response to acute stress (10 min restraint) (Figure 15). Corticosterone levels of tg mice and wt mice significantly increased after stress at 4 and 12 months of age. However, plasma corticosterone levels of wt and tg mice were indistinguishable (wt 4 months: basal: 6.60 ± 1.10 ng/ml vs. stress: 124.70 ± 7.35 ng/ml; tg 4 months: basal: 6.35 ± 1.10 ng/ml vs. stress: 113.00 ± 7.19 ng/ml and wt 12 months: basal: 3.02 ± 0.57 ng/ml vs. stress: 91.22 ± 6.94 ng/ml; tg 12 months: basal: 5.39 ± 1.25 ng/ml vs. stress: 89.25 ± 9.29 ng/ml). Interestingly, basal and stress levels of animals decreased with age (wt: basal: 4 months: 6.60 ± 1.10 ng/ml, 12 months: 3.02 ± 0.57 ng/ml, $p < 0.01$; stress: 4 months: 124.70 ± 7.35 ng/ml, 12 months: 91.22 ± 6.94 ng/ml, $p < 0.01$ and tg: basal: 4 months: 6.35 ± 1.09 ng/ml, 12 months: 4,56 ± 1.01 ng/ml, $p > 0.05$; stress: 4 months: 113.0 ± 7.19 ng/ml, 12 months: 89.25 ± 9.24 ng/ml, $p = 0.0546$).

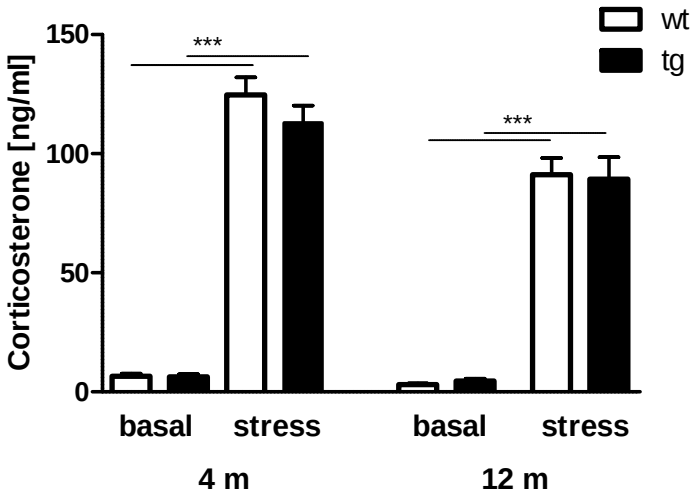

Figure 15. The HPA axis is fully functional in tg mice. Corticosterone levels were assessed in tg vs. wt mice under basal conditions and after acute stress (10 min restraint) at 4 and 12 months of age. Results are presented as means ± SEM; n=11-13; *** $p < 0.001$, Student´s t-test.

4.2.4. Assessment of basal emotionality in arcAß mice

The characterization of emotional behavior, including locomotion, anxiety-related and stress-coping behavior was conducted in tg vs. wt mice at 4, 8 and 12 months of age.

4.2.4.1. Assessment of locomotion in arcAß mice

Previously, Knobloch and colleagues (2007) observed increased locomotion in arcAß mice at 3 months of age in the open field (OF) and zeromaze test, whereas no difference was detectable in 6 and 9 months old mice.

We also assessed locomotion in the OF task. The distance travelled in the OF was significantly increased in tg mice at 8 and 12 months of age (Figure 16A). Accordingly, the immobility was reduced in this test (Figure 16B). In general, locomotion decreased with age. Along these lines, the distance travelled in the Y-maze task was increased in tg compared to wt animals at all ages (Figure 16C).

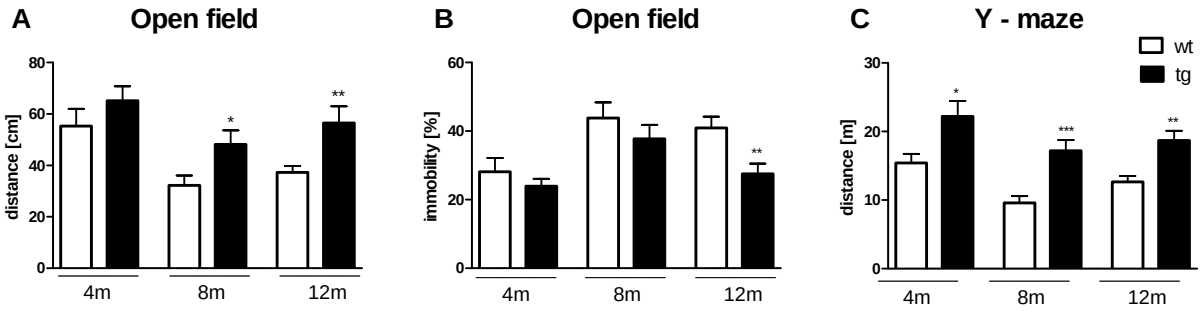

Figure 16. Locomotion is increased in tg mice. (A) Distance travelled and (B) immobility in the open field test and (C) distance travelled in the Y-maze task are presented in tg vs. wt mice at 4, 8 and 12 months of age. Data are presented as means ± SEM; n=11-13; * $p < 0.05$, ** $p < 0.01$, *** $p < 0.001$, Student´s t-test.

4.2.4.2. Assessment of anxiety-related behavior in arcAß mice

Anxiety-related behavior was assessed in the elevated plus maze (EPM), the dark/light box (DaLi) and the open field (OF) test. In the EPM the time in the open (Figure 17A) and closed arms (Figure 17B), in the DaLi the time in the lit compartment (Figure 17C) and in the OF the ratio of distance in the inner zone versus total distance (Figure 17D) were evaluated. None of the tests detected significant differences with respect to anxiety-related behavior in arcAß mice. This is in contrast to previous findings where mice spent less time on the open sectors of the zeromaze at 6 and 9 months of age suggesting reduced anxiety-related behavior.

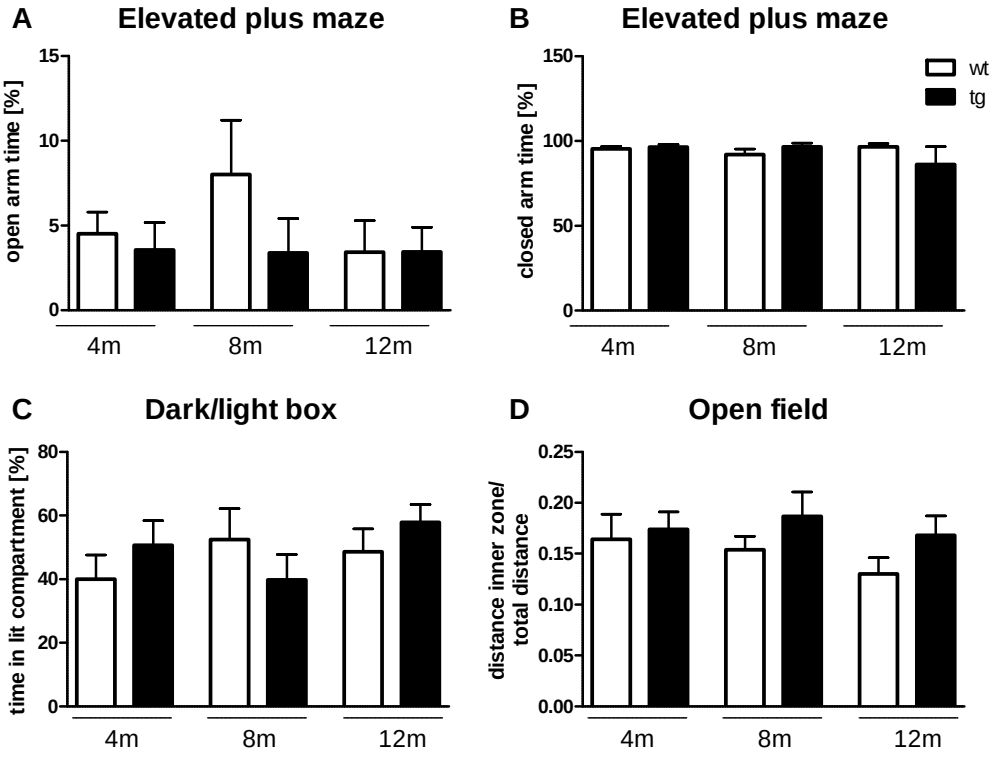

Figure 17. Anxiety-related behavior is not altered in arcAß (tg) mice. (A) Open and (B) closed arm time of the elevated plus maze test, (C) time in the lit compartment of the dark/light box and (D) the distance in the inner zone/total distance in the open field were assessed to evaluate anxiety in tg vs. wt mice at 4, 8 and 12 months of age. Data are presented as means ± SEM; n=11-13.

4.2.4.3. Assessment of stress-coping behavior in arcAß mice

Stress-coping or depression-like behavior was evaluated by analyzing the time struggling, swimming and floating in the forced swim test (FST). At 4 and 12 months of age tg mice showed a strong increase in active stress-coping behavior compared to wt littermates reflected by an increase in struggling (Figure 18A) and swimming (Figure 18B). Accordingly, the floating time (Figure 18C) was significantly decreased in tg mice compared to wt mice.

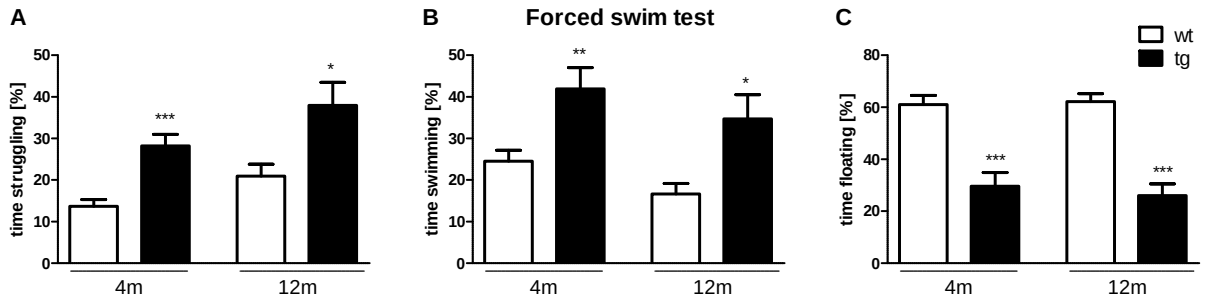

Figure 18. Tg mice show enhanced active stress-coping behavior in the forced swim test (FST). The time (A) struggling, (B) swimming and (C) floating was analyzed in the FST in tg compared to wt mice aged 4 and 12 months. Data are presented as means ± SEM; n=11-13. * $p < 0.05$, ** $p < 0.01$, *** $p < 0.001$, Student´s t-test.

4.2.5. Analysis of CRH and CRH-R1 expression in arcAß mice

In AD patients alterations in the CRH system have been reported repeatedly. Therefore, we analyzed the mRNA expression levels of CRH and CRH-R1 in arcAß mice by ISH (Figure 19). Compared to wt mice (=100 %) CRH levels in the cortex (CTX) of tg mice significantly increased with age, from 3 (106.2 ± 1.50 %, $p < 0.01$) to 6 (110.8 ± 3.57 %, $p < 0.01$) and 12 months (118.5 ± 2.25 %, $p < 0.001$). In contrast, CRH expression levels in the paraventricular nucleus (PVN) and the central amygdala (CeA) of tg animals did not differ from wt littermates at any time point (Figure 19A).

CRH-R1 expression in the CTX of 3 months old animals was elevated compared to wt mice (108.3 ± 1.31 %, $p < 0.001$), whereas CRH-R1 levels decreased with age (6 months: 102.1 ± 1.55 % and 12 months: 95.85 ± 1.72 %, $p < 0.05$; Figure 19B). In the CA1 region of the hippocampus (HIP) of tg animals CRH-R1 levels increased from 3 (102.0 ± 3.45 %, ns) to 6 (105.5 ± 2.02 %, $p < 0.05$) and to 12 months of age (111.0 ± 2.94 %, $p < 0.001$) compared to wt littermates.

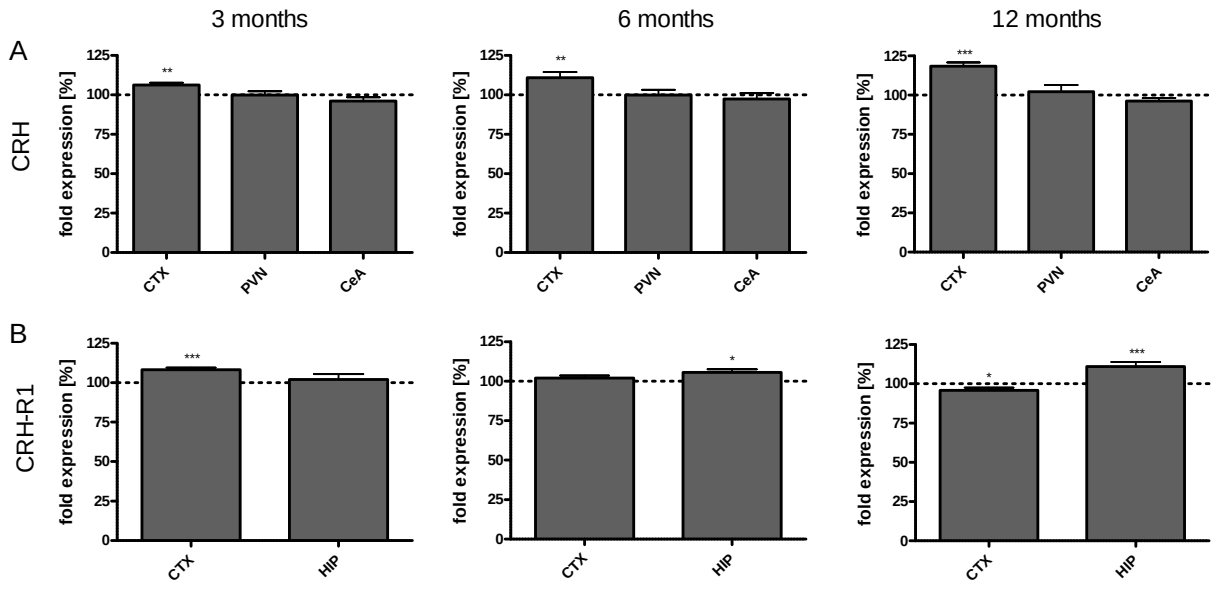

Figure 19. CRH and CRH-R1 mRNA expression analyses reveal significant alterations in tg mice compared to wt mice. (A) CRH expression in the cortex (CTX), paraventricular nucleus (PVN) and central amygdala (CeA). (B) CRH-R1 expression in the CTX and CA1 region of the hippocampus (HIP) of tg and wt mice at 3, 6 and 12 months of age was determined by ISH. Levels in tg mice are normalized to wt (= 100 %). Results are presented as means ± SEM; n=6-7; *** $p < 0.001$, ** $p < 0.01$, *$p < 0.05$, Student´s t-test.

4.3. Basal characterization of CRH-R1KO mice

Conventional CRH-R1 knockout (KO) mice exhibit increased locomotion and reduced anxiety-related behavior (Timpl et al., 1998). Similar to arcAß mice, we assessed basal emotionality and HPA axis activity in CRH-R1KO mice to estimate to what extent the pure CRH-R1KO might impact the cognitive phenotype of arcAß CRH-R1KO mice.

4.3.1. Assessment of bodyweight in CRH-R1KO mice

The assessment of the general health state did not reveal any significant differences between CRH-R1KO (ko) and wild-type (wt) mice. Bodyweight in both ko and wt mice increased from 4 to 8 months of age and slightly decreased in the 12 months aged group. The bodyweight in ko mice at the age of 8 and 12 months was significantly reduced compared to their wt littermates (Figure 20).

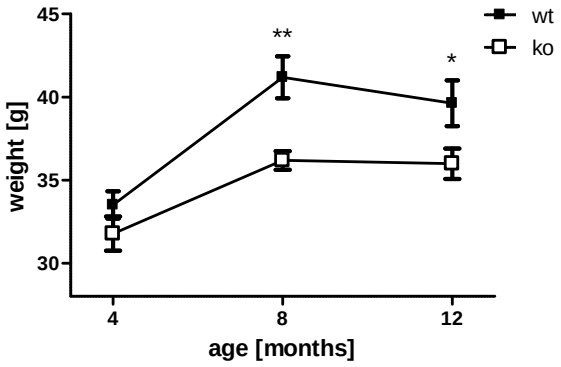

Figure 20. The bodyweight of CRH-R1KO (ko) mice is reduced compared to their wild-type (wt) littermates. Data are expressed as means ± SEM; n=11-13; * $p < 0.05$, ** $p < 0.01$, Student´s t-test.

4.3.2. HPA axis functionality in CRH-R1KO mice

Plasma corticosterone levels of wt mice significantly increased after stress ($p < 0.001$) (Figure 21). Levels of ko mice were at the detection limit, reflecting the compromised HPA axis activity due to CRH-R1 deletion in the pituitary. However, corticosterone levels of ko mice also increased slightly after stress ($p < 0.01$ at 4 months, $p < 0.05$ at 12 months), indicating residual functionality of the neuroendocrine stress response mediated most likely via compensatory action of arginine vasopressin.

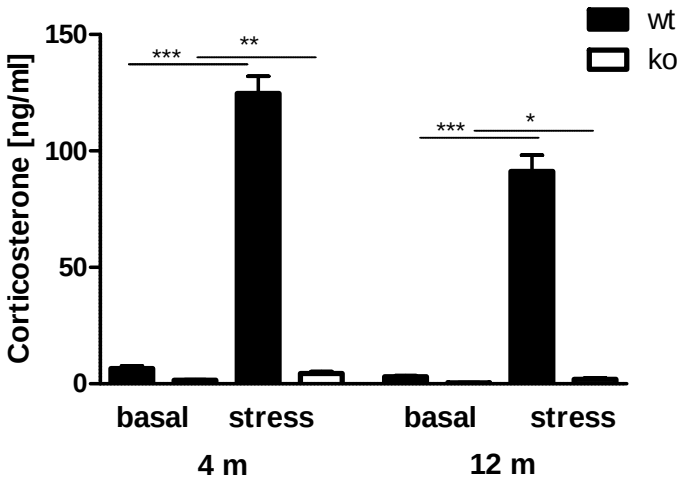

Figure 21. The HPA axis of ko mice is impaired in its functionality. Plasma Corticosterone levels were assessed in ko vs. wt mice under basal conditions and after stress (10 min restraint) at 4 and 12 months of age. Results are presented as means ± SEM; n=11-13; * $p < 0.05$, ** $p < 0.01$, *** $p < 0.001$, Student´s t-test.

4.3.3. Assessment of basal emotionality in CRH-R1KO mice

Characterization of emotional behavior including locomotion, anxiety-related and stress-coping behavior was conducted in ko vs. wt mice at 4, 8 and 12 months of age.

4.3.3.1. Assessment of locomotion in CRH-R1KO mice

Locomotion in ko mice aged 8 and 12 months was slightly increased in the OF as indicated by a longer total distance travelled (Figure 22A) and reduced immobility (Figure 22B). However, these differences were statistically not significant. In the Y-maze, the distance travelled was significantly increased in ko mice at 8 and 12 months of age (Figure 22C). These findings largely confirm previous results by Timpl and colleagues (1998).

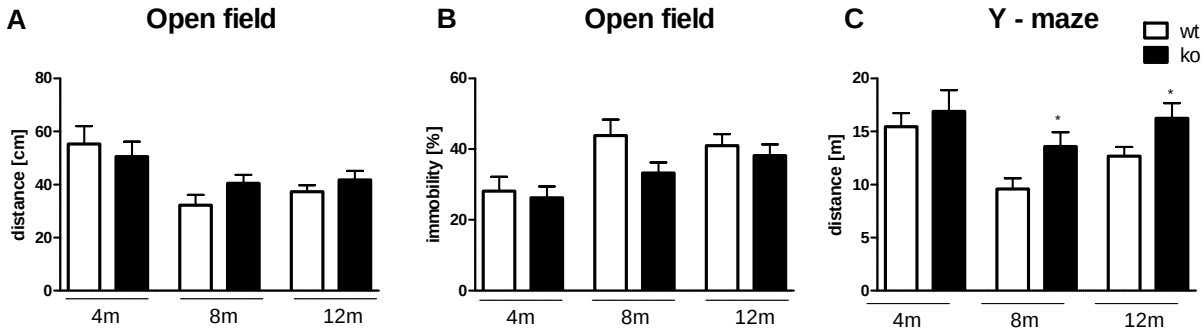

Figure 22. Locomotion is increased in ko mice. (A) Distance travelled and (B) immobility in the open field and (C) distance travelled in the Y-maze task are presented in ko vs. wt mice at 4, 8 and 12 months of age. Data are expressed as means ± SEM; n=11-13; * $p < 0.05$, Student´s t-test.

4.3.3.2. Assessment of anxiety-related behavior in CRH-R1KO mice

Anxiety-related behavior was reduced in ko mice aged 4 months as indicated by increased time spent in the open arms (Figure 23A) and a reciprocal reduction of time spent in the closed arms (Figure 23B) of the EPM. Also, at 8 and 12 months anxiety-related behavior was decreased, as reflected by a smaller ratio of the distance travelled in the inner zone versus the total distance in the OF (Figure 23D). Reduced anxiety-related behavior in CRH-R1KO mice has been previously demonstrated by Timpl and colleagues (1998) – CRH-R1KO mice spent more time in the lit compartment of the dark/light box (DaLi) (Timpl et al., 1998). In the DaLi paradigm we did not observe any difference (Figure 23C) under the used testing conditions (see 3.2.12.3 Methods DaLi).

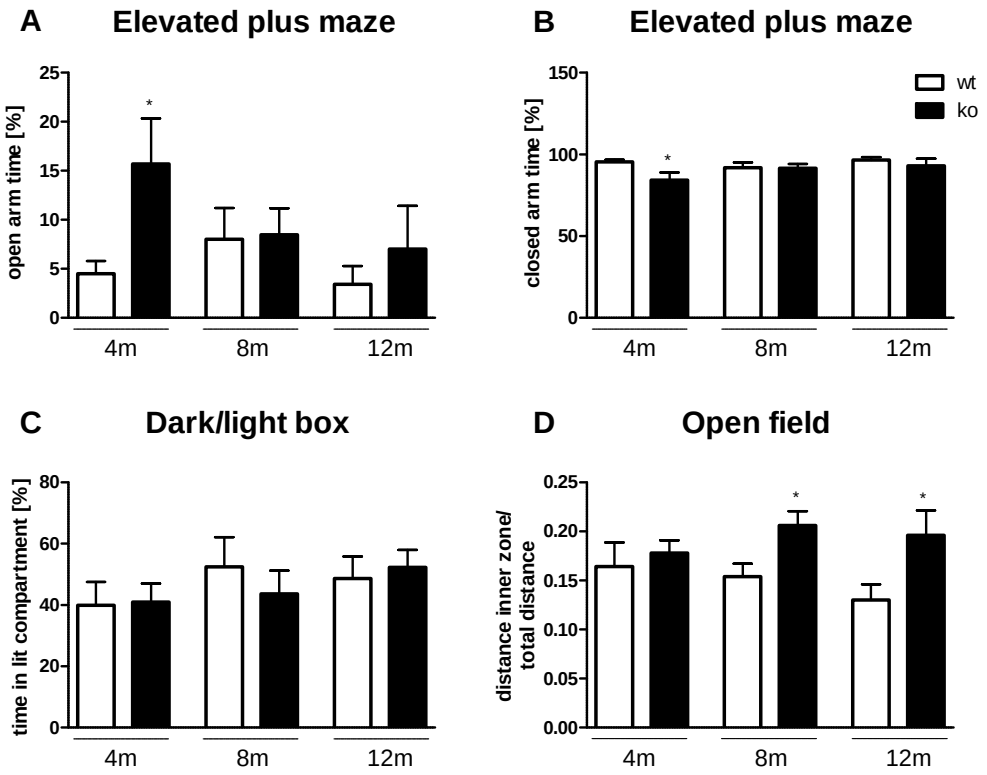

Figure 23. Anxiety-related behavior is reduced in ko mice. Time spent in the (A) open and (B) closed arm of the elevated plus maze test, (C) time spent in the lit compartment of the dark/ight box and (D) the distance in the inner zone/total distance in the open field was assessed to determine anxiety-related behavior in ko vs. wt mice at 4, 8 and 12 months of age. Data are expressed as means ± SEM; n=11-13; * $p < 0.05$, Student´s t-test.

4.3.3.3. Assessment of stress-coping behavior in CRH-R1KO mice

Stress-coping behavior was assessed in the forced swim test (FST). Ko mice showed a slight increase in active stress-coping behavior at 4 months of age as indicated by significantly more time spent struggling (Figure 24A) and reduced floating time (Figure 24C, $p = 0.38$). Ko mice aged 12 months tended to increase their time swimming (Figure 24B) and to reduce their time floating (Figure 24C), however, these results were statistically not significant.

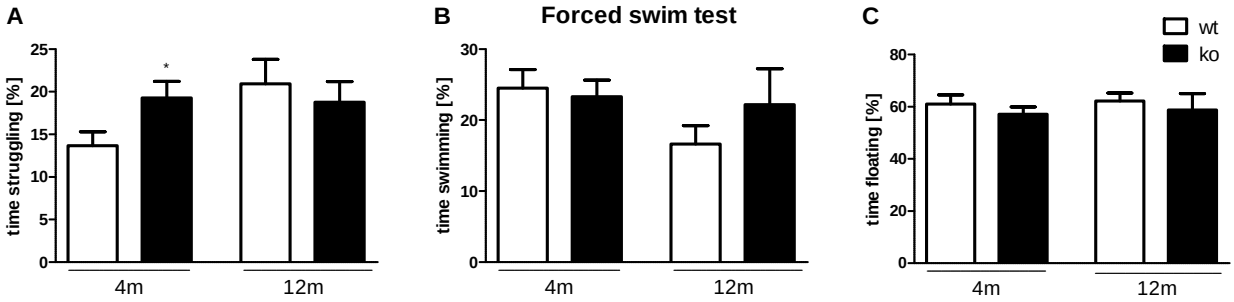

Figure 24. Ko mice show enhanced active stress-coping behavior at 4 months of age in the forced swim test. Ko and wt mice were analyzed regarding time (A) struggling, (B) swimming and (C) floating at 4 and 12 months of age. Data are expressed as means ± SEM; n=11-13. * $p < 0.05$, Student´s t-test.

4.4. The impact of the CRH-R1 on the onset and pathology of AD

To elucidate the impact of the CRH-R1 on the onset and progression of AD, CRH-R1KO mice were bred to arcAß mice. According to the breeding scheme depicted in Figure 25 mice of four genotypes of interest were obtained in the F_2-generation: wild-type (wt), transgenic arcAß (tg), CRH-R1KO (ko) and transgenic arcAß CRH-R1KO (tgko). These four genotypes of arcAß CRH-R1KO mice were submitted to comprehensive phenotyping at different ages.

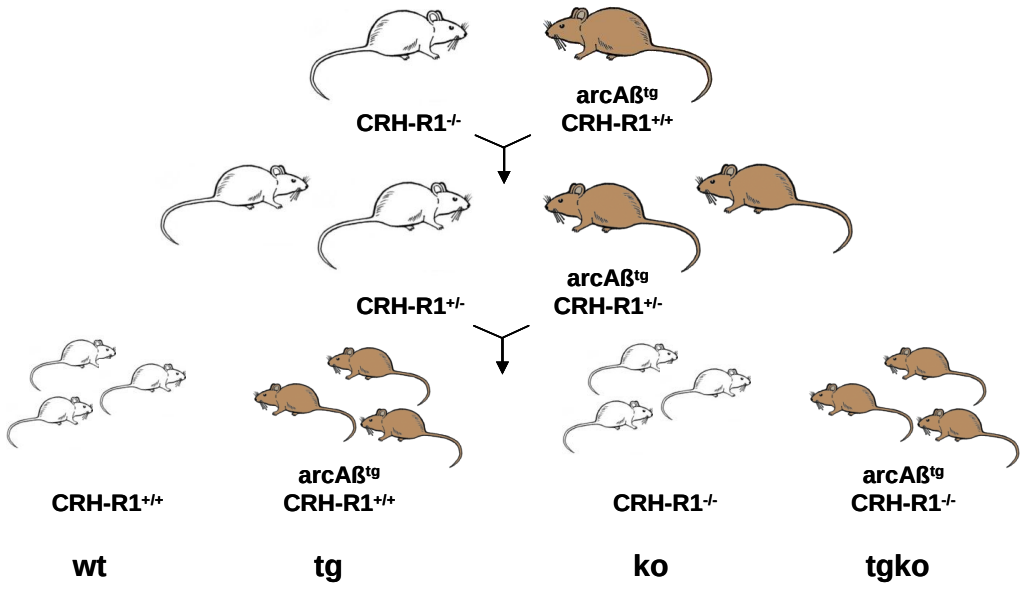

Figure 25. Breeding scheme of arcAß CRH-R1KO mice. Animals of the F_1-generation were bred among each other to gain the four genotypes of interest in the second generation: wild-type (wt), transgenic arcAß (tg), CRH-R1KO (ko) and transgenic arcAß CRH-R1KO (tgko). Brown fur color indicates mice carrying the arcAß transgene.

4.4.1. HPA axis functionality in arcAß CRH-R1KO mice

Plasma corticosterone levels were assessed in tg vs. tgko mice aged 12 months. As expected from CRH-R1KO mice (see also 4.3.2 HPA axis functionality in CRH-R1KO mice) tgko mice showed significantly reduced plasma corticosterone levels under basal conditions and a dramatically reduced HPA axis response to an acute stressor (10 min restraint; Figure 26).

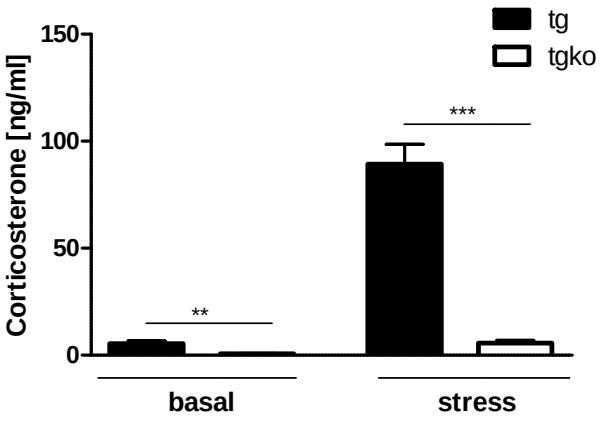

Figure 26. The activity of the HPA axis is impaired in tgko compared to tg mice aged 12 months. Corticosterone levels were assessed in tg vs. tgko mice at basal conditions and after stress (10 min restraint) at 12 months of age. Results are presented as means ± SEM; n=11-13; ** $p < 0.01$, *** $p < 0.001$, Student´s t-test.

4.4.2. Testing cognitive performance of arcAß CRH-R1KO mice

Memory impairment, in particular of recently learned facts, is one of the most prominent symptoms in AD. To assess the impact of the CRH-R1 in this context, we subjected arcAß CRH-R1KO mice to several tests aiming to address different learning and memory systems. Spontaneous alternation was tested in the Y-maze, spatial and response learning as well as cognitive flexibility in the water cross maze (WCM) and spontaneous object recognition (OR) in the OR test. Four genotypes of arcAß CRH-R1KO mice were analyzed in these tasks: wild-type (wt), CRH-R1KO (ko), transgenic arcAß (tg), transgenic arcAß CRH-R1KO (tgko).

4.4.2.1. Evaluation of spontaneous alternation in the Y-maze task

Working memory is the ability to hold memory in mind in order to solve complex tasks. In the Y-maze task, mice are confronted with the possibility to choose between three different arms, each presenting a different symbol at its end. Spontaneous alternation, assessed in the

Y-maze, is a natural tendency of rodents to explore different arms of a maze in successive runs (Middei et al., 2004). During a 5 min test session the sequence of arm entries was recorded and alternation calculated as successive entries into the three arms in overlapping triplet sets. In arcAß CRH-R1KO mice at 4, 8 and 12 months no significant changes were observed between the four genotypes (Figure 27).

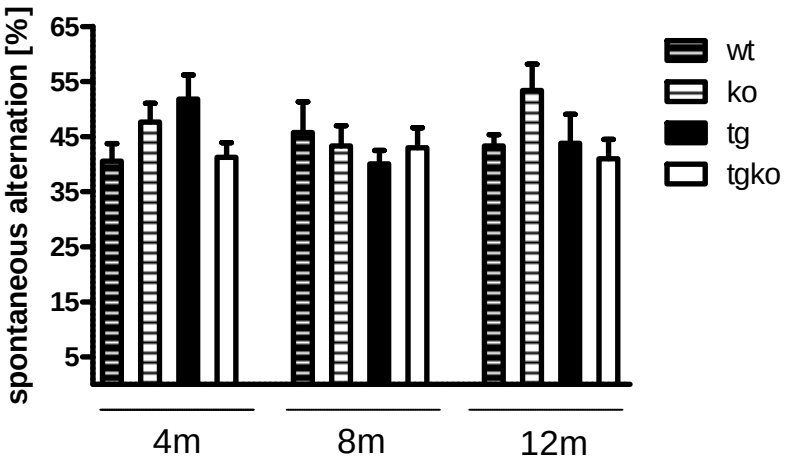

Figure 27. Spontaneous alternation is not significantly altered in arcAß CRH-R1KO mice. Wt, ko, tg and tgko mice at the age of 4, 8 and 12 months were subjected to the Y-maze task to test for spontaneous alternation. Percent alternation was calculated as the ratio of actual to possible alternations (defined as the total number of arm entries−2) x 100 %. Results are presented as means ± SEM; n=11-13, One-way-ANOVA.

4.4.2.2. Performance in the water cross maze (WCM) task

Mice of each genotype (wt, ko, tg, tgko) were tested in the WCM task to assess hippocampus-dependent spatial learning at the age of 4, 8 and 12 months (Figure 28A-D). In general, accuracy (to reach the platform in the first trial) decreases with age in all 4 genotypes (Figure 28A, B). Furthermore, at 4, 8 and 12 months of age tg and tgko mice performed worse than wt and ko mice did. Ko animals were the most accurate performers. Additionally, tgko mice at every age developed a high side bias which is the tendency to apply the same body turn at every trial irrespective of the starting arm what is an indication for response learning (Figure 28C, D). The preference of tgko mice to apply a response learning strategy was proven in the free-choice paradigm of the WCM test with mice aged 12 months (Figure 29A, B). Here, tg mice were delayed in their response learning ability in the first week (d1-d5), whereas tgko were not. In the second week (re-learning, d1r-d5r) the opposite body turn was enforced, which could not be done by tgko but by tg mice.

Consequently, performance of the second week suggests a more rigid, inflexible phenotype of tgko mice compared to tg mice.

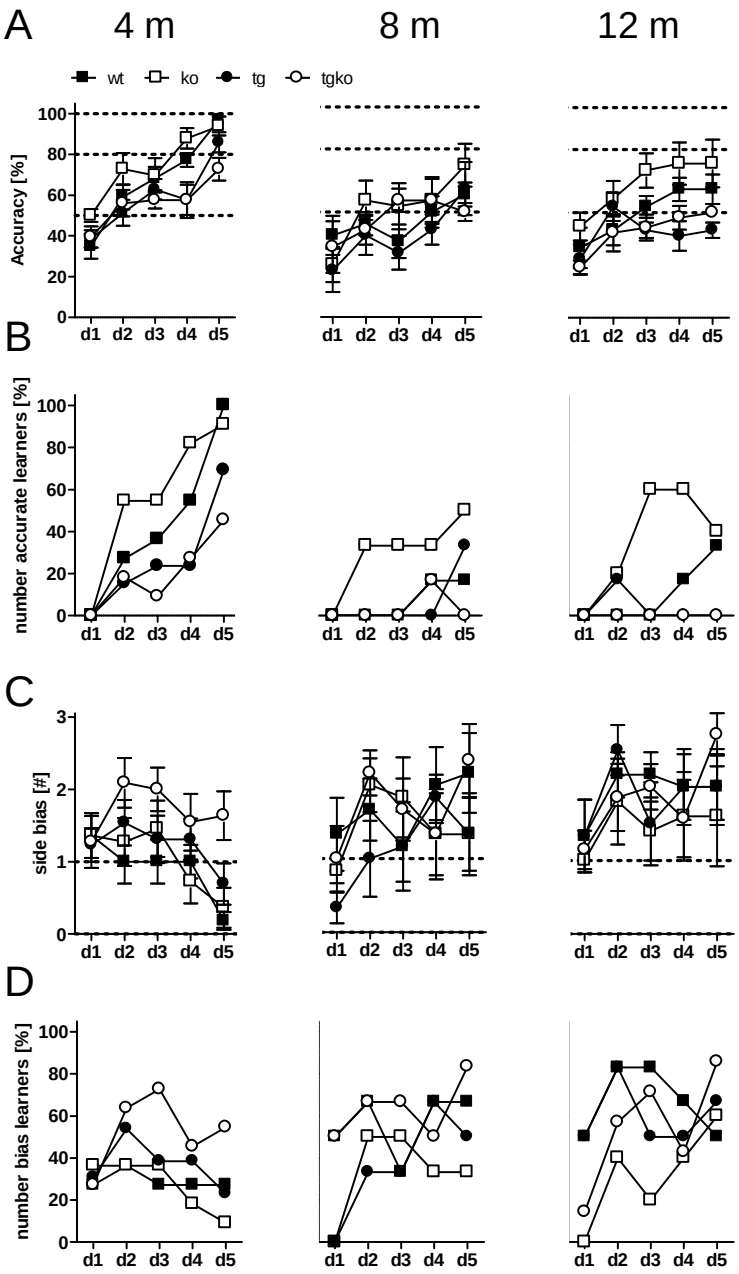

Figure 28. Loss of CRH-R1 in arcAß mice induces biased learning in the spatial protocol of the water cross maze (WCM). (A-D) Spatial learning was evaluated in wt, ko, tg and tgko mice at 4, 8 and 12 months of age. (A) Accuracy, (B) number of accurate learners, (C) side bias and (D) number of biased learners are shown. A: 4 months: wt-tgko d5 ($p < 0.05$); ko-tg d2 ($p < 0.05$), d4 ($p < 0.01$); 12 months: tg-ko d3 ($p < 0.05$), d4 ($p < 0.01$), d5 ($p < 0.05$); ko-tgko d3 ($p < 0.05$), d4 ($p < 0.05$); C: 4months: wt-tgko d5 ($p < 0.01$); ko-tgko d5 ($p < 0.05$). Data are presented as means ± SEM; n=6-12; Two-way repeated measures ANOVA, Bonferroni posttests.

Taken together, loss of CRH-R1 does not alter hippocampus-dependent spatial learning in arcAß mice, but induces a learning shift towards response learning in the WCM. In the spatial task, tgko mice at least developed a strategy, which was to apply always the same body turn. In the free-choice paradigm they were able to learn and accurately find the platform by applying a response learning strategy. Unlike tg mice, tgko littermates were unable to change their swimming strategy in the free-choice paradigm of the WCM due to a cognitive inflexibility and rigidity.

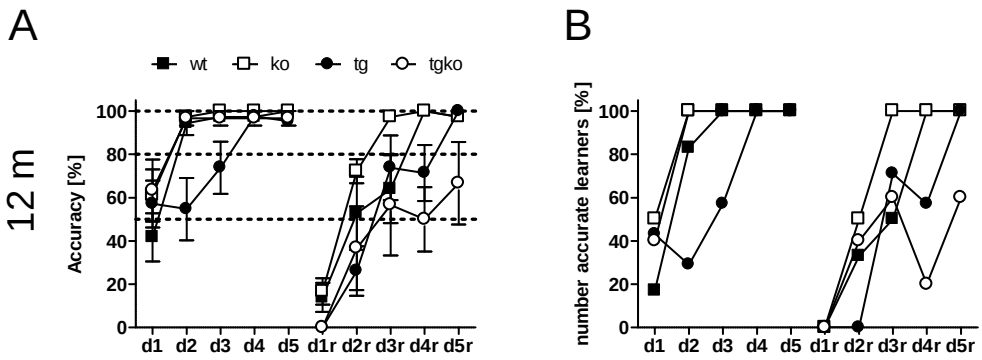

Figure 29. Tgko mice can solve the response learning task but have difficulties in cognitive flexibility in the free-choice paradigm of the WCM. The free-choice paradigm of the WCM was performed with wt, ko, tg and tgko mice aged 12 months. The response learning ability is assessed in the first week (d1-d5); cognitive flexibility is analyzed during the re-learning (r) trials (d1r-d5r) in the second week. (A) Accuracy and (B) number of accurate learners are shown. Week 1: tg-wt d2 ($p < 0.01$); ko-tg d2 ($p < 0.001$); tg-tgko d2 ($p < 0.01$); week 2: wt-tgko d4 ($p < 0.05$); tg-ko d2 ($p < 0.05$); tgko-ko d4 ($p < 0.05$). Data are expressed as means ± SEM; n=6-12; Two-way repeated measures ANOVA, Bonferroni posttests.

4.4.2.3. Evaluation of spontaneous object recognition memory

In order to test for declarative memory which depends on the hippocampus and the perirhinal cortex (PRh), arcAß CRH-R1KO mice (wt, ko, tg and tgko) aged 4 months were subjected to the spontaneous object recognition (OR) test (Figure 30). The recognition and preference of a novel object, which depends on temporal lobe areas, in particular the PRh (Aggleton and Brown, 1999;Bussey et al., 2000), was evaluated. Aggleton and Brown (1999) demonstrated that PRh-lesioned rats have impaired OR memory and that the hippocampus also contributes to the performance in this task, probably by combining spatial or contextual information with the specific object information processed by the PRh. We observed that tg mice do not discriminate between a novel and familiar object in the choice phase, whereas wt, ko and tgko mice do (Figure 30). Exploration time in the sample phase did not differ (wt:

27.7 ± 3.4 s; ko: 30.0 ± 4.3 s; tg: 32.1 ± 3.2 s; tgko: 33.1 ± 4.1 s). Interestingly, the loss of CRH-R1 in arcAß mice could at least partly compensate the learning deficit in tg mice (exploration %: wt: 68.4 ± 1.9, ko: 62.7 ± 2.6, tg: 53.77 ± 2.3, tgko: 64.3 ± 2.4).

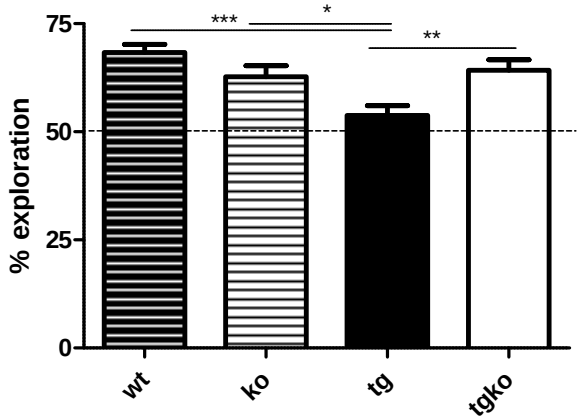

Figure 30. ArcAß mice have deficits in spontaneous object recognition (OR) memory which are rescued by disruption of CRH-R1. OR was conducted for wt, ko, tg and tgko mice at 4 months of age. Percentage exploration = novel object exploration time / total object exploration in the choice phase x 100%. Dotted line indicates the chance level of 50 %. Results are presented as means ± SEM; n=8; * $p < 0.05$, ** $p < 0.01$, *** $p < 0.001$, One-way ANOVA, Turkey´s multiple comparison posttest.

4.4.3. Electrophysiological evaluation in arcAß CRH-R1KO mice

Disruption of synaptic plasticity, caused by Aß oligomers rather than Aß plaques (Lesne et al., 2006;Oddo et al., 2003), is suggested to be the best pathological correlate to cognitive impairment (Gouras et al., 2010;Tampellini and Gouras, 2010). To identify the nature of this defect, electrophysiological studies have been conducted in diverse transgenic AD mouse models, foremost in the hippocampus as one of the major players in memory encoding.

To gain insight into these neuropathololgical features and in order to have a correlate to our cognitive findings, we performed long-term potentiation (LTP) measurements in the CA1 region of the hippocampus as well as long-term depression (LTD) measurements in the perirhinal cortex (PRh) of arcAß CRH-R1KO (wt, ko, tg, tgko) mice at the age of 12 months.

LTP in the CA1 area was not significantly altered between the four genotypes as indicated by traces of individual field excitatory postsynaptic potentials (fEPSPs) of wt, ko, tg and tgko mice (Figure 31A, B). Previously, LTP impairment was observed in arcAß mice at 3.5 and 7.5 months of age (Knobloch et al., 2007b). However, in our study tg mice tended to show increased fEPSPs (Figure 31A, B).

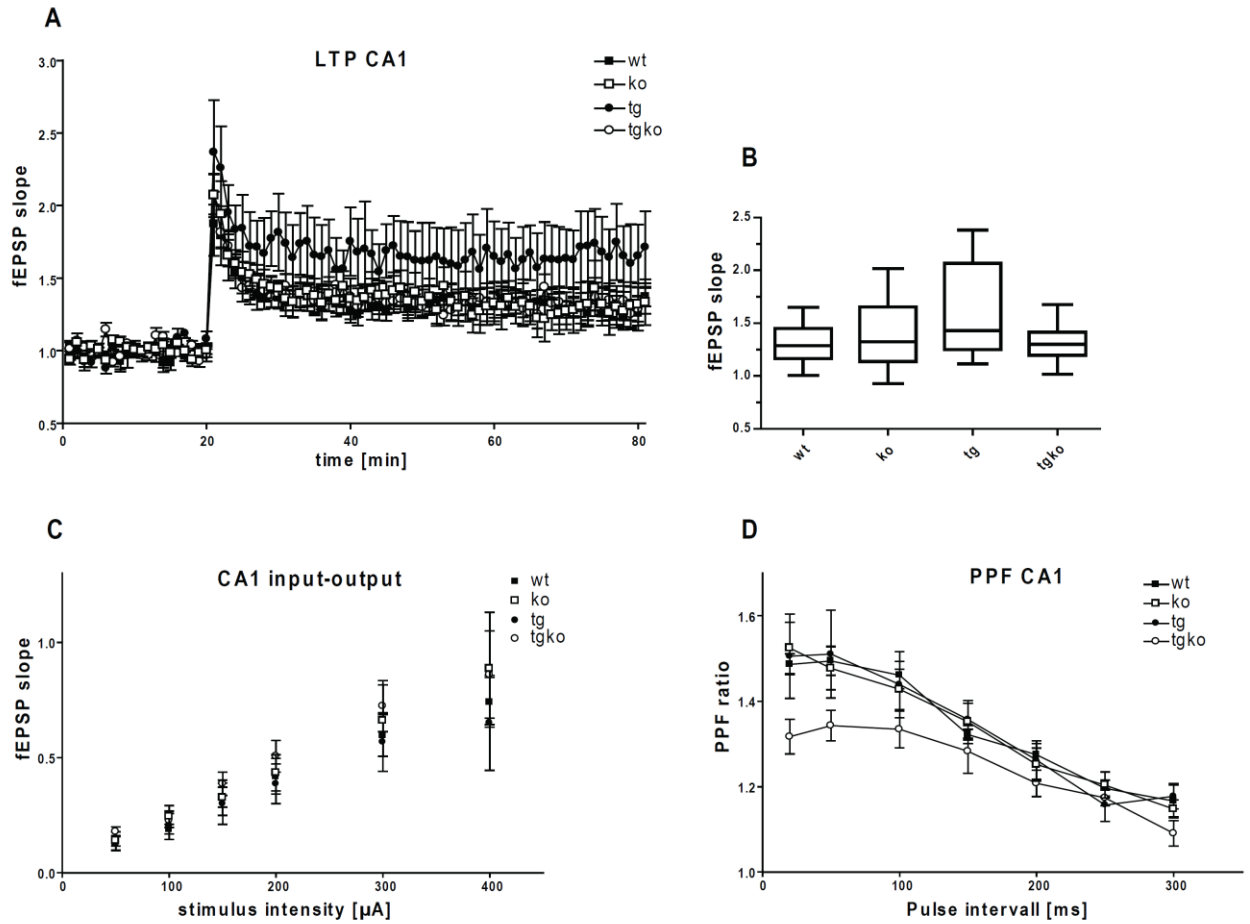

Figure 31. CA1 hippocampal long-term potentiation (LTP) is not altered in arcAß CRH-R1KO mice aged 12 months. (A) Individual fEPSP traces for wt, ko, tg and tgko. (B) Final 10 minutes of fEPSP slope. (C) Input-output curve. (D) Paired-pulse facilitation (PPF). Significances for a pulse interval of 20 ms: tgko vs. wt, tg ($p < 0.05$); tgko vs. ko ($p < 0.01$), Two-way ANOVA. Values represent means ± SEM; n=5-7.

Basal transmission was normal as indicated by the Input-output curve (Figure 31C). Paired-pulse facilitation (PPF), the ratio of the second response over the first response elicited with an interstimulus interval from 20 ms to 300 ms, is a marker for presynaptic release probability. Evaluation of the PPF ratio resulted in lower levels for tgko mice versus wt, tg ($p < 0.05$) and ko ($p < 0.01$) mice at a pulse interval of 20 ms indicating a higher release of glutamate from the presynaptic cell in tgko mice (Figure 31D).

LTD in the PRh of mice at 12 months did not differ between wt, ko, tg and tgko mice (Figure 32A, B). The input-output curve indicates normal basal transmission (Figure 32C).

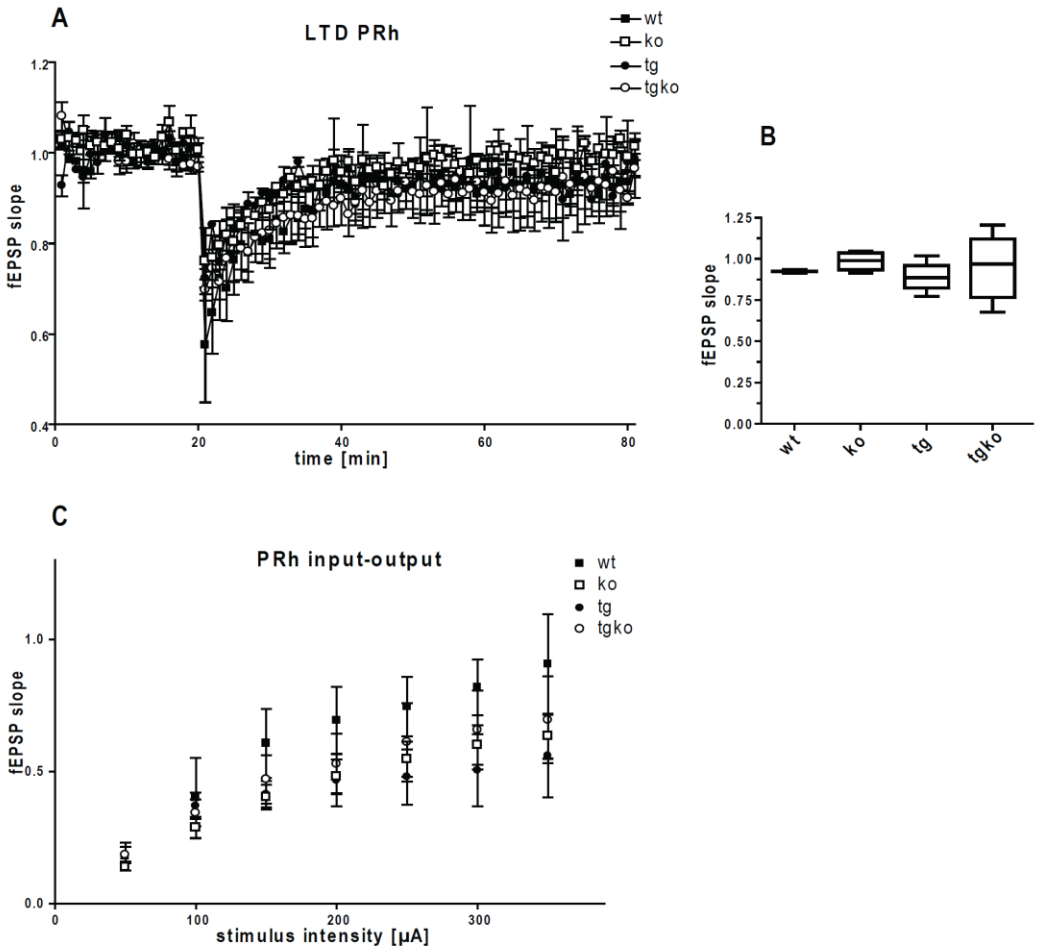

Figure 32. Long-term depression (LTD) in the perirhinal cortex (PRh) is not altered. (A) Individual fEPSP traces for wt, ko, tg and tgko. (B) Final 10 minutes of fEPSP slope. (C) Input-output curve. Values represent means ± SEM; n=5-7; One-way ANOVA.

4.4.4. Neuropathological analyses in arcAß CRH-R1KO mice

4.4.4.1. The influence of the CRH-R1 on Aß levels in arcAß mice

Aß accumulation has been shown to correlate with mnesic impairment (Selkoe, 2002). Since arcAß mice strongly overexpress APP, Aß levels and Aß plaque burden were investigated in arcAß CRH-R1KO mice to provide insight into the role of CRH-R1 in Aß generation in arcAß mice. We performed Sandwich ELISAs of $Aß_{38}$ (not shown), $Aß_{40}$ and $Aß_{42}$ levels in arcAß CRH-R1KO mice. We analyzed soluble and insoluble fractions of combined hippocampal and cortical tissue of tg vs. tgko mice aged 6.5, 9.5 and 12.5 months. Analyses revealed a significant reduction of insoluble levels of $Aß_{40}$ (tg: 1733.53 ± 319.90 ng/mg vs. tgko: 941.45 ± 226.92 ng/mg; $p < 0.01$) and $Aß_{42}$ (tg: 206.40 ± 25.36 ng/mg vs. tgko: 126.98 ± 28.09

ng/mg; $p < 0.01$) in tgko mice at 12.5 months of age (Figure 33A). In the soluble fraction a reduction of $Aß_{40}$ levels was observed in tgko mice at 9.5 months of age (tg: 447.25 ± 92.53 pg/mg vs. tgko: 238.95 ± 24.74 pg/mg; $p < 0.01$). Insoluble $Aß_{40}$ and $Aß_{42}$ did not differ between tg and tgko mice at 6.5 and 9.5 months, neither did soluble levels of 5.5 and 12.5 months aged animals. For all soluble values large deviations have to be taken into consideration.

To exclude that differences in Aß levels are due to altered APP processing, lysates of the soluble (DEA) fraction were analyzed by Western blotting. Immunoblot analysis of the soluble fraction of tg and tgko mice at 7, 9.5 and 12.5 months for APP (22C11), αAPPs (Aß rod), βAPPs (192 wt) and huAPP (5313) (Figure 33B) revealed no differences in tg vs. tgko mice, implying that alterations of Aß levels in the ELISA were not due to changes in APP processing.

In summary, $Aß_{40}$ and $Aß_{42}$ levels in hippocampal and cortical tissue of tgko compared to tg mice at 12.5 months were reduced, as was soluble $Aß_{40}$ at 9.5 months, while APP processing was unchanged.

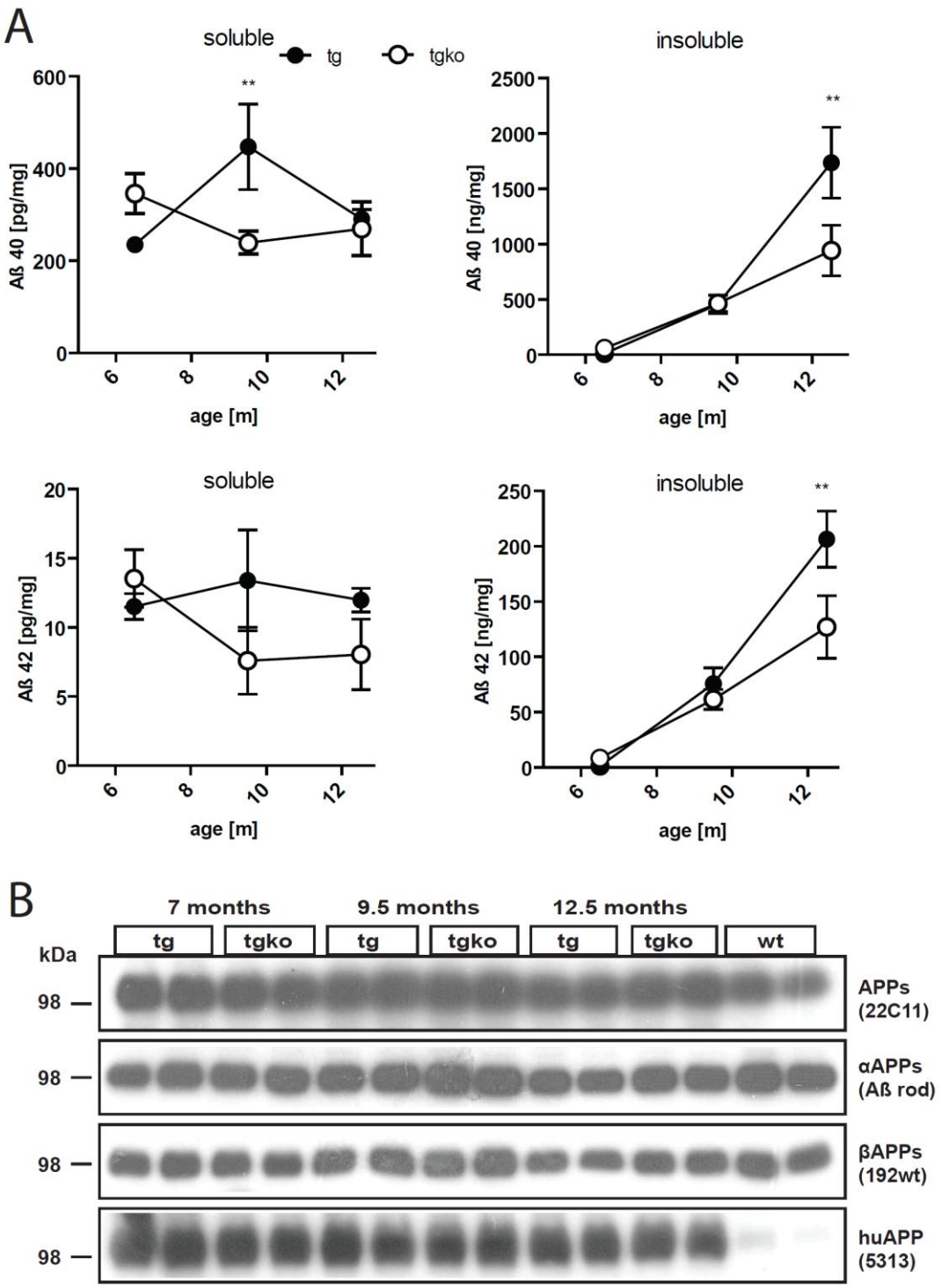

Figure 33. Aß levels are reduced in tgko mice compared to tg mice. (A) Determination of the amounts of soluble and insoluble $Aß_{40}$ and $Aß_{42}$ by ELISA in tg and tgko mice. Data are presented as means ± SEM; n=7-13; ** $p < 0.01$, Two-way ANOVA, Bonferroni posttests. (B) Immunoblot analysis of soluble fraction of tg and tgko mice at 7, 9.5 and 12.5 months for APP (22C11), αAPPs (Aß rod), βAPPs (192 wt) and huAPP (5313) in order to reveal differences in APP processing in tg vs. tgko mice. Antibodies used for detection of APP isoforms are depicted in brackets at the right. Wild-type (wt) extracts served as a control.

4.5. APP processing in CRH-R1KO mice

To exclude that alterations in Aß levels in arcAß CRH-R1KO mice are not due to changes in endogenous APP processing in CRH-R1-deficient mice, we analyzed hemispheres of CRH-R1KO (ko) mice (Timpl et al., 1998). After gel electrophoresis of the soluble diethylamine (DEA) fraction (see 3.2.6 Extraction and quantification of secreted Aß and APP processing forms), Western blotting was conducted with antibodies against total sAPP (22C11; for binding specificity see Figure 12) and against sAPPβ (192wt). Levels of total sAPP and sAPPβ were indistinguishable between ko and wt mice (Figure 34) aged 3 months, indicating similar expression of endogenous APP in ko mice and no preferred cleavage by α- or β-secretase (BACE1).

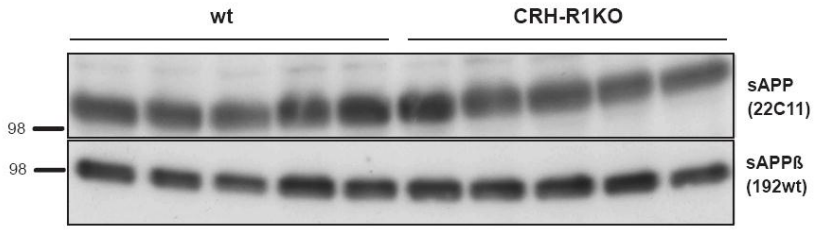

Figure 34. Endogenous sAPP levels in CRH-R1KO (ko) mice do not differ from wild-type (wt) littermates. Diethylamine (DEA) fraction of wt and ko mice aged 3 months. Antibodies against sAPP (22C11) and sAPPß (192wt) were used for detection. Protein sizes are depicted in kDa.

Beta-secretase (BACE1) is supposed to play a crucial role in the myelination of peripheral nerve cells. Consistently, expression of BACE1 in mice was found to be highest in early postnatal stages, declined in the second postnatal week and decreased onwards to low levels in adult mice (Willem et al., 2006).

To get more detailed insights into APP processing in CRH-R1KO mice, we analyzed brains of CRH-R1KO mice (ko, heterozygous and wt) at P5.5 with respect to BACE1 regulation. To this end, membranes were prepared. In addition, expression of APP (22C11) and α-secretase (ADAM 10) were analyzed (Figure 35A). The DEA fraction (see 3.2.6 Extraction and quantification of secreted Aß and APP processing forms) was analyzed regarding total sAPP (22C11), sAPPβ (192wt) and sAPPα (Figure 35B). Although the Western blot suggests that more APP is expressed in wt mice (lane 1-3, Figure 35A, B), levels of α-secretase (ADAM) and β-secretase (BACE1) remained the same in wt, heterozygous and total ko mice (Figure 35B). Accordingly, the levels of the processing products (sAPP, sAPPβ, sAPPα) were not changed (Figure 35 B).

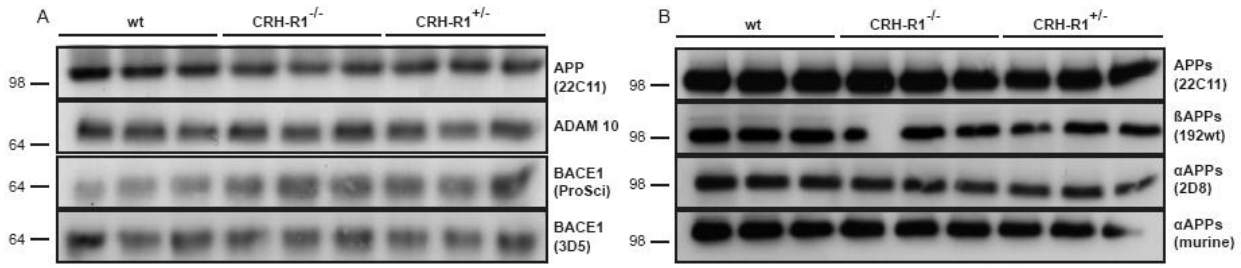

Figure 35. BACE and ADAM activity in CRH-R1KO mice at P5.5. Brains of wild-type (wt), homozygous (CRH-R1$^{-/-}$) and heterozygous (CRH-R1$^{+/-}$) CRH-R1KO mice at P5.5. (A) Membrane preparation reveals levels of APP (22C11), ADAM 10 and BACE1 (ProSci and 3D5). (B) DEA fractions were analyzed with respect to sAPP (22C11), sAPPß (192wt) and αAPPs (2D8 and murine). Protein sizes are depicted in kDa.

4.5.1.1. The influence of the CRH-R1 on Aß plaque formation in arcAß mice

To further substantiate the biochemical findings in arcAß CRH-R1KO mice we conducted a detailed plaque analysis. Plaque number (Figure 36A, D), the area occupied by plaques (Figure 36B, E) and the mean plaque area (Figure 36C, F) within the hippocampus and prefrontal cortex (PFC) were determined. For the prefrontal cortex (PFC) 3-4 coronal sections from bregma +2.22 to +1.78 mm and for the hippocampus 3 sections from bregma -1.70 to -2.06 mm per animal were chosen according to the stereotaxic atlas (Paxinos and Franklin, 2001). Sections of tg vs. tgko mice at 9.5 and 12.5 months of age were stained with antibody A2275 specific for the N-terminus of human amyloid ß. Photomicrographs were taken and analyzed automatically using the particle measurement programme of ImageJ. In the PFC similar Aß plaque load and appearance were found in tg and tgko mice at 9.5 and 12.5 months of age (Figure 36D, E, F). In the hippocampus the plaque number, the area occupied by plaques and the mean plaque area increased with age in both genotypes (Figure 36A, B, C). Furthermore, the number of plaques in the hippocampus was significantly decreased in tgko mice compared to tg mice at 12.5 months of age (tg: 26.68 ± 3.61 vs. tgko: 13.47 ± 2.09; $p < 0.01$). The plaque area at 9.5 months (tg: 0.375 ± 0.04 vs. tgko: 0.23 ± 0.03; $p < 0.05$) and at 12.5 months (tg: 1.61 ± 0.32 vs. tgko: 0.65 ± 0.12; $p < 0.01$) was also decreased in tgko mice compared to tg littermates.

Taken together, the number of plaques and the area occupied by plaques were reduced in the hippcampus of tgko mice at 12.5 months, as was the area occupied by plaques in the hippocampus at 9.5 months.

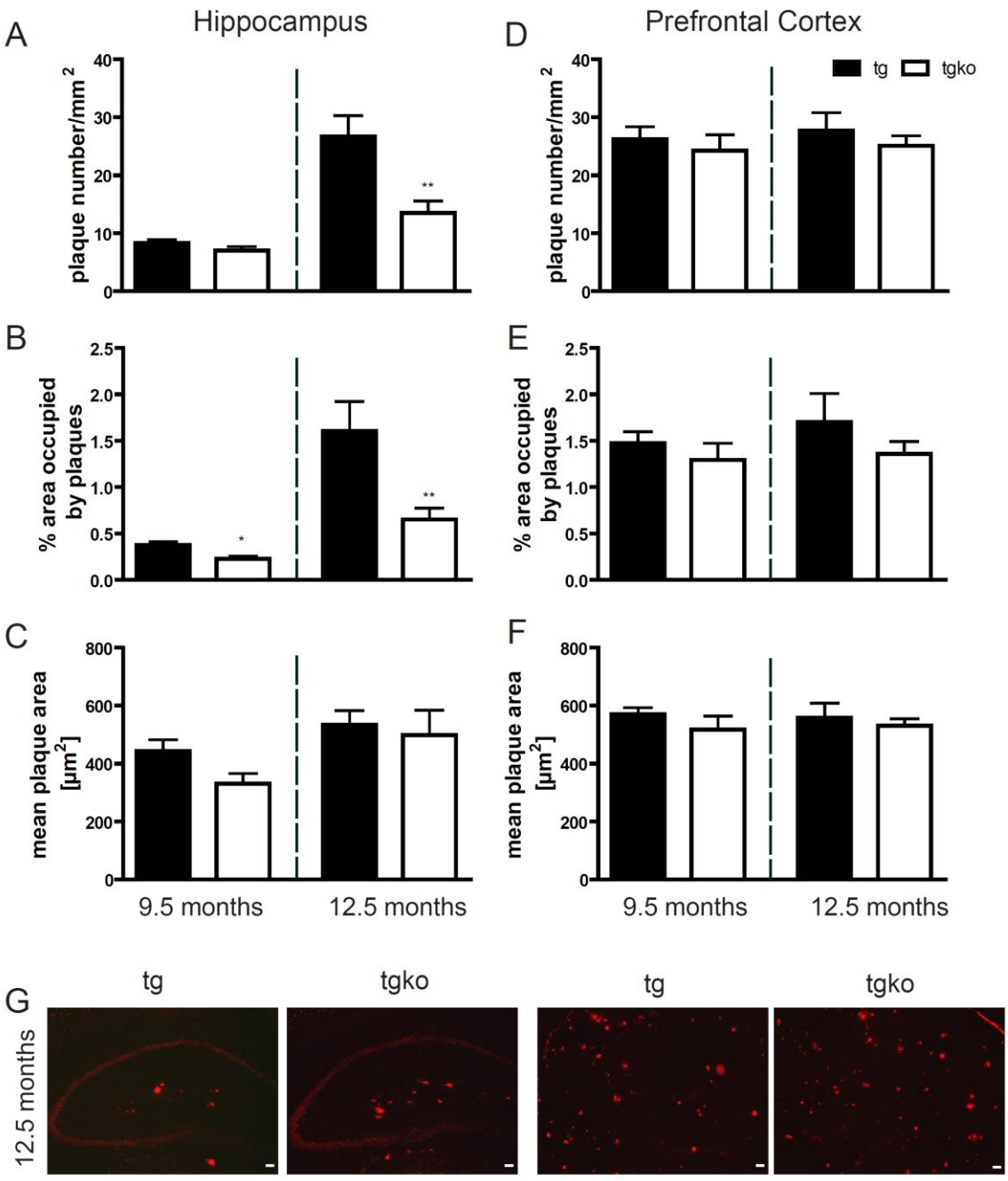

Figure 36. Loss of CRH-R1 reduces Aß plaque formation in the hippocampus of arcAß mice. A detailed analysis of plaque quantification was conducted to determine (A, D) the plaque number, (B, E) the area occupied by plaques and (C, F) the mean plaque area of tg (solid bar) and tgko (open bar) mice (A, B, C) in the hippocampus (bregma -1.70 to -2.06 mm) and (D, E, F) the prefrontal cortex (bregma +2.22 to +1.78 mm) at 9.5 and 12.5 months of age. (G) Photomicrographs show Aß immunostaining of the hippocampus (left) and the prefrontal cortex (right). Analysis is based on anti Aß-immunoreactivity (antibody A2275, red, specific for the N-terminus of human Aß). Data are presented as means ± SEM; n=4-8; * $p < 0.05$, ** $p < 0.01$, Student´s t-test.

4.5.1.2. The influence of the CRH-R1 on neuroinflammation in arcAß mice

Infiltration of activated microglia and astrocytes is observed in the brains of human AD patients and transgenic AD mouse models (Stalder et al., 1999;Matsuoka et al., 2001) as a response to injury in the brain. To dissect the role of CRH-R1 deficiency in this context we performed co-stainings of Aß plaques with markers for microglia and astrocytes in the hippocampus and prefrontal cortex (PFC) of tg vs. tgko mice aged 9.5 and 12.5 months, respectively. Results are exemplarily depicted for the PFC of mice at 12.5 months of age (Figure 37A-C). Astrocytes, stained for glial fibrillary acidic protein (GFAP, red), are similarily distributed around Aß plaques (A2275, green) of tg and tgko mice (Figure 37A). Also, microglia surrounding Aß plaques in tg and tgko mice show similar spatial distributions and frequencies (Figure 37B, C). Figure 37B shows microglia stained with tomato lectin (green) around Aß plaques (A2275, red); in Figure 37C microglia are detected by expression of ionized calcium-binding adaptor molecule 1 (Iba-1, red), Aß plaques by 6E10 antibody specific for the 1-17 fragment of human Aß (green). No differences in infiltration of microglia and astrocytes were to be seen in tg vs. tgko mice.

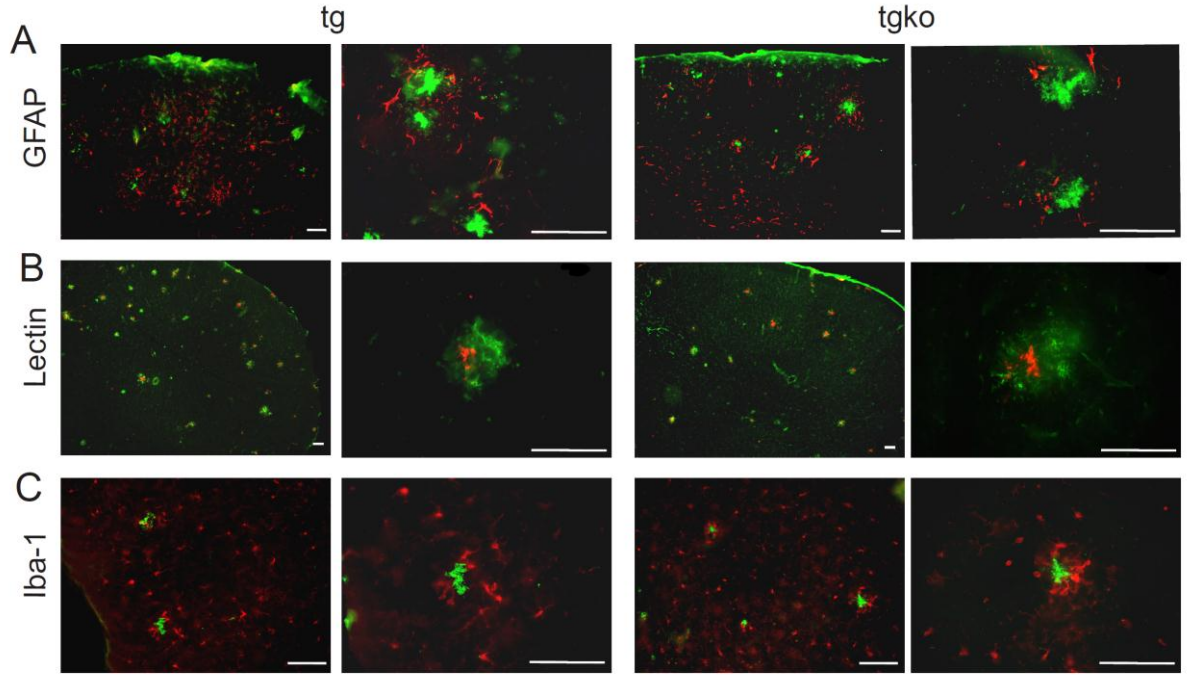

Figure 37. Microglia and astrocytes are equally accumulated around plaques in tg and tgko mice. (A-C) Inflammation in the prefrontal cortex of tg and tgko mice at 12.5 months of age. (A) Astrocytes (GFAP, red) are assembled around Aß plaques (A2275, green). (B, C) Microglia surrounding Aß plaques are present in tg and tgko mice; (B) Microglia (tomato lectin, green) and Aß plaques (A2275, red); (C) Microglia (Iba-1, red) and Aß plaques (6E10, green). Scale bars, 100 µm.

4.6. Basal characterization of CRH-COE^{CNS} mice

To elucidate the effects of CRH in the context of AD, we used mice with conditional, CNS restricted overexpression of CRH (CRH-COE^{CNS}, generated by Lu et al. 2008). CRH-COE^{CNS} mice were screened for basal emotionality to assess effects of potential phenotypes on cognitive performance of arcAß CRH-COE^{CNS} mice. In general, CRH-COE^{CNS} mice were hyperactive and aroused during handling in all experiments.

4.6.1. Assessment of bodyweight in CRH-COE^{CNS} mice

Bodyweight in CRH-COE^{CNS} mice (coe) was significantly reduced at 4 months of age ($p < 0.01$). At the age of 8 and 12 months coe mice showed a tendency towards decreased bodyweight (Figure 38).

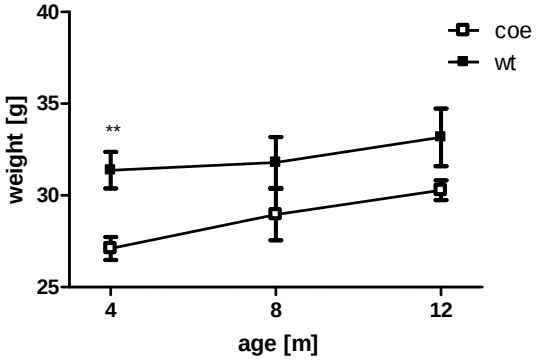

Figure 38. The bodyweight of CRH-COE^{CNS} (coe) mice is reduced compared to their wild-type (wt) littermates. Data are presented as means ± SEM; n=11-13; ** $p < 0.01$, Student´s t-test.

4.6.2. HPA axis functionality in CRH-COE^{CNS} mice

HPA axis activity, reflected by corticosterone levels, in coe mice at 12 months of age was determined (Figure 39). Under basal housing conditions plasma corticosterone levels were indistinguishable between wt and coe mice. In contrast, plasma corticosterone levels after acute stress (10 min restraint) were significantly increased in coe mice compared to control littermates, indicating an exaggerated activation of the HPA axis in response to stress. These results confirm previous findings by Lu and colleagues (2008).

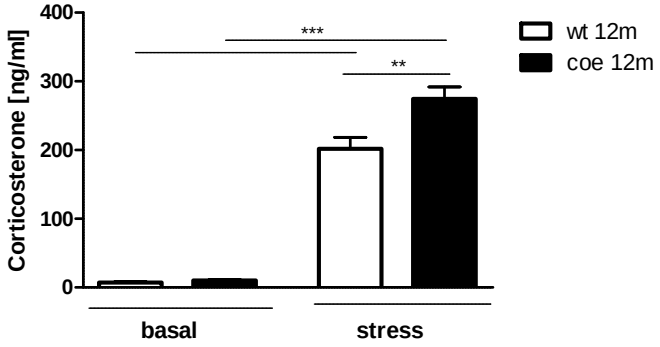

Figure 39. The HPA axis in coe mice is hyperreactive to stress.
Corticosterone levels were assessed in wt vs. coe mice at basal conditions and following stress (10 min restraint) at 12 months of age. Results are presented as means ± SEM; n=11-13; ** $p < 0.01$, *** $p < 0.001$, Student´s t-test.

4.7. Assessment of basal emotionality in CRH-COE^{CNS} mice

The characterization of emotional behavior, including locomotion, anxiety-related and stress-coping behavior was conducted in coe vs. wt mice at 4, 8 and 12 months of age.

4.7.1.1. Assessment of locomotion in CRH-COE^{CNS} mice

Locomotion of coe mice at all ages was increased in the open field (OF) (Figure 40A, B) and in the Y-maze task (Figure 40C).

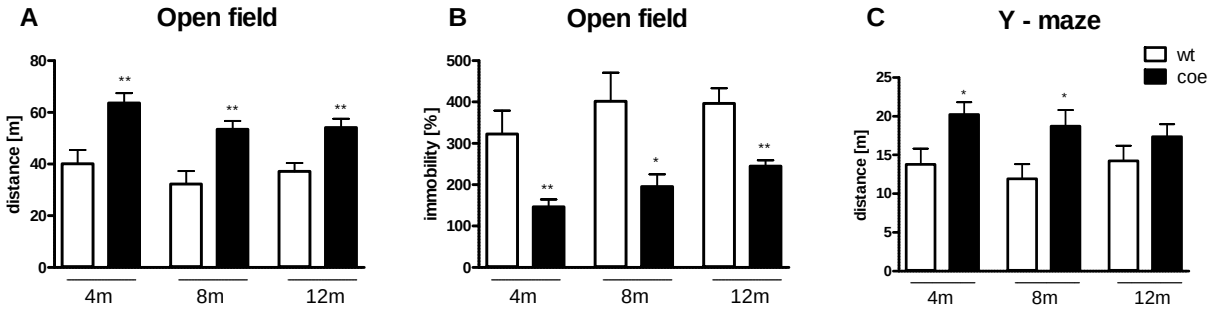

Figure 40. Locomotion is increased in coe mice. (A) Distance travelled and (B) immobility in the open field and (C) distance travelled in the Y-maze task are presented in wt vs. coe mice at 4, 8 and 12 months of age. Data are expressed as means ± SEM; n=11-13; * $p < 0.05$, ** $p < 0.01$, Student´s t-test.

4.7.1.2. Assessment of anxiety-related behavior in CRH-COE^{CNS} mice

Anxiety-related behavior of coe mice was assessed in the dark/light box (DaLi) and the OF. Additionally, the elevated plus maze test was performed, but the results cannot be taken into account since a huge proportion of mice dropped off the maze and remaining numbers were too small. Coe mice aged 4 months showed a significant increase in the time spent in the lit compartment of the DaLi (Figure 41A), indicating a less anxious phenotype. In the OF no alteration in anxiety-related behavior was detected between coe and wt mice at 4, 8 and 12 months (Figure 41B).

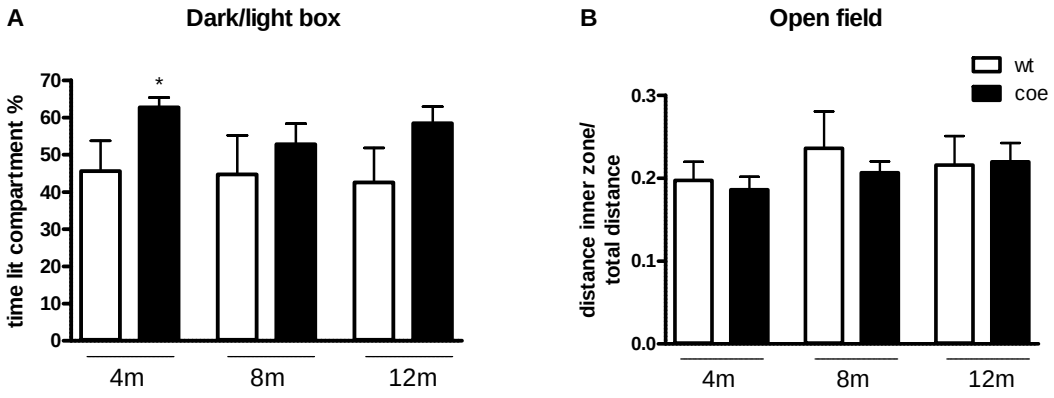

Figure 41. Anxiety-related behavior is reduced in coe mice. (A) Time in the lit compartment of the dark/light box and (B) the distance in the inner zone/total distance in the open field were determined in order to assess anxiety-related behavior in coe vs. wt mice at 4, 8 and 12 months of age. Data are presented as means ± SEM; n=11-13; * $p < 0.05$, Student´s t-test.

4.7.1.3. Assessment of stress-coping behavior in CRH-COE^{CNS} mice

Lu and colleagues demonstrated that coe mice show enhanced active stress-coping behavior (Lu et al., 2008). We could partly confirm these results as we observed that coe mice aged 12 months float less (Figure 42C). However, we could not observe enhanced active stress-coping behavior in coe mice at the age of 4 months (Figure 42A-C).

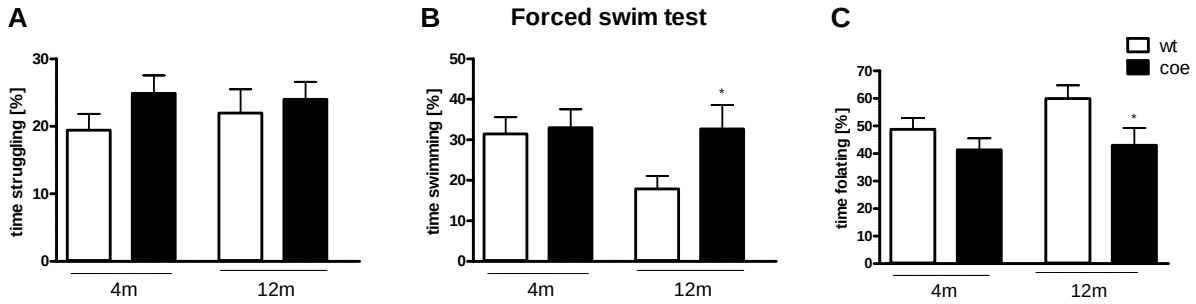

Figure 42. Coe mice show enhanced active stress-coping behavior at 12 months of age in the forced swim test. Coe and wt mice were analyzed regarding time (A) struggling, (B) swimming and (C) floating at 4 and 12 months of age. Data are presented as means ± SEM; n=11-13. * $p < 0.05$, Student´s t-test

4.8. The impact of CRH overexpression on the onset and pathology of AD

To study the impact of CRH overexpression in an AD mouse model, arcAß mice were bred to CRH-COE^{CNS} mice according to the breeding scheme depicted in Figure 43. Four genotypes of interest of arcAß CRH-COE^{CNS} mice were generated and subjected to comprehensive phenotyping: wild-type (wt), transgenic arcAß (tg), CRH-COE^{CNS} (coe) and transgenic arcAß CRH-COE^{CNS} (tgcoe).

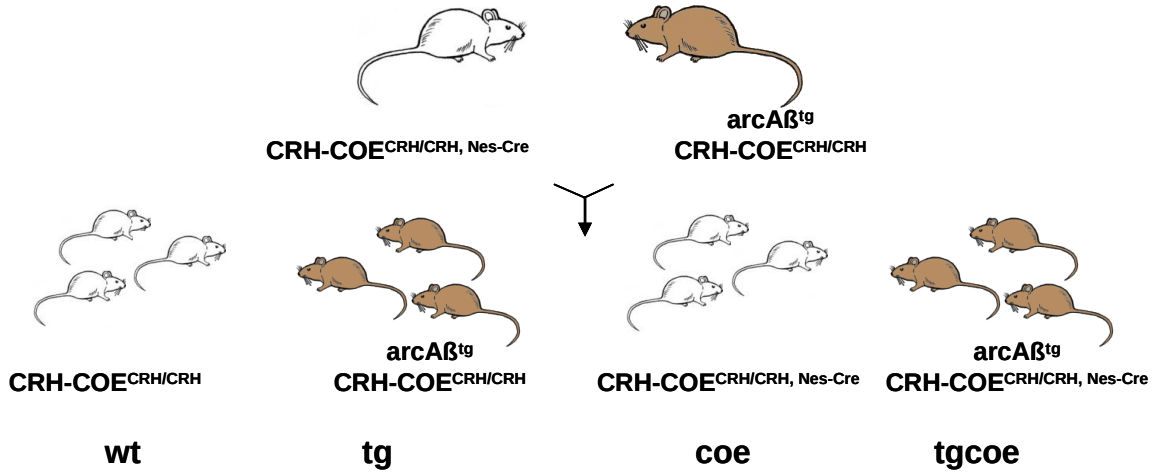

Figure 43. Breeding scheme of arcAß CRH-COE^{CNS} mice. Four genotypes were generated: wild-type (wt), transgenic arcAß (tg), CRH-COE^{CNS} (coe) and transgenic arcAß CRH-COE^{CNS} (tgcoe). Brown fur color indicates mice carrying the arcAß transgene.

4.8.1. HPA axis functionality in arcAß CRH-COE^{CNS} mice

Plasma corticosterone levels were assessed in tg vs. tgcoe mice at 12 months of age. Assessment revealed elevated basal ($p = 0.056$) and stress ($p < 0.05$) levels in tgcoe mice (Figure 44) indicating an hyperactivated and hyperreactive HPA axis in those mice.

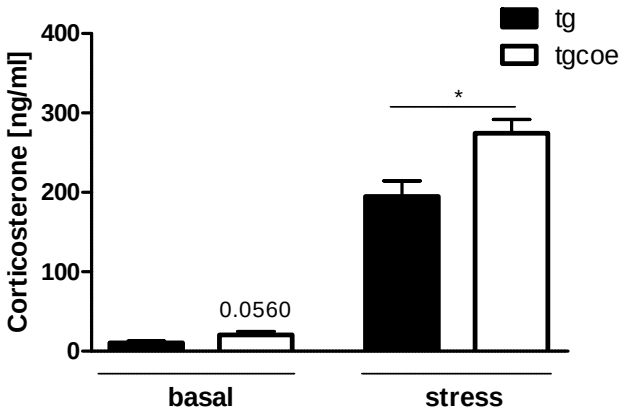

Figure 44. HPA axis is hyperactivated and hyperreactive in tgcoe compared to tg mice.
Basal and stress-induced plasma corticosterone levels in tg vs. tgcoe mice at 12 months of age. Results are presented as means ± SEM; n=11-13; * $p < 0.05$, Student´s t-test.

4.8.2. Testing cognitive performance of arcAß CRH-COE^{CNS} mice

Similar to the assessment of cognition in arcAß CRH-R1KO mice, the cognitive abilities were investigated in arcAß CRH-COE^{CNS} mice. Four genotypes, wild-type (wt), CRH-COE^{CNS} (coe), arcAß transgenic (tg) and arcAß transgenic CRH-COE^{CNS} (tgcoe), were submitted to the Y-maze, the spatial paradigm of the water cross maze (WCM) and the spontaneous object recognition (OR) task.

4.8.2.1. Evaluation of spontaneous alternation in the Y-maze task

In the Y-maze task, mice can choose between three different arms to explore, each presenting a different symbol at its end. Spontaneous alternation, assessed in the Y-maze, is a natural tendency of rodents to explore different arms of a maze on successive runs (Middei et al., 2004). During a 5 min test session the sequence of arm entries was recorded and alternation calculated as successive entries into the three arms in overlapping triplet sets. Spontaneous alternation was not significantly altered in wt, coe, tg and tgcoe mice at 4, 8 and 12 months of age (Figure 45).

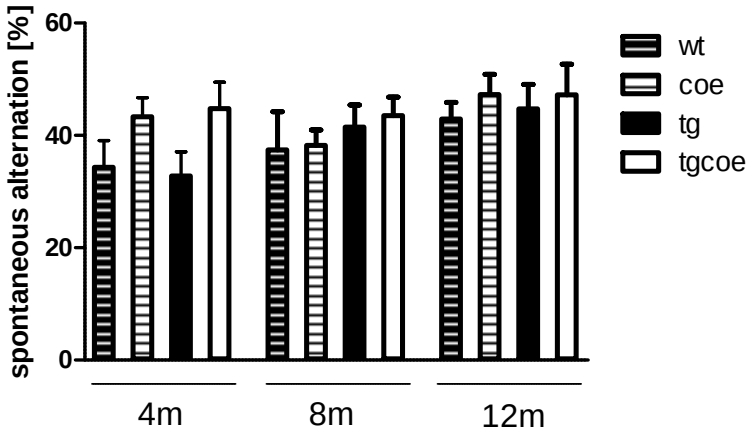

Figure 45. Spontaneous alternation is not significantly altered in arcAß CRH-COE^{CNS} mice. Wt, coe, tg and tgcoe mice at the age of 4, 8 and 12 months were submitted to the Y-maze task to test spontaneous alternation. Percent alternation was calculated as the ratio of actual to possible alternations (defined as the total number of arm entries−2) × 100 %. Results are presented as means ± SEM; n=11-13, One-way-ANOVA.

4.8.2.2. Performance in the water cross maze (WCM) task

Wt, coe, tg and tgcoe mice aged 8 months were subjected to the spatial paradigm of the WCM. Accuracy was clearly reduced in tg and tgcoe mice compared to wt and coe mice (Figure 46A, B). None of the tg animals passed the chance level of 50 %. These findings indicate a decline in hippocampus-dependent spatial learning in tg mice with or without CRH overexpression compared to non-tg mice. Side bias did not significantly deviate between the genotypes (Figure 46C, D).

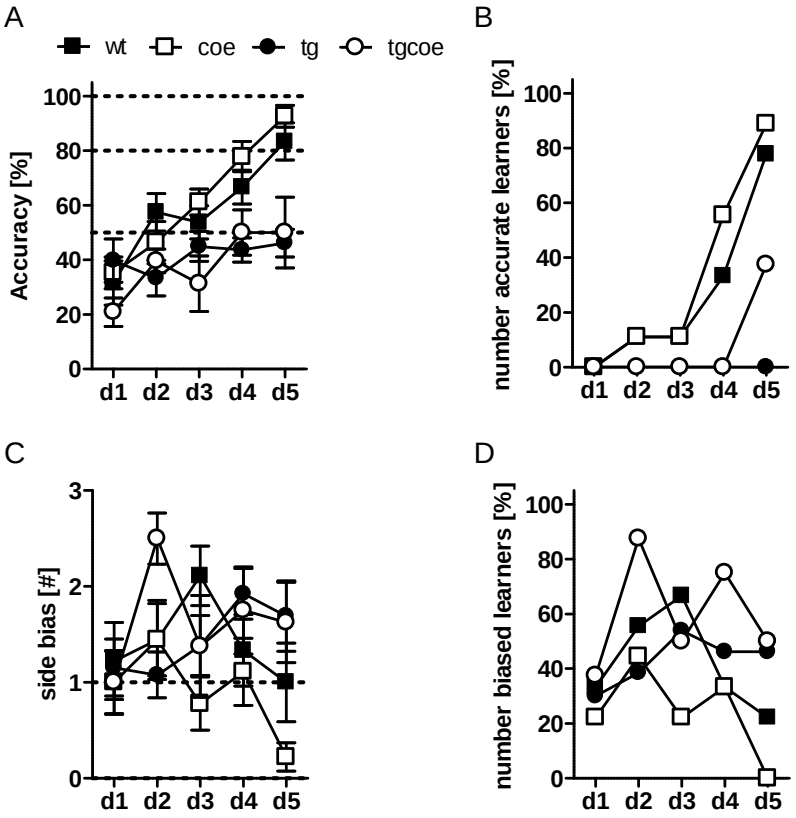

Figure 46. CRH overexpression does not alter spatial performance of arcAß mice in the WCM task. (A-D) Spatial learning was evaluated in wt, coe, tg and tgcoe mice at 8 months of age. (A) Accuracy, (B) number of accurate learners, (C) side bias and (D) number of biased learners are shown. A: wt-tg d2 *, d5 ***; wt-tgcoe d5 ***; coe-tg d4 **, d5 ***; coe-tgcoe d3 *, d4 *, d5 ***. Data are presented as means ± SEM; n=6-12; * $p < 0.05$, ** $p < 0.01$, *** $p < 0.001$, Two-way repeated measures ANOVA, Bonferroni posttests.

4.8.2.3. Evaluation of spontaneous object recognition memory

ArcAß CRH-COE^{CNS} mice were tested for spontaneous object recognition at the age of 4 months (Figure 47). Contrary to wt mice, which discriminated between novel and familiar object (67.03 ± 9.95 %), coe (48.93 ± 12.59 %) and tg (50.80 ± 16.16 %) mice were not able to discriminate, i.e. their exploration score was at the chance level. Tgcoe mice (55.25 ± 10.89 %) did not significantly differ in the task compared to wt mice, although their exploration score was low and below the predicted ability of object distinction. However, no additive effects of the tg and coe phenotype were seen in the OR performance of tgcoe mice.

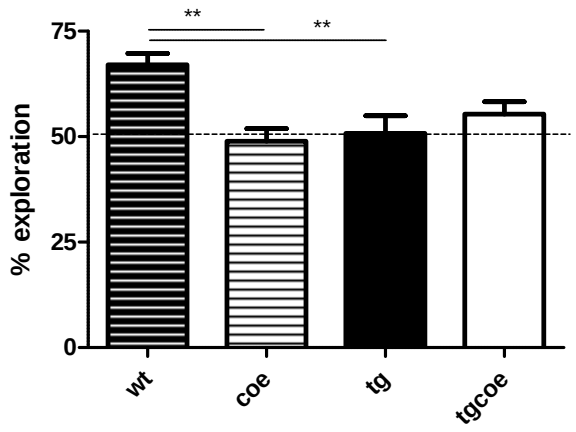

Figure 47. Tg and coe mice are impaired in performing the spontaneous object recognition (OR) task. OR was conducted for wt, coe, tg and tgcoe mice at 4 months of age. Percentage exploration = novel object exploration time / total object exploration in the choice phase x 100%. Results are presented as means ± SEM; n=8; ** $p < 0.01$, One-way ANOVA, Turkey´s multiple comparison posttest.

4.8.3. Neuropathological analyses in arcAß CRH-COE^{CNS} mice

4.8.3.1. The influence of CRH overexpression on Aß levels in arcAß mice

In order to investigate the impact of CRH overexpression on Aß generation in brains of arcAß mice, we performed a Sandwich ELISA for $Aß_{38}$ (not shown), $Aß_{40}$ and $Aß_{42}$ on brain extracts from tg vs. tgcoe mice at the age of 5.5, 9 and 11.5 months. Therefore, combined hippocampal and cortical tissue was processed to a soluble and insoluble fraction. Results revealed elevated $Aß_{40}$ and $Aß_{42}$ levels in both the soluble and insoluble fraction for tgcoe mice at 11.5 months, significant for the insoluble levels (Figure 48A) ($Aß_{40}$: tg: 1692.66 ± 155.14 ng/mg vs. tgcoe: 2366.01 ± 239.70 ng/mg; $p < 0.01$ and $Aß_{42}$: tg: 237.98 ± 16.85 ng/mg vs. tgcoe: 316.87 ± 21.03 ng/mg; $p < 0.001$). In the soluble fraction $Aß_{40}$ and $Aß_{42}$ levels were already increased at the age of 9 months, but due to high variability this effect was not significant. Insoluble Aß did not differ between tg and tgcoe at 9 months. For the earliest time point no differences in either fraction were observed.

To preclude that altered Aß levels are a consequence of a modified APP processing in arcAß CRH-COE^{CNS} mice, lysates of the soluble (DEA) fraction were analyzed by Western blotting. Immunoblot analysis of the soluble fraction of tg and tgcoe mice at 6, 9 and 12 months for APP (22C11), αAPPs (Aß rod), βAPPs (192 wt) and huAPP (5313) (Figure 48B) revealed no differences in tg vs. tgcoe mice, implying that alterations of Aß levels in the ELISA are not due to shifted APP processing.

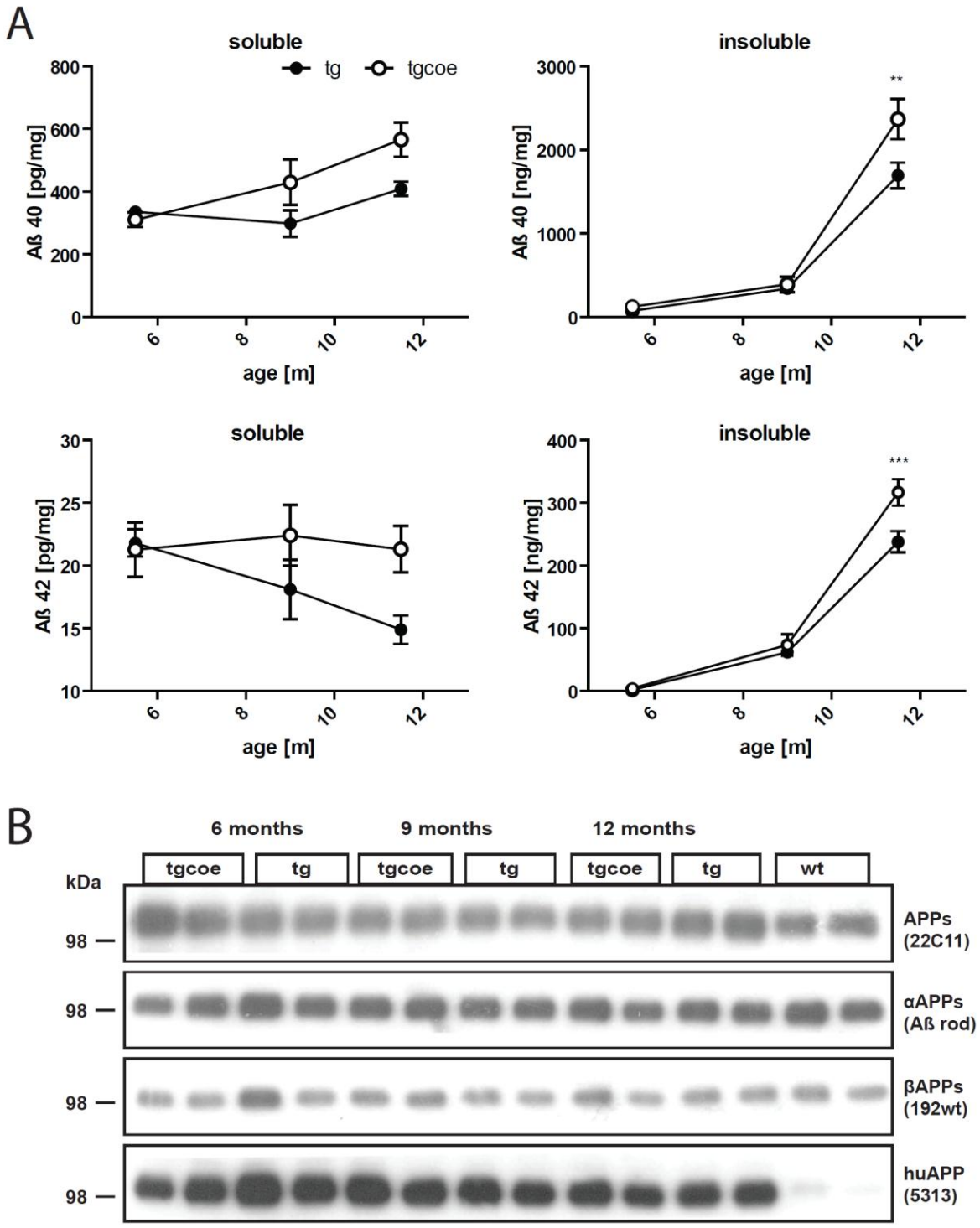

Figure 48. Aß levels are increased in tgcoe mice compared to tg mice. (A) Determination of the amounts of soluble and insoluble $Aß_{40}$ and $Aß_{42}$ by ELISA in tg and tgcoe mice at different time points. Data are presented as means ± SEM; n=7-13; ** $p < 0.01$, Two-way ANOVA, Bonferroni posttests. (B) Immunoblot analysis of soluble fraction of tg and tgcoe mice at 6, 9 and 12 months for APP (22C11), αAPPs (Aß rod), βAPPs (192 wt) and huAPP (5313) in order to reveal differences in APP processing in tg vs. tgcoe mice. Wild-type (wt) samples served as a negative control.

4.8.3.2. The influence of CRH overexpression on Aß plaque formation in arcAß mice

To further substantiate the biochemical findings of arcAß CRH-COE^{CNS} mice we conducted a detailed plaque analysis. Plaque number (Figure 49A, D), the area occupied by plaques (Figure 49B, E) and the mean plaque area (Figure 49C, F) in the hippocampus (bregma -1.70 to -2.06 mm) and prefrontal cortex (PFC, bregma +2.22 to +1.78 mm) were determined. Therefore, sections of tg vs. tgcoe mice at 9 and 12 months of age were stained with the antibody A2275 specific for the N-terminus of human amyloid ß. Photomicrographs were taken and analyzed automatically using the particle measurement programme of ImageJ.

In the PFC a similar Aß plaque load and appearance of plaques was observed in tg and tgcoe mice at 9 and 12 months of age with a general increase in plaque number from 9 to 12 months (Figure 49D, E, F). In the hippocampus of mice aged 9 months the plaque number was significantly increased in tgcoe compared to tg, as was the area occupied by plaques (not significant) but not the size of the individual plaques (Figure 49A, B, C). The hippocampi of arcAß CRH-COE^{CNS} mice aged 12 months did not show alterations regarding plaque number, area occupied by plaques or mean plaque area compared to arcAß control mice.

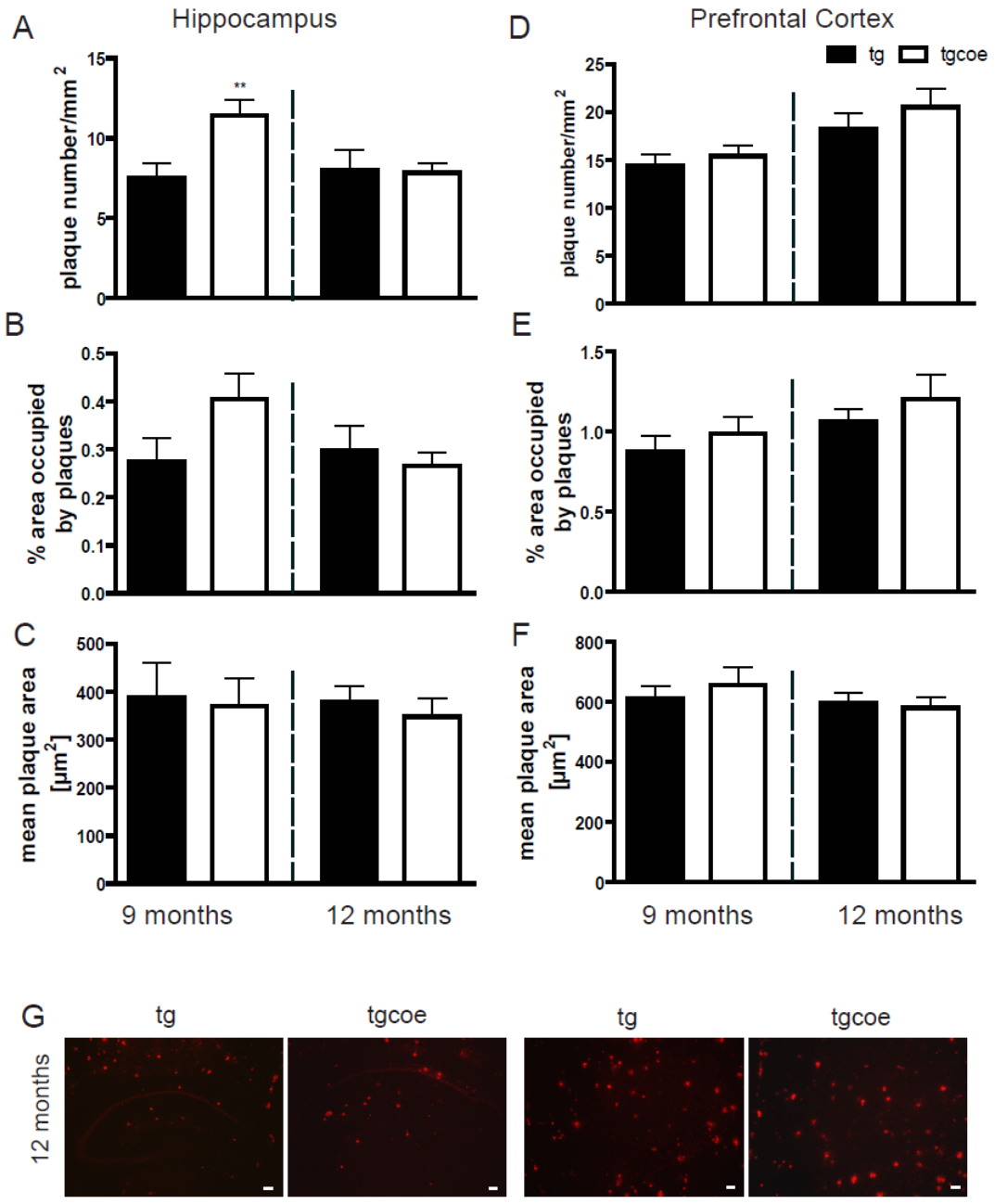

Figure 49. CRH overexpression increases hippocampal plaque load at 9 months. A detailed quantification of plaques was conducted to determine (A, D) plaque number, (B, E) percentage area occupied by plaques and (C, F) mean plaque area of tg (solid bar) and tgcoe (open bar) in the hippocampus (bregma -1.70 to -2.06 mm) (left column) and prefrontal cortex (bregma +2.22 to +1.78 mm) (right column) at 9 and 12 months of age. (G) Visualization of amyloid plaques is based on anti Aß-immunoreactivity (A2275, red). Data are presented as means ± SEM; n=4-8; ** $p < 0.01$, Student´s t-test.

4.8.3.3. The influence of CRH overexpression on neuroinflammation in arcAß mice

Similar to arcAß CRH-R1 mice, inflammation was assessed in arcAß CRH-COE^{CNS} mice: co-stainings of Aß plaques with markers for microglia and astrocytes in the hippocampus and prefrontal cortex (PFC) of tg vs. tgcoe mice aged 9 and 12 months were performed. Results are exemplary depicted for the PFC of mice at 12 months of age (Figure 50A-C). GFAP positive astrocytes (red) are assembled to similar extent around Aß plaques (A2275, green) of tg and tgcoe mice (Figure 50A). Also, microglia surrounding Aß plaques are present to a similar extent in tg and tgcoe mice (Figure 50B, C): Figure 50B shows microglia stained with tomato lectin (green) around Aß plaques (A2275, red); in Figure 50C microglia are detected by Iba-1 (red), Aß plaques by 6E10 antibody (green). No differences in infiltration of microglia and astrocytes were visible in tg vs. tgcoe mice.

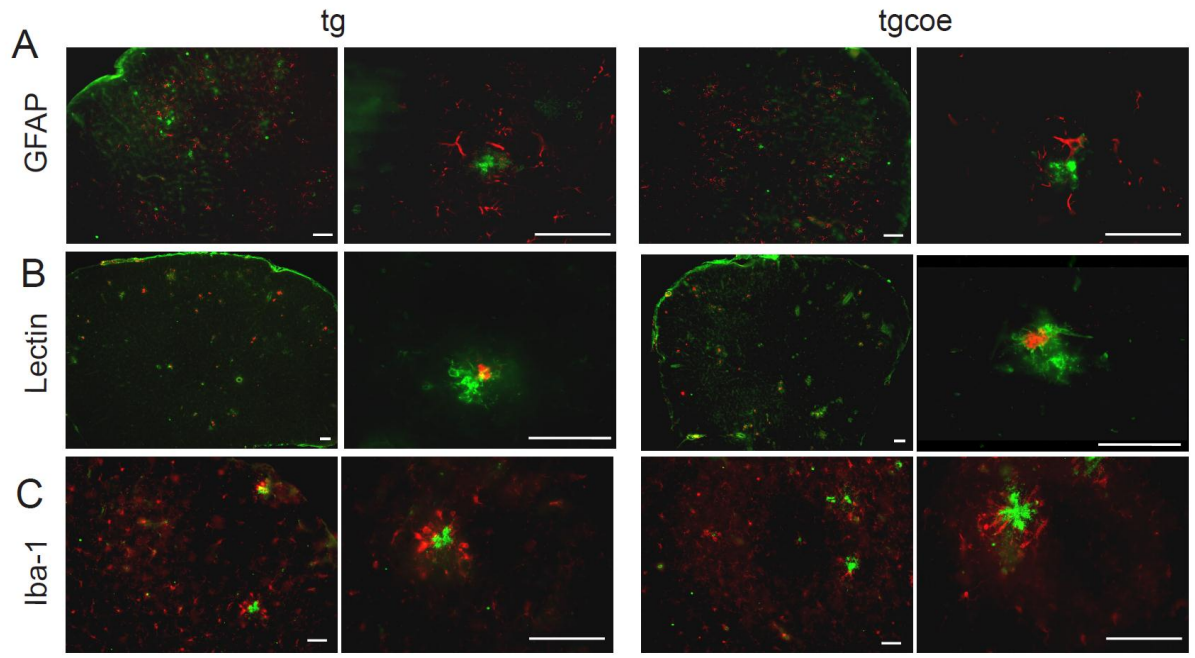

Figure 50. Activated microglia and astrocytes are similarily surrounding plaques in tg and tgcoe mice. (A-C) Inflammation in the prefrontal cortex of tg and tgcoe mice at 12 months of age. (A) Astrocytes (GFAP, red) are assembled around Aß plaques (A2275, green). (B, C) Microglia are surrounding Aß plaques: (B) Microglia (tomato lectin, green) and Aß plaques (A2275, red); (C) Microglia (Iba-1, red) and Aß plaques (6E10, green). Scale bars, 100 µm.

5. Discussion

Alterations of the CRH/CRH-R1 system and in this context of the HPA axis have been repeatedly reported in Alzheimer´s disease (AD). Furthermore, a hyperactivity of the HPA axis, which manifests in elevated glucocorticoid (GC) levels, has been shown to accelerate the onset and progression of the disease. GCs can enhance Aß generation (Catania et al., 2009;Sotiropoulos et al., 2008b;Lee et al., 2009;Sotiropoulos et al., 2011) as well as tau phoshporylation (Sotiropoulos et al., 2008a) and are at high levels detrimental for cognitive functionality (Gurevich et al., 1990;Lupien et al., 1998). In addition, stress induced tau phosphorylation has been shown to be mediated via CRH-R1 (Rissman et al., 2007;Carroll et al., 2011) and Aß increase in the interstitial fluid after acute stress has also been demonstrated to be CRH dependent (Kang et al., 2007b). In contrast, CRH has been shown to exert neuroprotective effects against Aß mediated toxicity in *in vitro* models (Bayatti et al., 2003;Facci et al., 2003;Lezoualc'h et al., 2000).

5.1. Neuroprotective effects of CRH *in vitro*

Neuroprotective effects of CRH against Aß mediated toxicity in *in vitro* models have been shown before (Bayatti et al., 2003;Facci et al., 2003;Lezoualc'h et al., 2000).

We observed neuroprotective effects of CRH pretreatment against Aß toxicity dependent on the amount of CRH-R1 and concentration of CRH. In AtT20 cells, which endogenously express CRH-R1, CRH treatment had no effect on cell survival, whereas in HT22 C3 cells, pretreated with 500 nM CRH, cell survival was elevated applying Aß 10-40 µM. In HT22 C2 cells, which overexpress more than 400-fold of CRH-R1, cell survival after CRH treatment was clearly increased for all concentrations of CRH and Aß. Here, we reveal a neuroprotective capacity of CRH and hence, to some extent confirm previous findings mentioned above. Apparantly, in cells carrying the CRH-R1, CRH can exert neuroprotective effects against Aß treatment in a concentration-dependent manner.

At first glance, the neuroprotective effects in cell models seem contradictory to our *in vivo* results, in which the CRH system turned out to act rather adversely. It has to be considered that these conflicting results emerge from fundamentally different systems. *In vitro* data cannot directly be correlated to findings in animal models.

5.2. Basal characterization of arcAß mice

5.2.1. Emotional behavior of arcAß mice

Assessment of basal emotionality in arcAß mice (tg vs. wt) revealed an increase in locomotion at 4, 8 and 12 months, unchanged anxiety-like behavior and an enhanced active stress-coping phenotype. Knobloch and colleagues only found increased locomotion in tg mice at 3 months of age while tg mice at older ages were indistinguishable from their wt littermates (Knobloch et al., 2007a). Furthermore, Knobloch and colleagues observed reduced anxiety-like behavior in tg mice at the age of 6 and 12 months (Knobloch et al., 2007a). These discrepancies most likely can be ascribed to the difference in the genetic background of the used mouse strains, the age of mice, housing and testing conditions including the used test apparatuses.

Increased locomotor activity is frequently observed in APP mouse models, e.g. in Tg2576 mice (Bardgett et al., 2011). Interestingly, hippocampus lesioned mice (Ibotenic acid) exhibit a similar hyperactivated phenotype with increased locomotion in the open field (OF) task (C. Wotjak, unpublished results). In light of these findings it remains questionable why Knobloch and colleagues did not observe increased locomotion in older mice.

Previous analyses of stress-coping behavior in APPswe/PS1 mice revealed a higher immobility of tg mice compared to controls in the forced swim test (FST) supporting a depression-like phenotype in that AD mouse model (Filali et al., 2009). We observed enhanced active stress-coping behavior in the FST, which was reflected by increased struggling and reduced floating time. These findings in the FST might also be related to the hyperactive phenotype of arcAß mice. Similarily, the reduced bodyweight in tg mice might also be a consequence of a higher energy expenditure related to the hyperactivity.

5.2.2. HPA axis activity in arcAß mice

Many AD patients exhibit elevated cortisol levels suggesting that AD causes a dysregulation of the HPA axis (Rothman and Mattson, 2010;Davis et al., 1986;Csernansky et al., 2006;Rasmuson et al., 2001). Along these lines, basal and stress-induced corticosterone levels were elevated in several transgenic human APP mouse models of AD. In TgCRND8 mice basal and stress-induced corticosterone levels were elevated in aged animals (Touma et al. 2004). Tg2576 mice showed elevated basal corticosterone levels (Lee et al., 2009;Dong et al., 2008). Similarily, Carroll and colleagues observed increased basal and stress-induced corticosterone levels at 4 months of age in Tg2576 mice (Carroll et al., 2011) and at 9 months. Along these lines, older 3xTg-AD mice have significantly higher corticosterone levels than non-tg mice (Green et al., 2006). Taken together, these

observations indicate that the AD-like pathology in these APP mouse models induces a dysfunction of the HPA axis. This might be explained by the decline of the hippocampus following Aß plaque deposition and the accompanying reduced sensitivity of the HPA axis to negative feedback of GCs (Goncharova and Lapin, 2002;Bao et al., 2008;Raadsheer et al., 1994b).

In contrast to these findings, assessment of basal and stress levels of plasma corticosterone did not reveal any changes of basal or stress-induced corticosterone levels in arcAß mice compared to control littermates at 4 or 12 months of age. Apparently, in this specific AD model the HPA axis is not altered in its function. Interestingly, basal and stress levels of corticosterone significantly decreased with age in wt animals. In contrast to this finding, the HPA axis has been demonstrated to be more activated during aging in humans (Bao et al., 2008). Numerous studies on rats also point towards an increased HPA axis activity during aging (de Kloet, 1992), although some reported an aging-associated decline (Cizza et al., 1995). In C57BL/6 mice aged 3, 9 and 16 months the circadian pattern of corticosterone showed age-related changes: the peak of corticosterone secretion at the end of the light phase/beginning of the dark phase was at its highest level in mice at 3 months of age, whereas mice aged 9 months reached peak corticosterone concentrations about 2 hours earlier and the lowest levels of GCs were observed in 16 months aged mice. However, the total levels of corticosterone were rather equal (Dalm et al., 2005).

5.2.3. Analysis of CRH and CRH-R1 expression in arcAß mice

Since changes in the CRH system were shown in AD patients, we analyzed CRH and CRH-R1 mRNA expression in arcAß mice at 3, 6 and 12 months of age.

Consistent with data from AD patients, cortical CRH mRNA expression was already increased at 3 months of age and continuously increased with age in arcAß mice. In contrast, CRH-R1 levels in the cortex of tg mice were elevated at 3 months of age, but decreased with age until they were below the wt levels at 12 months. The reciprocal expression of CRH and CRH-R1 mRNA in the progression of the disease might result from a compensatory mechanism, i.e. that increased CRH levels might result in a downregulation of CRH-R1. Similar observations on the transcriptional level have been made in depressed patients. Here the upregulation of CRH emerged concomitantly with CRH-R1 downregulation in the prefrontal cortex (Swaab et al., 2005).

Contrary to the cortex, CRH-R1 expression in the CA1 region of the hippocampus increases with age. This is most likely due to the hippocampal damage in arcAß mice caused by Aß deposition. Thus, the CRH-R1 density in the hippocampus is reduced and the signaling

compromised. Therefore, the CRH-R1 is probably upregulated in order to compensate these deficits.

5.3. The impact of CRH-R1 on the onset and progression of AD

Previous studies demonstrated an increase in Aß production and tau phosphorylation by GC treatment and stress (Catania et al., 2009;Sotiropoulos et al., 2008a;Sotiropoulos et al., 2011;Lee et al., 2009). Recently, stress induced tau phosphorylation has been shown to be mediated via the CRH-R1 (Rissman et al., 2007;Carroll et al., 2011). Also stress-related increase of Aß levels in the interstitial fluid has been demonstrated to be CRH dependent (Kang et al., 2007d). Further confirming the role of the CRH/CRH-R1 system in AD pathology apart from GCs, neuroprotective effects of CRH by binding to CRH-R1 against Aß-induced toxicity have been shown *in vitro* (Bayatti and Behl, 2005). Moreover, CRH treatment stimulated the release of non-amyloidogenic sAPP *in vitro* (Lezoualc'h et al., 2000). Taken together, there is increasing evidence that both the CRH-R1 and GC are crucial players in this devastating disease.

To shed light on this interplay we generated an AD mouse model lacking CRH-R1. In this model CRH-R1 signaling throughout the brain and the pituitary is disrupted. These conventional CRH-R1 knockout (KO) mice have a non-functional HPA axis, characterized by low circulating corticosterone levels under basal conditions and following stress. However, CRH-R1KO mice show residual HPA axis activity in response to stress indicated by a slight increase of plasma corticosterone levels ($p < 0.01$ at 4 months, $p < 0.05$ at 12 months). This basal GC secretion in CRH-R1KO mice might result from an increased secretion of arginine vasopressin (AVP) from the PVN, which is able to maintain basal ACTH secretion and thus HPA axis activity (Muller et al., 2000).

GCs play an essential role in processes related to memory formation (Sotiropoulos et al., 2008b;Sandi, 2011). Sandi (2008) suggested an inverted-U shape model for the relation between stress/GCs dosage and learning: the peak is located in the learning improvement zone, whereas the lower branches, reflecting too low and high levels of stress/GC, are accompanied by impaired learning. This model gained validation for hippocampus- and PFC-dependent learning tasks (Sandi, 2011).

5.3.1. Correlating cognitive to neuropathological results

All four genotypes of arcAß CRH-R1KO mice were comprehensively tested for their cognitive abilities: wild-type (wt), CRH-R1KO (ko), transgenic arcAß (tg) and transgenic arcAß CRH-R1KO (tgko). Since Aß-related pathologies were only observed in APP transgenic mice, neuropathological and biochemical analyses were performed in tg vs. tgko mice.

In the spontaneous object recognition (OR) test tg animals aged 4 months were significantly impaired in exploration of the novel object compared to wt animals indicating a cognitive deficit due to overexpression of APP. Interestingly, CRH-R1 deficiency was able to rescue the OR deficits in tg mice. Since no Aß plaques were detectable in arcAß mice at 4 months of age, this behavioral phenotype can be ascribed to the detrimental effects of soluble Aß oligomers. Accordingly, there is evidence, that impairment in cognitive function, learning and memory correlates with soluble Aß oligomers rather than with total Aß (insoluble and soluble) or Aß plaques (Lue et al., 1999;McLean et al., 1999;Lesne et al., 2006;Selkoe, 2008). Thus, there is no strict correlation between learning capabilities and plaque burden, in particular in younger mice, where no Aß deposits are detectable but cognitive decline can already be observed. Moreover, the arcAß mouse model is characterized by strong and early accumulation of intracellular Aß oligomers, which could explain the early deficits in the OR task.

In the water cross maze (WCM) task we discovered a general age-related decline in hippocampus-dependent spatial memory performance, but did not observe alterations in execution of the spatial task comparing tg versus tgko mice. However, striatum-mediated biased/response learning was dominant in tgko mice during the spatial paradigm. In the free-choice paradigm, which is testing for response learning in the first week of the experiment, accurate response learning was only accomplished by tgko mice, not by tg mice. In the reversal phase of that test, which relies on re-learning and thus cognitive flexibility, which primarily depends on the PFC, tgko were impaired while tg mice were able to re-learn.

The key neuropathological finding of arcAß CRH-R1KO mice was that $Aß_{40}$ and $Aß_{42}$ levels in hippocampal and cortical tissue of tgko compared to tg mice at 12.5 months were significantly reduced. Accordingly, also the plaque number and the area occupied by plaques were reduced in hippocampi of tgko mice in comparison to tg mice at 12.5 months. Soluble $Aß_{40}$ was reduced in tgko mice at 9.5 months, as was the area occupied by plaques in the hippocampus at this age. Since the plaque analysis in the PFC did not reveal any significant differences between the genotypes, alterations in Aß levels measured by ELISA are suggested to originate primarily from the hippocampal alterations. APP processing was not altered when comparing tg and tgko mice, indicating that the decreased Aß levels in tgko mice are not a consequence of decreased Aß production but rather a result of enhanced Aß clearance. To preclude that alterations in Aß levels in arcAß CRH-R1KO mice are not due to changes in APP processing in CRH-R1-deficient mice, processing of endogenous APP was assessed in CRH-R1KO mice (wt vs. ko). Levels of sAPP did not differ between the genotypes, indicating equal processing of the protein. To further confirm this result, ß-secretase (BACE1) activity and APP processing were determined in CRH-R1KO mice at

postnatal day 5.5. At this stage BACE1 activity and thus potential changes in APP processing are at their maximum (Willem et al., 2006). Again, no alterations were detectable, suggesting that the decreased insoluble Aß levels in tgko compared to tg mice at 12 months of age are in fact a consequence of accelerated clearance rather than of alterations in the generation of Aß.

It becomes clear that CRH-R1 deficiency induces a shift in learning strategies in arcAß mice, rescues object recognition memory impairment and leads to reduced Aß levels and plaque load in the hippocampus. The neuropathological findings including the increased insoluble Aß levels in the hippocampus and cortex as well as the increased hippocampal plaque load are in full agreement with the cognitive and mnesic decline observed whenever APP is overexpressed. More pronounced striatum based learning cannot be attributed to the plaque load in that region as the striatum is a region where hardly any plaques were found. Cognitive flexibility was compromised in tgko mice compared to tg mice at 12 months of age. However, the plaque analysis in the PFC, which is crucially involved in cognitive flexibility, did not reveal any differences between tg and tgko mice. GCs play a crucial role in cognitive function related to the PFC and it has been demonstrated that reduced endogenous GC levels can induce dysfunction of the PFC (Mizoguchi et al., 2004). Accordingly, compromised cognitive flexibility in tgko mice might partly be explained by low GC levels. However, non-transgenic ko mice were not impaired, suggesting the combination of APP overexpression and low GC levels to induce the deficit in cognitive flexibility. On the other hand, stress and chronically elevated GCs disturbed hippocampus-dependent memory and PFC-mediated behavioral flexibility. The latter is also impaired by centrally applied Aß (Sotiropoulos et al., 2011).

When correlating Aß plaque burden to cognitive performance, the growing evidence which demonstrated that the number of senile plaques often does not correlate with the severity of memory impairment has to be considered. Soluble Aß oligomers much better correlate with mnesic decline (Lue et al., 1999;McLean et al., 1999;Lesne et al., 2006;Lesne et al., 2008;Selkoe, 2008). In particular, deficits in spatial learning have been shown to correlate directly with Aß protofibril levels, but not with total Aß (Lord et al., 2009). In this context, it is worth mentioning that Aß oligomers are with respect to their biochemical properties fundamentally different from plaques. Consequently, statements concerning Aß oligomers need to be reviewed critically. Moreover, a positive relationship between soluble Aß levels and synaptic loss and accordingly severe cognitive impairment has been established (Pleckaityte, 2010). Synaptic loss, specifically the loss of synaptophysin as a presynaptic marker, is one of the best pathological correlates of cognitive impairment in AD subjects (Gouras et al., 2010;Tampellini and Gouras, 2010). Besides, synaptic activity is thought to

promote Aß secretion and one known function of APP is to inhibit synapses (Priller et al., 2006).

Previous studies reported increased GC levels to promote Aß generation and to decrease Aß degeneration (Green et al., 2006). Thus, the corticosterone deficit might be causally related to the reduction of Aß levels as well as to the improvement of cognition in arcAß CRH-R1KO mice in the OR task.

Furthermore, Aß deposits in the hippocampus and resulting hippocampal damage have been demonstrated to enhance HPA axis dysregulation and to increase basal levels of GC (Kulstad et al., 2005;Breyhan et al., 2009;Nuntagij et al., 2009). Due to the blockade of the HPA axis this potentially exacerbating mechanism is disrupted in our model. In fact, not only is this aggravating mechanism sidestepped, but almost the entire stress hormone cascade including its ultimate effector - GCs. By deleting CRH-R1 in arcAß mice we could neither prevent the disease nor its progression in general, but could alleviate onset and symptoms like cognitive deficits and Aß plaque burden. Whether these effects are due to disruption of CRH-R1 signaling in general or due to the blockade of the HPA axis and accompanying low circulating GCs, remains to be elucidated. However, most probably disruption of the reinforcing HPA axis/GC circuit contributed to the alleviation of the disease. It is out of question that the GC-cascade with its powerful feed-forward loop is not the initial cause of AD since for expample depressed patients, which often show a hyperactive HPA axis, do not show neuropathological hallmarks such as Aß deposits. There is also no indication that GC treatment elicits AD neuropathological changes like Aß plaques (Lucassen et al., 2001). Though, dysregulation of the HPA axis may rather worsen the symptoms of the disease. The increased incidence of AD in aged, depressed and stressed subjects and the concomitant hyperactivation of the HPA axis in those subjects support the strong coherency of AD and the HPA axis.

The detrimental effects of high dose GCs are evident. What is the particular role of CRH-R1 in this interplay? Previously it has been demonstrated that GC treatment could trigger Aß generation (Sotiropoulos et al., 2008a;Catania et al., 2009), which could be reversed by pharmacologically blocking the CRH-R1 (Lee et al., 2009). Also Carroll and colleagues showed that restrained and isolation stress enhanced Aß generation and reduced microglial activation in Tg2576 mice, which could not be mimicked by GC-administration but prevented by CRH-R1-antagonists (Carroll et al., 2011). In addition, they observed increased tau phosphorylation and aggregation after stress in PS19 mice expressing human tau, which similarily could be prevented by CRH-R1-antagonism. Accordingly, Rissman and colleagues discovered stress-induced tau phosphorylation to be mediated by CRH-R1 in mice (Rissman et al., 2007).

Our data confirm the involvement of the CRH-R1 in the progression of AD. In a transgenic mouse model of AD we demonstrate that the deletion of CRH-R1 can defer Aß pathology and improve memory and learning.

5.4. The impact of CRH on the onset and progression of AD

To elucidate effects of CRH in the context of AD, we used CRH-COE^{CNS} mice, overexpressing CRH in the CNS (Lu et al., 2008). Basal screening of CRH-COE^{CNS} mice (wt vs. coe) revealed enhanced locomotion and a general arousal of coe mice, which most likely also entail their reduced bodyweight. The aroused phenotype might influence cognitive performance as it could be accompanied by attention deficits.

HPA axis function at basal conditions was not altered in coe mice as indicated by corticosterone levels which were similar to wt mice. However, stress-induced plasma corticosterone levels were significantly increased in coe mice, indicating an exaggerated response of the HPA axis to stressful conditions.

Interestingly, corticosterone assessment in arcAß CRH-COE^{CNS} mice revealed elevated levels in tgcoe compared to tg mice, which were marginally significant at basal conditions ($p = 0.056$) and significantly increased after stress. Apparantly, the combination of the APP transgene and CRH overexpression triggers HPA axis activity and enhanced drive of GCs. As discussed above, in AD elevated GC levels enhance Aß plaque formation and induce memory impairment.

5.4.1. Correlating cognitive to neuropathological results

Following arcAß CRH-R1KO mice, four genotypes of arcAß CRH-COE^{CNS} mice (wild-type (wt), CRH-COE^{CNS} (coe), arcAß transgenic (tg) and arcAß transgenic CRH-COE^{CNS} (tgcoe)) were subjected to cognitive testing. Neuropathological and biochemical analyses were conducted in tg vs. tgcoe mice.

Cognitive performance of arcAß CRH-COE^{CNS} mice (wt, coe, tg, tgcoe) in the Y-maze revealed no significant alterations. However, at 4 months of age mice overexpressing CRH (coe and tgcoe) tended to have a higher percentage of spontaneous alternation. This observation might be ascribed to the increased hyperactivity and arousal observed in coe mice, which might increase the chance of higher alternation.

The cognitive performance of wt, coe, tg and tgcoe mice aged 8 months in the WCM revealed impaired spatial memory of all tg mice, whereas there was no difference between tg and tgcoe mice in this particular task. These findings confirm those in arcAß CRH-R1KO mice in terms of hippocampal decline.

In contrast to wt mice, tg and coe mice aged 4 months failed to perform the OR task as their exploration score was at the chance level. In arcAß CRH-R1KO we similarily experienced tg mice to have impaired object recognition memory. Interestingly, CRH overexpression induces equal deficits, which probably again can be ascribed to the attention deficit due to their aroused state. However, the deficits seen in single transgenic tg and coe mice did not summate in double transgenic tgcoe mice. In contrast, tgcoe rather showed an improved performance in the task.

In contrast to the OR task, the aroused phenotype did not compromise the performance of coe mice in the WCM. The strong motivation to escape the highly aversive test situation might probably override the attention deficit observed in the OR test. Along this line, the WCM is strongly driven by the aversive motivation to escape the water while in the OR task attention might be more essential for the recognition of an object.

Mice with a central overexpression of CRH, which involves hypercorticosteronism and signs of cushing´s syndrome, show learning deficits (Stenzel-Poore et al., 1992). In particular the acquisition of learned behavior in the Water T-maze as well as in the Morris water maze are compromised (Heinrichs et al., 1996).

In the neuropathological analysis of arcAß CRH-COE^{CNS} mice, elevated levels of insoluble Aß$_{40}$ and Aß$_{42}$ were observed in hippocampal and cortical tissue of tgcoe mice compared to tg mice at 12 months. APP processing in tgcoe mice was indistinguishable from tg mice.This finding points to a lower degradation rate in tgcoe mice compared to tg mice. In accordance, the hippocampal plaque load of tgcoe mice aged 9 months was increased in comparison to tg mice. However, this increase in plaque load in tgcoe vs. tg mice was not observed at 12 months of age when a significant increase in Aß$_{40}$ and Aß$_{42}$ levels was detected.

These results are in line with previous findings, where restraint stress and repeated CRH activation in the amygdala increased APP and Aß levels (Ray et al., 2011). Moreover, a recent study by Carroll and colleagues (2011) discovered elevated levels of paired-helical-filaments (PHF1) without changes in total tau levels in CRH-overexpressing mice aged 10 months, supporting a detrimental role of CRH and GC not only in Aß pathology. In contrast, Hanstein and colleagues, using CRH-COE^{CNS} mice, demonstrated a neuroprotective role of CRH overexpression against kainate-induced cell death in the CA3 region of the hippocampus which is highly sensitive to excitotoxic stress (Hanstein et al., 2008). Interestingly, they also observed no signs of neuroinflammation in coe mice after kainate injection, whereas control animals showed both activated astrocytes and microglia. In our study, astrocytes and microglia were activated and accumulated in particular around Aß plaques to the same extent in tg and tgcoe mice. Here, of course, it has to be considered that our analysis of inflammation was only applied to APP transgenic animals which exhibited Aß

plaques, whereas Hanstein and colleagues used non-transgenic mice which obtained acute kainate injections. The fact that we saw no alteration in the inflammatory response in tg compared to tgcoe mice might be due to the strong inflammatory response in APP transgenic arcAß mice mice which easily might mask minor differences.

In summary, CRH overexpression exacerbated the AD neuropathology by increasing the Aß load. From the cognitive finding of the OR task we can hardly draw a conclusion as arcAß CRH-COE^{CNS} mice suffered attention deficits and therefore were basically impaired in mastering this task. However, performance in the WCM task was impaired in tg and tgcoe mice to a similar extent at 8 months of age.

5.5. Cognitive performance of arcAß CRH-R1KO and arcAß CRH-COE^{CNS} mice

5.5.1. Performance in the water cross maze (WCM) task

In the water cross maze (WCM) test all transgenic (tg, tgko, tgcoe) animals were equally impaired in their spatial hippocampus-dependent performance compared to non-transgenic mice (wt, ko, coe). Although no difference in allocentric spatial accomplishment of the task became apparent among the APP transgenic mice, tgko mice preferentially solved the task by predominant use of an egocentric response strategy, indicated by a high side bias. In the free-choice paradigm of the WCM, enforcing response learning during the first week of training, tgko mice performed as accurate as wt and ko mice did, whereas correct performance of tg mice was severely delayed. Consequently, striatum-mediated response learning is the predominant learning strategy in tgko compared to tg mice.

Our data support previous findings regarding the decline of hippocampal function and consequent acquisition of a striatum-based compensatory mechanism. In general, hippocampus lesioned mice showed an impaired performance in spatial water maze tasks (Arns et al., 1999). Middei and colleagues observed that hippocampal dysfunction induced by APP mutations promotes striatum-based compensatory mechanisms. Hence, response learning became the predominant strategy in Tg2576 mice (Middei et al., 2004). Others also showed that impairment of hippocampal function enhances striatum-dependent procedural learning in rodents tested in various cross mazes (Schroeder et al., 2002;Chang and Gold, 2003a). Interestingly, we observed compensation of spatial cognitive deficits by response learning only in tgko mice, suggesting CRH-R1 deficiency to trigger that shift in learning.

Acetylcholine is a marker for learning activity and has also been implicated in switching of learning strategies. It has been shown that depending on the level of acetylcholine in the hippocampus or the striatum the solution strategy with respect to place (spatial) or response

could be predicted in rodents (Chang and Gold, 2003b). It is notable, that here the ratio of the neurotransmitter was important in both structures rather than the overall content (Pych et al., 2005). For example, higher acetylcholine levels in the striatum compared to the hippocampus predicted a response solution in a respective task. This might suggest that in tgko mice compared to tg mice the cholinergic transmission in the striatum is enhanced in comparison to the hippocampus.

Unlike the accurate egocentric performance of tgko mice in the first week of the free-choice paradigm, the second week, testing for cognitive flexibility, revealed poor performance of tgko mice in comparison to tg mice. This suggests an impairment in cognitive flexibility of tgko mice compared to tg mice. Cognitive flexibility is largely mediated by PFC-hippocampus circuits. PFC-hippocampus circuits and thus behavioral flexibility have been shown to be affected by chronic GR activation (Cerqueira et al., 2007). Furthermore, Cerqueira and colleagues found that hippocampal functions are more sensitive to detrimental effects of GCs than other regions (Cerqueira et al., 2005). In contrast, we did not observe alterations in hippocampus-based spatial function in APP transgenic mice with normal versus low GC levels. However, the functionality of the PFC was impaired in tgko mice compared to tg mice, although tgko mice have lower GC levels.

Taken together, these findings suggest that a loss of CRH-R1 in arcAß mice might promote a shift towards striatum-based response learning as we have seen in a task testing for spatial memory, whereas PFC-mediated cognitive flexibility was deteriorated. In conclusion, the predominant use of the striatum in tgko mice might act complementary to the disabled hippocampus and might also act complementary to the PFC. Such a complementary activity pattern of the striatum and the PFC was reported before (Ragozzino and Choi, 2004).

Nevertheless, it has to be remarked that previously mentioned memory circuits are not independently operating units but are intermingled. Most experiences require integration of information across different neural systems. Supression of one system facilitates other systems, probably in a more pronounced manner than under physiological conditions necessary for the respective cognitive task.

5.5.2. Evaluating object recognition memory

Object recognition (OR) memory which depends on temporal lobe areas, in particular the perirhinal cortex (PRh) (Bussey et al., 2000), was impaired in tg mice aged 4 months, whereas tgko mice showed exploration scores similar to wt mice. Perirhinal neuronal response mechanisms also depend on cholinergic transmission (Massey et al., 2001). For example, blocking of muscarinic receptors by scopolamine impaired preferential exploration

of novel over familiar objects (Warburton et al., 2003). This suggests that loss of CRH-R1 might induce enhanced cholinergic transmission in the PRh in arcAß mice.
At the same age of 4 months, non-APP-transgenic mice overexpressing CRH (coe) were unable to perform the OR task. This deficit might be related to their aroused, hyperactive phenotype and connected to reduced attention.

5.5.3. Linking cognitive results to cholinergic transmission

Decline of cholinergic transmission caused by loss of cholinergic neurons, decrease in cholinergic receptors and reduction in choline acetyltransferase and acetylcholinesterase enzyme activities resemble the oldest hypothesis of AD (Coyle et al., 1983). However, therapeutic strategies addressing the acetylcholine deficit by inhibiting acetylcholinesterases are not able to cure the disease but can only treat symptoms in an early state. Thus, acetylcholine deficiency may not be the initiator of AD but rather the consequence of a widespread neuronal damage. In this process insufficient cholinergic neurotransmission may participate in the ongoing neuropathology and cognitive decline.
Both the cholinergic and the CRH system are linked to memory and learning processes. Steckler and Holsboer (2001) observed both systems to interact in the modulation of spatial learning. Specifically, blockade of the muscarinic receptor by scopolamine induced spatial learning deficits which were aggravated by concomitant intracerebroventricular CRH administration. Nicotinic antagonism had no effect in this respect (Steckler and Holsboer, 2001).
These findings support the hypothesis that acetylcholine-dependent circuits are involved in the altered cognitive competence of arcAß CRH-R1KO and arcAß CRH-COE^{CNS} mice. In general, the cholinergic system in APP transgenic mouse models is supposed to be impaired similarily to AD patients (Bornemann and Staufenbiel, 2000). In CRH-R1 deficient arcAß mice (tgko) some cognitive abilities e.g. OR memory are sustained compared to tg mice. The decreased plaque load in tgko versus tg and tgcoe mice could preserve cholinenergic transmission. Pointing to the relation between the cholinergic and the CRH system, chronic muscarinic blockade led to increased cortical expression of CRH-receptors in rats (De Souza and Battaglia, 1986). As CRH aggravates the cognitive damage (Steckler and Holsboer, 2001), it is reasonable to assume that no additional CRH-induced damage can occur in CRH-R1KO (ko, tgko) mice. In contrast, in mice overexpressing CRH (coe, tgcoe) this leads to a deficit in attention and thus learning is even more deteriorated. This scenario could also explain the accurate performance of ko mice in the WCM tasks. In addition, the loss of CRH-R1 and the decreased GC levels could result in enhanced cholinergic activity for instance in the PRh and striatum. Vice versa, a cholinergic deficit would rather be aggravated by excess

CRH. Moreover, the increased levels of stress-induced GCs in CRH-COE^{CNS} mice might over the lifetime lead to aggravated cognitive function. Additional evidence corroborating the cholinergic hypothesis in the context of cognitive findings in arcAß CRH-R1KO and arcAß CRH-COE^{CNS} mice are the reciprocal Aß levels in both lines. Aß deposition locally deteriorates cholinergic transmission as demonstrated by decreased cholinergic enzyme activity in APP transgenic mice (Boncristiano et al., 2002). In conflict to that, we did not observe differences in plaque burden between the genotypes (tg vs. tgko) in the PFC, but only in the hippocampus and behaviorally we observed no change in hippocampus-dependent spatial performance, only in cognitive flexibility. In this context, the hippocampus holds a pivotal role as it is consolidating information of other parts of the brain. Thus, the hippocampal Aß burden should be considered a general indicator for the learning capabilities.

5.6. Electrophysiological evaluation in arcAß CRH-R1KO mice

Disruption of synaptic plasticity, caused by soluble Aß oligomers rather than insoluble Aß plaques (Oddo et al., 2003;Lesne et al., 2006), is suggested to be the best pathological correlate to cognitive impairment (Gouras et al., 2010;Tampellini and Gouras, 2010) in AD. To identify the nature of this defect, electrophysiological studies have been performed in various AD transgenic mouse models, foremost in the CA1 region of the hippocampus, which is one of the major players in memory encoding. Knobloch and colleagues observed severely impaired CA1 hippocampal long-term potentiation (LTP) in slices from arcAß mice (tg vs. wt) aged 3.5 and 7.5 months (Knobloch et al., 2007b). They claim, that the deficit was not due to impaired synaptic plasticity as basal transmission in tg slices was normal, but caused by Aß oligomers as it could be reversed by pretreatment with the 6E10 antibody (against Aß 1-17 sequence). Electrophysiological recordings in the CA1 region of the hippocampus of arcAß CRH-R1KO mice (wt, ko, tg, tgko) aged 12 months revealed a tendency to increased field excitatory postsynaptic potentials (fEPSPs) in tg mice compared to wt, ko and tgko mice after stimulation. Basal transmission and therewith synaptic plasticity was normal as indicated by the input-output curve. Determination of paired-pulse facilitation (PPF) predicated a higher presynaptic release probability of glutamate in tgko mice compared to tg, ko and wt mice. This effect was detectable at the short inter-stimulus interval of 20 ms. With longer pulse intervals the PPF ratio of tgko mice was similar to those of tg, ko and wt mice.

At first glance, our results are opposing to those of Knobloch and colleagues. In this context, it is worth to mention that in the multitude of electrophysiological studies, contrasting results have been yielded in different AD transgenic mouse models, even in the same model by different research groups (Marchetti and Marie, 2011). Marchetti and Marie, who review the outcome of manifold hippocampal electrophysiological studies in AD transgenic mouse

models, report for 20 APP-based models in the age of 3-10 months mixed results: nine showed normal CA1 hippocampal LTP, 10 impaired LTP and one increased LTP. For a few APP mouse models even opposing data are evident, for example Tg2576 mice show either normal LTP or an age-dependent reduction in CA1 LTP. Middei and colleagues observed reduced potentiation only after submitting APP23 mice to training in the Morris water maze, pointing to the hypothesis that detection of hippocampal plasticity deficit ensues from prior challenge of its function (Middei et al., 2010). However, the current canon in the AD research field proposes acute exposure to synthetic or naturally secreted Aß to induce deficits in hippocampal LTP (Wang et al., 2002;Wei et al., 2010b;Klyubin et al., 2008;Klyubin et al., 2005). Along these lines, it would be of interest to perform electrophysiological recordings in our mice after testing of cognition in order to record from already activated respective brain regions (Middei et al., 2010).

FEPSPs after LTP stimulation tended to be increased in tg mice compared to tgko, ko and wt mice. In contrast, soluble $Aß_{40}$ and $Aß_{42}$ levels, which are believed to cause LTP impairment, showed an opposite trend with higher levels in tg mice compared to tgko mice. However, fEPSPs results were not significant and it can not be ruled out that they are a result of high variability. As Knobloch and colleagues did not evaluate LTP of arcAß mice older than 7.5 months we cannot directly correlate our findings to their results. In aged mice, physiological conditions are different to young animals. Additionally, they used a different stimulus (100 Hz for 3 trains of 1 s tetanus separated by 20 s, whereas our stimulus was: 1 x 100 Hz / 100 pulses).

In the spontaneous object recognition (OR) task we observerd a decline in exploration of tg mice which was rescued by CRH-R1KO. Perfomance of the task largely depends on the perirhinal cortex (PRh). To correlate these findings to a neuropathologic phenotype, we analyzed long-term depression (LTD) in this brain region. We did not observe alterations when comparing the four genotypes. To this end, it has to be taken into account that OR results were obtained from mice aged 4 months, whereas LTD measurements were done in mice aged 12 months. Probably, at 4 months of age, enhanced levels of Aß oligomers might have influenced the PRh of tg mice, whereas at 12 months oligomers assembled to plaques which do not differ in tg vs. tgko mice.

While trying to correlate electrophysiological outcome to cognitive results it is noteworthy that LTP and LTD only mirrors memory acquisition, not e.g. the course of memory acquisition or extinction. Thus the results of the electrophysiological recordings can reliably be related only to the performance in the WCM on the first day of the test. Usually, the first day of comprehensive memory tasks like the WCM or the Morris water maze does not provide any prediction about the final mastering of the task. On day one of the WCM hippocampus-

dependent spatial paradigm, arcAß CRH-R1KO mice at every age did not significantly differ among each other, only during later testing tg and tgko showed a deficit. Consistent with this, hippocampal LTP, which reflects acquisition at day one, did not differ in all groups tested.

5.7. The role of corticosterone in arcAß CRH-R1KO and arcAß CRH-COE^{CNS} mice

Besides loss of CRH-R1 and overexpression of CRH, tgko and tgcoe mice show a different activity of the HPA axis (Figure 51). GC levels under basal and stress conditions are lower in tgko and higher in tgcoe compared to their respective tg controls. The basal plasma corticosterone levels of tgcoe vs. tg mice are marginally and the response of the HPA axis to stress is significantly increased. Consequently, it has to be assumed that the corticosterone load over the lifetime is higher in tgcoe mice.

Aß levels and plaque load were reduced in tgko compared to tg mice and increased in tgcoe mice. These reciprocal findings reflect the levels of corticosterone, which were also oppositely regulated in tgko and tgcoe mice. The detrimental effects of GCs in this regard are proven. Thus, we might hypothesize that low circulating corticosterone delays the onset and progression of AD, whereas elevated levels accelerate the disease progression in arcAß mice.

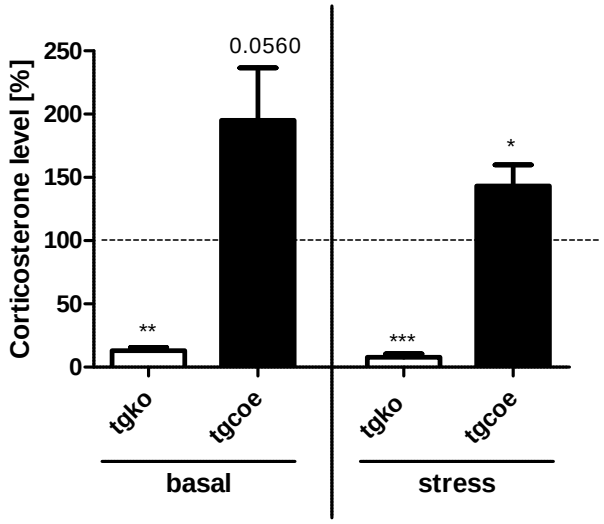

Figure 51. HPA axis activity in tgko and tgcoe compared to tg mice at 12 months. Illustrated are the basal and stress-induced corticosterone levels of tgko and tgcoe mice normalized to levels of their respective tg littermates (= 100 %). Results are presented as means ± SEM; n=11-13; * $p < 0.05$, ** $p < 0.01$, *** $p < 0.001$, Student´s t-test.

5.8. Limitations and outlook of this study

The genetic approach applied in this study has some limitations with respect to the specificity and spatial resolution. On the one hand we used conventional CRH-R1KO mice and on the other hand mice overexpressing CRH throughout the central nervous system. In both cases not only the CRH/CRH-R1 system is affected in the entire brain but also the HPA axis is compromised. Therefore, it is not possible to clearly discriminate CRH/CRH-R1 effects from those related to GCs or to assign effects to specific brain areas. Moreover, the study is restricted to a single transgenic AD mouse model which has its specific characteristics that cannot be fully generalized.

Taken together, the present study cannot unequivocally discriminate between actions of GCs and the CRH/CRH-R1 system but provides strong evidence that both systems participate in the pathogenesis of AD. Chronic excess of GCs as well as of CRH exacerbate the disease, whereas the disruption of central CRH-R1 signaling and of the HPA axis alleviates the pathology. More definite roles of these crucial systems could originate from conditional mouse mutants with e.g. i) CRH-R1 deletion specifically in the pituitary to disrupt only the HPA axis, ii) CRH-R1 deletion in the brain but not in the pituitary to maintain HPA function or iii) confined CRH overexpression to the PVN in the hypothalamus resulting in a hyperactive HPA axis without CRH overexpression throughout the brain.

In these conditional mutants cognitive assessment for all ages would be instructive, in particular tests enforcing learning shifts to further dissect the findings in arcAß CRH-R1KO mice. In this context, the evaluation of cholinergic transmission e.g. by detection of acetylcholinesterase activity would be necessary to test the cholinergic hypothesis. In addition, assessment of neuropathological correlates in young APP mice at ages where no senile plaques are visible yet could help to address the pathophysiology in more detail.

Furthermore, chronic stress has been demonstrated to trigger Aß generation and tau hyperphosphorylation in dependence of the CRH-R1/CRH system (Kang et al., 2007c;Rissman et al., 2007). To this end, it would be of interest to evaluate the impact of stress in the used models.

In general, reduced sex hormones are a risk factor for AD (Atwood et al., 2005). The prevalence of AD is higher in women, most likely due to hormonal fluctuations in the menstrual cycle and a decline in estrogens during the menopause and therewith the lacking neuroprotective function of the hormone as ROS scavenger (Bachman et al., 1992;Letenneur et al., 2000;Selkoe, 2001;Swaab et al., 2003;Sotiropoulos et al., 2008b). Therefore, it is necessary to distinguish between males and females in studies concerning AD. In AD studies involving rodents, it is advisable to also include female animals to learn more about gender differences in this disease.

The current number and future estimations of AD cases are enormous: about 36 million people are affected by dementia worldwide (Ferri et al., 2005) and the numbers are predicted to double every 20 years. In the Global burden of disease study, depression is estimated to become the leading cause of disability by the year 2020 (Murray and Lopez, 1996). The increasing burden of both AD and depression and the higher prevalence in women, draws the attention to the overlay of pathologies and symptoms of both diseases. Assessing the interfaces, which partly manifest in CRH/GC system alterations, could probably yield in a more profound understanding of the genesis of either disease and eventually to more effective therapeutic strategies.

CRH-R1 antagonists have gained attention as a potential novel class of antidepressants. CRH-R1 antagonist R121919 significantly reduced depression and anxiety scores in patients (Zobel et al., 2000). It is noteworthy that increased REM-sleep is a common feature of depressed patients, leading to a reduced release of growth hormones and enhanced secretion of CRH. So far, approved antipressants failed to improve REM-sleep conditions, however, CRH-R1 antagonist R121919 reduced REM-sleep duration to normal levels (Zobel et al., 2000).

In contrast, two other CRH-R1 antagonists failed in the treatment of depressive symptoms: Pexacerfont (Bristol-Myers Squibb) did not demonstrate efficacy compared to placebo in generalized anxiety disorders (Coric et al., 2010) and CP-316,311 (Pfizer) also failed in treating major depression (Binneman et al., 2008). These discrepancies might be led back to the fact that not every depressed patient exhibits a hyperactive CRH system. Therefore, only a subpopulation reacts to CRH-R1 antagonism. Accordingly, targeting the CRH-R1 could prove to be successful at least in a sub-population of depressed patients and, in the light of similarities, might also be a promising target for the treatment of AD. In our study, CRH-R1 turned out to be crucial for the onset and progression of AD and disruption of its signaling to defer the disease. Consequently, our data support the concept of CRH-R1 antagonism as a potential treatment strategy.

6. Conclusion

In Alzheimer´s disease (AD), alterations of the CRH system and in this context of the HPA axis have been reported. Furthermore, hyperactivity of the HPA axis, manifested by elevated glucocorticoid (GC) levels, has been shown to accelerate the onset and progression of the disease.

To elucidate the role of CRH and CRH-R1 we generated AD mouse models with alterations of the CRH/CRH-R1 system. To this end, we bred arcAß mice, a transgenic human amyloid precursor protein (APP) AD mouse model, to i) conventional CRH-R1KO mice obtaining arcAß CRH-R1KO and ii) conditional CRH-overexpressing mice CRH-COE^{CNS} obtaining arcAß CRH-COE^{CNS} mice. Four genotypes of either line, i) wild-type (wt), CRH-R1KO (ko), transgenic arcAß (tg), transgenic arcAß CRH-R1KO (tgko) and ii) wild-type (wt), CRH-COE^{CNS} (coe), arcAß transgenic (tg) and arcAß transgenic CRH-COE^{CNS} (tgcoe) mice, were submitted to cognitive testing at 4, 8 and 12 months of age. Neuropathological as well as biochemical analyses were performed in tg mice and compared to their respective mutants (tgko, tgcoe mice).

Our data provide evidence for the involvement of the CRH system and the HPA axis in the onset and progression of AD: we observed impaired object recognition (OR) memory in tg mice at 4 months, which was restored by CRH-R1 deficiency (tgko). Furthermore, all tg mice aged 8 months and older had deteriorated spatial memory in the water cross maze (WCM) task. Interestingly, tgko mice shifted to a striatum-dependent egocentric strategy by which they were able to perform a task of the WCM enforcing response learning more easily than tg mice. However, tgko mice exhibited less cognitive flexibility compared to tg mice. Different learning patterns might be ascribed to cholinergic signaling which is supposed to be related to the CRH system.

Mice overexpressing CRH (coe, tgcoe) exhibited an aroused phenotype, which is accompanied by attention deficits and thus cognitive impairment as observed in the OR task.

Compared to tg mice, Aß levels in hippcampal and cortical tissue of tgko mice were reduced as well as the hippocampal pIaque load. In tgcoe mice opposite effects were observed.

In summary, in a tg mouse model of AD we could demonstrate that CRH-R1 deficiency can improve memory and learning and defer Aß pathology, whereas CRH overexpression had rather detrimental effects. Whether the effects are due to circulating GC levels, which are decreased in CRH-R1KO and elevated in CRH-COE^{CNS} mice or due to CRH-R1/CRH signaling per se remains to be investigated.

7. References

Aggleton JP, Brown MW (1999) Episodic memory, amnesia, and the hippocampal-anterior thalamic axis. Behav Brain Sci 22:425-444.

Arns M, Sauvage M, Steckler T (1999) Excitotoxic hippocampal lesions disrupt allocentric spatial learning in mice: effects of strain and task demands. Behav Brain Res 106:151-164.

Atwood CS, Meethal SV, Liu T, Wilson AC, Gallego M, Smith MA, Bowen RL (2005) Dysregulation of the hypothalamic-pituitary-gonadal axis with menopause and andropause promotes neurodegenerative senescence. J Neuropathol Exp Neurol 64:93-103.

Bachman DL, Wolf PA, Linn R, Knoefel JE, Cobb J, Belanger A, D'Agostino RB, White LR (1992) Prevalence of dementia and probable senile dementia of the Alzheimer type in the Framingham Study. Neurology 42:115-119.

Baddeley A (2003) Working memory: looking back and looking forward. Nat Rev Neurosci 4:829-839.

Ballard C, Gauthier S, Corbett A, Brayne C, Aarsland D, Jones E (2011) Alzheimer's disease. Lancet 377:1019-1031.

Ballard C, Waite J (2006) The effectiveness of atypical antipsychotics for the treatment of aggression and psychosis in Alzheimer's disease. Cochrane Database Syst RevCD003476.

Bao AM, Meynen G, Swaab DF (2008) The stress system in depression and neurodegeneration: Focus on the human hypothalamus. Brain Research Reviews 57:531-553.

Bardgett ME, Davis NN, Schultheis PJ, Griffith MS (2011) Ciproxifan, an H3 receptor antagonist, alleviates hyperactivity and cognitive deficits in the APP Tg2576 mouse model of Alzheimer's disease. Neurobiol Learn Mem 95:64-72.

Bayatti N, Zschocke J, Behl C (2003) Brain region-specific neuroprotective action and signaling of corticotropin-releasing hormone in primary neurons. Endocrinology 144:4051-4060.

Bayatti N, Behl C (2005) The neuroprotective actions of corticotropin releasing hormone. Ageing Research Reviews 4:258-270.

Behl C (1997) Amyloid beta-protein toxicity and oxidative stress in Alzheimer's disease. Cell Tissue Res 290:471-480.

Berendse HW, Galis-de GY, Groenewegen HJ (1992) Topographical organization and relationship with ventral striatal compartments of prefrontal corticostriatal projections in the rat. J Comp Neurol 316:314-347.

Binneman B, Feltner D, Kolluri S, Shi Y, Qiu R, Stiger T (2008) A 6-week randomized, placebo-controlled trial of CP-316,311 (a selective CRH1 antagonist) in the treatment of major depression. Am J Psychiatry 165:617-620.

Bissette G, Reynolds GP, Kilts CD, Widerlov E, Nemeroff CB (1985) Corticotropin-releasing factor-like immunoreactivity in senile dementia of the Alzheimer type. Reduced cortical and striatal concentrations. JAMA 254:3067-3069.

Blanchard V, Moussaoui S, Czech C, Touchet N, Bonici B, Planche M, Canton T, Jedidi I, Gohin M, Wirths O, Bayer TA, Langui D, Duyckaerts C, Tremp G, Pradier L (2003) Time sequence of maturation of dystrophic neurites associated with Abeta deposits in APP/PS1 transgenic mice. Exp Neurol 184:247-263.

Block AE, Dhanji H, Thompson-Tardif SF, Floresco SB (2007) Thalamic-prefrontal cortical-ventral striatal circuitry mediates dissociable components of strategy set shifting. Cereb Cortex 17:1625-1636.

Blurton-Jones M, LaFerla FM (2006) Pathways by which Abeta facilitates tau pathology. Curr Alzheimer Res 3:437-448.

Boncristiano S, Calhoun ME, Kelly PH, Pfeifer M, Bondolfi L, Stalder M, Phinney AL, Abramowski D, Sturchler-Pierrat C, Enz A, Sommer B, Staufenbiel M, Jucker M (2002) Cholinergic changes in the APP23 transgenic mouse model of cerebral amyloidosis. J Neurosci 22:3234-3243.

Bonotis K, Krikki E, Holeva V, Aggouridaki C, Costa V, Baloyannis S (2008) Systemic immune aberrations in Alzheimer's disease patients. J Neuroimmunol 193:183-187.

Bornemann KD, Staufenbiel M (2000) Transgenic mouse models of Alzheimer's disease. Ann N Y Acad Sci 908:260-266.

Bossy-Wetzel E, Schwarzenbacher R, Lipton SA (2004) Molecular pathways to neurodegeneration. Nat Med 10 Suppl:S2-S9.

Braak H, Braak E (1991) Neuropathological stageing of Alzheimer-related changes. Acta Neuropathol 82:239-259.

Bredesen DE, Rao RV, Mehlen P (2006) Cell death in the nervous system. Nature 443:796-802.

Breyhan H, Wirths O, Duan K, Marcello A, Rettig J, Bayer TA (2009) APP/PS1KI bigenic mice develop early synaptic deficits and hippocampus atrophy. Acta Neuropathol 117:677-685.

Buee L, Bussiere T, Buee-Scherrer V, Delacourte A, Hof PR (2000) Tau protein isoforms, phosphorylation and role in neurodegenerative disorders. Brain Res Brain Res Rev 33:95-130.

Buonassisi V, Sato G, COHEN AI (1962) Hormone-producing cultures of adrenal and pituitary tumor origin. Proc Natl Acad Sci U S A 48:1184-1190.

Busciglio J, Lorenzo A, Yeh J, Yankner BA (1995) beta-amyloid fibrils induce tau phosphorylation and loss of microtubule binding. Neuron 14:879-888.

Bussey TJ, Duck J, Muir JL, Aggleton JP (2000) Distinct patterns of behavioural impairments resulting from fornix transection or neurotoxic lesions of the perirhinal and postrhinal cortices in the rat. Behav Brain Res 111:187-202.

Butovsky O, Kunis G, Koronyo-Hamaoui M, Schwartz M (2007) Selective ablation of bone marrow-derived dendritic cells increases amyloid plaques in a mouse Alzheimer's disease model. Eur J Neurosci 26:413-416.

Byers AL, Yaffe K (2011) Depression and risk of developing dementia. Nat Rev Neurol 7:323-331.

Carroll JC, Iba M, Bangasser DA, Valentino RJ, James MJ, Brunden KR, Lee VM, Trojanowski JQ (2011) Chronic Stress Exacerbates Tau Pathology, Neurodegeneration, and Cognitive Performance through a Corticotropin-Releasing Factor Receptor-Dependent Mechanism in a Transgenic Mouse Model of Tauopathy. J Neurosci 31:14436-14449.

Catania C, Sotiropoulos I, Silva R, Onofri C, Breen KC, Sousa N, Almeida OF (2009) The amyloidogenic potential and behavioral correlates of stress. Mol Psychiatry 14:95-105.

Cerqueira JJ, Catania C, Sotiropoulos I, Schubert M, Kalisch R, Almeida OF, Auer DP, Sousa N (2005) Corticosteroid status influences the volume of the rat cingulate cortex - a magnetic resonance imaging study. J Psychiatr Res 39:451-460.

Cerqueira JJ, Mailliet F, Almeida OF, Jay TM, Sousa N (2007) The prefrontal cortex as a key target of the maladaptive response to stress. J Neurosci 27:2781-2787.

Chalmers DT, Lovenberg TW, De Souza EB (1995) Localization of novel corticotropin-releasing factor receptor (CRF2) mRNA expression to specific subcortical nuclei in rat brain: comparison with CRF1 receptor mRNA expression. J Neurosci 15:6340-6350.

Chang Q, Gold PE (2003a) Intra-hippocampal lidocaine injections impair acquisition of a place task and facilitate acquisition of a response task in rats. Behav Brain Res 144:19-24.

Chang Q, Gold PE (2003b) Switching memory systems during learning: changes in patterns of brain acetylcholine release in the hippocampus and striatum in rats. J Neurosci 23:3001-3005.

Chishti MA, et al. (2001) Early-onset amyloid deposition and cognitive deficits in transgenic mice expressing a double mutant form of amyloid precursor protein 695. J Biol Chem 276:21562-21570.

Cizza G, Gold PW, Chrousos GP (1995) Aging is associated in the 344/N Fischer rat with decreased stress responsivity of central and peripheral catecholaminergic systems and impairment of the hypothalamic-pituitary-adrenal axis. Ann N Y Acad Sci 771:491-511.

Cohen NJ, Poldrack RA, Eichenbaum H (1997) Memory for items and memory for relations in the procedural/declarative memory framework. Memory 5:131-178.

Coric V, Feldman HH, Oren DA, Shekhar A, Pultz J, Dockens RC, Wu X, Gentile KA, Huang SP, Emison E, Delmonte T, D'Souza BB, Zimbroff DL, Grebb JA, Goddard AW, Stock EG (2010) Multicenter, randomized, double-blind, active comparator and placebo-controlled trial of a corticotropin-releasing factor receptor-1 antagonist in generalized anxiety disorder. Depress Anxiety 27:417-425.

Coyle JT, Price DL, DeLong MR (1983) Alzheimer's disease: a disorder of cortical cholinergic innervation. Science 219:1184-1190.

Craft JM, Watterson DM, Hirsch E, Van Eldik LJ (2005) Interleukin 1 receptor antagonist knockout mice show enhanced microglial activation and neuronal damage induced by intracerebroventricular infusion of human beta-amyloid. J Neuroinflammation 2:15.

Csernansky JG, Dong H, Fagan AM, Wang L, Xiong C, Holtzman DM, Morris JC (2006) Plasma cortisol and progression of dementia in subjects with Alzheimer-type dementia. Am J Psychiatry 163:2164-2169.

Dagerlind A, Friberg K, Bean AJ, Hokfelt T (1992) Sensitive mRNA detection using unfixed tissue: combined radioactive and non-radioactive in situ hybridization histochemistry. Histochemistry 98:39-49.

Dalm S, Enthoven L, Meijer OC, van der Mark MH, Karssen AM, de Kloet ER, Oitzl MS (2005) Age-related changes in hypothalamic-pituitary-adrenal axis activity of male C57BL/6J mice. Neuroendocrinology 81:372-380.

Davies P, Maloney AJ (1976) Selective loss of central cholinergic neurons in Alzheimer's disease. Lancet 2:1403.

Davis KL, Davis BM, Greenwald BS, Mohs RC, Mathe AA, Johns CA, Horvath TB (1986) Cortisol and Alzheimer's disease, I: Basal studies. Am J Psychiatry 143:300-305.

Davis KL, Mohs RC, Marin DB, Purohit DP, Perl DP, Lantz M, Austin G, Haroutunian V (1999) Neuropeptide abnormalities in patients with early Alzheimer disease. Arch Gen Psychiatry 56:981-987.

de Kloet ER (1992) Corticosteroids, stress, and aging. Ann N Y Acad Sci 663:357-371.

de Kloet ER, Joels M, Holsboer F (2005) Stress and the brain: from adaptation to disease. Nat Rev Neurosci 6:463-475.

de Lau LM, Breteler MM (2006) Epidemiology of Parkinson's disease. Lancet Neurol 5:525-535.

De Souza EB, Battaglia G (1986) Increased corticotropin-releasing factor receptors in rat cerebral cortex following chronic atropine treatment. Brain Res 397:401-404.

Deiana S, Platt B, Riedel G (2011) The cholinergic system and spatial learning. Behav Brain Res 221:389-411.

Delarasse C, Auger R, Gonnord P, Fontaine B, Kanellopoulos JM (2011) The Purinergic Receptor P2X7 Triggers {alpha}-Secretase-dependent Processing of the Amyloid Precursor Protein. J Biol Chem 286:2596-2606.

Deussing JM, Wurst W (2005) Dissecting the genetic effect of the CRH system on anxiety and stress-related behaviour. C R Biol 328:199-212.

Dias R, Aggleton JP (2000) Effects of selective excitotoxic prefrontal lesions on acquisition of nonmatching- and matching-to-place in the T-maze in the rat: differential involvement of the prelimbic-infralimbic and anterior cingulate cortices in providing behavioural flexibility. Eur J Neurosci 12:4457-4466.

Dong H, Yuede CM, Yoo HS, Martin MV, Deal C, Mace AG, Csernansky JG (2008) Corticosterone and related receptor expression are associated with increased beta-amyloid plaques in isolated Tg2576 mice. Neuroscience 155:154-163.

Drachman DA, Leavitt J (1974) Human memory and the cholinergic system. A relationship to aging? Arch Neurol 30:113-121.

Duff K, Eckman C, Zehr C, Yu X, Prada CM, Perez-tur J, Hutton M, Buee L, Harigaya Y, Yager D, Morgan D, Gordon MN, Holcomb L, Refolo L, Zenk B, Hardy J, Younkin S (1996) Increased amyloid-beta42(43) in brains of mice expressing mutant presenilin 1. Nature 383:710-713.

Duyckaerts C, Potier MC, Delatour B (2008) Alzheimer disease models and human neuropathology: similarities and differences. Acta Neuropathol 115:5-38.

Eichenbaum H, Clegg RA, Feeley A (1983) Reexamination of functional subdivisions of the rodent prefrontal cortex. Exp Neurol 79:434-451.

El Khoury J., Luster AD (2008) Mechanisms of microglia accumulation in Alzheimer's disease: therapeutic implications. Trends Pharmacol Sci 29:626-632.

El Khoury J., Toft M, Hickman SE, Means TK, Terada K, Geula C, Luster AD (2007) Ccr2 deficiency impairs microglial accumulation and accelerates progression of Alzheimer-like disease. Nat Med 13:432-438.

Elder GA, Gama Sosa MA, De GR (2010) Transgenic mouse models of Alzheimer's disease. Mt Sinai J Med 77:69-81.

Facci L, Stevens DA, Pangallo M, Franceschini D, Skaper SD, Strijbos PJLM (2003) Corticotropin-releasing factor (CRF) and related peptides confer neuroprotection via type 1 CRF receptors. Neuropharmacology 45:623-636.

Fath T, Eidenmuller J, Brandt R (2002) Tau-mediated cytotoxicity in a pseudohyperphosphorylation model of Alzheimer's disease. J Neurosci 22:9733-9741.

Ferri CP, Prince M, Brayne C, Brodaty H, Fratiglioni L, Ganguli M, Hall K, Hasegawa K, Hendrie H, Huang Y, Jorm A, Mathers C, Menezes PR, Rimmer E, Scazufca M (2005) Global prevalence of dementia: a Delphi consensus study. Lancet 366:2112-2117.

Filali M, Lalonde R, Rivest S (2009) Cognitive and non-cognitive behaviors in an APPswe/PS1 bigenic model of Alzheimer's disease. Genes Brain Behav 8:143-148.

Forwood SE, Winters BD, Bussey TJ (2005) Hippocampal lesions that abolish spatial maze performance spare object recognition memory at delays of up to 48 hours. Hippocampus 15:347-355.

Francis PT, Palmer AM, Snape M, Wilcock GK (1999) The cholinergic hypothesis of Alzheimer's disease: a review of progress. J Neurol Neurosurg Psychiatry 66:137-147.

Fratiglioni L, De RD, guero-Torres H (1999) Worldwide prevalence and incidence of dementia. Drugs Aging 15:365-375.

Fu HJ, Liu B, Frost JL, Lemere CA (2010) Amyloid-beta immunotherapy for Alzheimer's disease. CNS Neurol Disord Drug Targets 9:197-206.

Fuchs E, Czeh B, Kole MH, Michaelis T, Lucassen PJ (2004) Alterations of neuroplasticity in depression: the hippocampus and beyond. Eur Neuropsychopharmacol 14 Suppl 5:S481-S490.

Furth J, Dent J.N., Burnett WT, Gadsen EL (1955) The mechanism of induction and the characteristics of pituitary tumors induced by thyroidectomy. J Clin Endocrinol Metab 15:81-97.

Gallagher JP, Orozco-Cabal LF, Liu J, Shinnick-Gallagher P (2008) Synaptic physiology of central CRH system. Eur J Pharmacol 583:215-225.

Geschwind DH (2003) Tau phosphorylation, tangles, and neurodegeneration: the chicken or the egg? Neuron 40:457-460.

Goedert M, Spillantini MG (2000) Tau mutations in frontotemporal dementia FTDP-17 and their relevance for Alzheimer's disease. Biochim Biophys Acta 1502:110-121.

Gold PW, Chrousos GP (2002) Organization of the stress system and its dysregulation in melancholic and atypical depression: high vs low CRH/NE states. Mol Psychiatry 7:254-275.

Gold PW, Drevets WC, Charney DS (2002) New insights into the role of cortisol and the glucocorticoid receptor in severe depression. Biol Psychiatry 52:381-385.

Gold PW, Licinio J, Wong ML, Chrousos GP (1995) Corticotropin releasing hormone in the pathophysiology of melancholic and atypical depression and in the mechanism of action of antidepressant drugs. Ann N Y Acad Sci 771:716-729.

Goncharova ND, Lapin BA (2002) Effects of aging on hypothalamic-pituitary-adrenal system function in non-human primates. Mech Ageing Dev 123:1191-1201.

Gotz J, Chen F, van DJ, Nitsch RM (2001) Formation of neurofibrillary tangles in P301l tau transgenic mice induced by Abeta 42 fibrils. Science 293:1491-1495.

Gotz J, Ittner LM (2008) Animal models of Alzheimer's disease and frontotemporal dementia. Nat Rev Neurosci 9:532-544.

Gouras GK, Tampellini D, Takahashi RH, Capetillo-Zarate E (2010) Intraneuronal beta-amyloid accumulation and synapse pathology in Alzheimer's disease. Acta Neuropathol 119:523-541.

Grammatopoulos DK, Chrousos GP (2002) Functional characteristics of CRH receptors and potential clinical applications of CRH-receptor antagonists. Trends Endocrinol Metab 13:436-444.

Green KN, Billings LM, Roozendaal B, McGaugh JL, LaFerla FM (2006) Glucocorticoids increase amyloid-beta and tau pathology in a mouse model of Alzheimer's disease. J Neurosci 26:9047-9056.

Griffin WS, Mrak RE (2002) Interleukin-1 in the genesis and progression of and risk for development of neuronal degeneration in Alzheimer's disease. J Leukoc Biol 72:233-238.

Grimm MO, Rothhaar TL, Hartmann T (2011) The role of APP proteolytic processing in lipid metabolism. Exp Brain Res.

Grosgen S, Grimm MO, Friess P, Hartmann T (2010) Role of amyloid beta in lipid homeostasis. Biochim Biophys Acta 1801:966-974.

Gurevich D, Siegel B, Dumlao M, Perl E, Chaitin P, Bagne C, Oxenkrug G (1990) HPA axis responsivity to dexamethasone and cognitive impairment in dementia. Prog Neuropsychopharmacol Biol Psychiatry 14:297-308.

Hanger DP, Anderton BH, Noble W (2009) Tau phosphorylation: the therapeutic challenge for neurodegenerative disease. Trends Mol Med 15:112-119.

Hanstein R, Lu A, Wurst W, Holsboer F, Deussing JM, Clement AB, Behl C (2008) Transgenic overexpression of corticotropin releasing hormone provides partial protection against neurodegeneration in an in vivo model of acute excitotoxic stress. Neuroscience 156:712-721.

Hardy JA, Higgins GA (1992) Alzheimer's disease: the amyloid cascade hypothesis. Science 256:184-185.

Heinrichs SC, Stenzel-Poore MP, Gold LH, Battenberg E, Bloom FE, Koob GF, Vale WW, Pich EM (1996) Learning impairment in transgenic mice with central overexpression of corticotropin-releasing factor. Neuroscience 74:303-311.

Herman JP, Cullinan WE (1997) Neurocircuitry of stress: central control of the hypothalamo-pituitary-adrenocortical axis. Trends Neurosci 20:78-84.

Hewett SJ, Csernansky CA, Choi DW (1994) Selective potentiation of NMDA-induced neuronal injury following induction of astrocytic iNOS. Neuron 13:487-494.

Holmes C, Cunningham C, Zotova E, Woolford J, Dean C, Kerr S, Culliford D, Perry VH (2009) Systemic inflammation and disease progression in Alzheimer disease. Neurology 73:768-774.

Hsiao K, Chapman P, Nilsen S, Eckman C, Harigaya Y, Younkin S, Yang F, Cole G (1996) Correlative memory deficits, Abeta elevation, and amyloid plaques in transgenic mice. Science 274:99-102.

Ittner LM, Ke YD, Delerue F, Bi M, Gladbach A, van EJ, Wolfing H, Chieng BC, Christie MJ, Napier IA, Eckert A, Staufenbiel M, Hardeman E, Gotz J (2010) Dendritic function of tau mediates amyloid-beta toxicity in Alzheimer's disease mouse models. Cell 142:387-397.

Jankovic J (2008) Parkinson's disease: clinical features and diagnosis. J Neurol Neurosurg Psychiatry 79:368-376.

Jeong YH, Park CH, Yoo J, Shin KY, Ahn SM, Kim HS, Lee SH, Emson PC, Suh YH (2006) Chronic stress accelerates learning and memory impairments and increases amyloid deposition in APPV717I-CT100 transgenic mice, an Alzheimer's disease model. FASEB J 20:729-731.

Johnson GVW, Stoothoff WH (2004) Tau phosphorylation in neuronal cell function and dysfunction. J Cell Sci 117:5721-5729.

Johnston H, Boutin H, Allan SM (2011) Assessing the contribution of inflammation in models of Alzheimer's disease. Biochem Soc Trans 39:886-890.

Kang JE, Cirrito JR, Dong H, Csernansky JG, Holtzman DM (2007d) Acute stress increases interstitial fluid amyloid-beta via corticotropin-releasing factor and neuronal activity. Proc Natl Acad Sci U S A 104:10673-10678.

Kang JE, Cirrito JR, Dong H, Csernansky JG, Holtzman DM (2007b) Acute stress increases interstitial fluid amyloid-beta via corticotropin-releasing factor and neuronal activity. Proc Natl Acad Sci U S A 104:10673-10678.

Kang JE, Cirrito JR, Dong H, Csernansky JG, Holtzman DM (2007a) Acute stress increases interstitial fluid amyloid-beta via corticotropin-releasing factor and neuronal activity. Proc Natl Acad Sci U S A 104:10673-10678.

Kang JE, Cirrito JR, Dong H, Csernansky JG, Holtzman DM (2007c) Acute stress increases interstitial fluid amyloid-beta via corticotropin-releasing factor and neuronal activity. Proc Natl Acad Sci U S A 104:10673-10678.

Kawahara M, Negishi-Kato M, Sadakane Y (2009) Calcium dyshomeostasis and neurotoxicity of Alzheimer's beta-amyloid protein. Expert Rev Neurother 9:681-693.

Kim J, Basak JM, Holtzman DM (2009) The role of apolipoprotein E in Alzheimer's disease. Neuron 63:287-303.

Kim J, Ragozzino ME (2005) The involvement of the orbitofrontal cortex in learning under changing task contingencies. Neurobiol Learn Mem 83:125-133.

Klyubin I, Betts V, Welzel AT, Blennow K, Zetterberg H, Wallin A, Lemere CA, Cullen WK, Peng Y, Wisniewski T, Selkoe DJ, Anwyl R, Walsh DM, Rowan MJ (2008) Amyloid beta protein dimer-containing human CSF disrupts synaptic plasticity: prevention by systemic passive immunization. J Neurosci 28:4231-4237.

Klyubin I, Walsh DM, Lemere CA, Cullen WK, Shankar GM, Betts V, Spooner ET, Jiang L, Anwyl R, Selkoe DJ, Rowan MJ (2005) Amyloid beta protein immunotherapy neutralizes Abeta oligomers that disrupt synaptic plasticity in vivo. Nat Med 11:556-561.

Knobloch M, Konietzko U, Krebs DC, Nitsch RM (2007a) Intracellular Abeta and cognitive deficits precede beta-amyloid deposition in transgenic arcAbeta mice. Neurobiol Aging 28:1297-1306.

Knobloch M, Farinelli M, Konietzko U, Nitsch RM, Mansuy IM (2007b) A{beta} Oligomer-Mediated Long-Term Potentiation Impairment Involves Protein Phosphatase 1-Dependent Mechanisms. J Neurosci 27:7648-7653.

Kok EH, Luoto T, Haikonen S, Goebeler S, Haapasalo H, Karhunen PJ (2011) CLU, CR1 and PICALM genes associate with Alzheimer's-related senile plaques. Alzheimers Res Ther 3:12.

Kulstad JJ, McMillan PJ, Leverenz JB, Cook DG, Green PS, Peskind ER, Wilkinson CW, Farris W, Mehta PD, Craft S (2005) Effects of chronic glucocorticoid administration on insulin-degrading enzyme and amyloid-beta peptide in the aged macaque. J Neuropathol Exp Neurol 64:139-146.

LaFerla FM, Green KN, Oddo S (2007) Intracellular amyloid-beta in Alzheimer's disease. Nat Rev Neurosci 8:499-509.

Langui D, Girardot N, El Hachimi KH, Allinquant B, Blanchard V, Pradier L, Duyckaerts C (2004) Subcellular topography of neuronal Abeta peptide in APPxPS1 transgenic mice. Am J Pathol 165:1465-1477.

Lee KW, Kim JB, Seo JS, Kim TK, Im JY, Baek IS, Kim KS, Lee JK, Han PL (2009) Behavioral stress accelerates plaque pathogenesis in the brain of Tg2576 mice via generation of metabolic oxidative stress. J Neurochem 108:165-175.

Lee YJ, Han SB, Nam SY, Oh KW, Hong JT (2010) Inflammation and Alzheimer's disease. Arch Pharm Res 33:1539-1556.

Lehnert H, Schulz C, Dieterich K (1998) Physiological and neurochemical aspects of corticotropin-releasing factor actions in the brain: the role of the locus coeruleus. Neurochem Res 23:1039-1052.

Lesne S, Koh MT, Kotilinek L, Kayed R, Glabe CG, Yang A, Gallagher M, Ashe KH (2006) A specific amyloid-beta protein assembly in the brain impairs memory. Nature 440:352-357.

Lesne S, Kotilinek L, Ashe KH (2008) Plaque-bearing mice with reduced levels of oligomeric amyloid-beta assemblies have intact memory function. Neuroscience 151:745-749.

Letenneur L, Launer LJ, Andersen K, Dewey ME, Ott A, Copeland JR, Dartigues JF, Kragh-Sorensen P, Baldereschi M, Brayne C, Lobo A, Martinez-Lage JM, Stijnen T, Hofman A (2000) Education and the risk for Alzheimer's disease: sex makes a difference. EURODEM pooled analyses. EURODEM Incidence Research Group. Am J Epidemiol 151:1064-1071.

Lezoualc'h F, Engert S, Berning B, Behl C (2000) Corticotropin-Releasing Hormone-Mediated Neuroprotection against Oxidative Stress Is Associated with the Increased Release of Non-amyloidogenic Amyloid {beta} Precursor Protein and with the Suppression of Nuclear Factor-{kappa}B. Mol Endocrinol 14:147-159.

Li Y, Maher P, Schubert D (1997) A role for 12-lipoxygenase in nerve cell death caused by glutathione depletion. Neuron 19:453-463.

Livak KJ, Schmittgen TD (2001) Analysis of relative gene expression data using real-time quantitative PCR and the 2(-Delta Delta C(T)) Method. Methods 25:402-408.

Lord A, Englund H, Soderberg L, Tucker S, Clausen F, Hillered L, Gordon M, Morgan D, Lannfelt L, Pettersson FE, Nilsson LN (2009) Amyloid-beta protofibril levels correlate with spatial learning in Arctic Alzheimer's disease transgenic mice. FEBS J 276:995-1006.

Lu A, Steiner MA, Whittle N, Vogl AM, Walser SM, Ableitner M, Refojo D, Ekker M, Rubenstein JL, Stalla GK, Singewald N, Holsboer F, Wotjak CT, Wurst W, Deussing JM (2008) Conditional mouse mutants highlight mechanisms of corticotropin-releasing hormone effects on stress-coping behavior. Mol Psychiatry 13:1028-1042.

Lucassen PJ, Muller MB, Holsboer F, Bauer J, Holtrop A, Wouda J, Hoogendijk WJ, de Kloet ER, Swaab DF (2001) Hippocampal apoptosis in major depression is a minor event and absent from subareas at risk for glucocorticoid overexposure. Am J Pathol 158:453-468.

Lue LF, Kuo YM, Roher AE, Brachova L, Shen Y, Sue L, Beach T, Kurth JH, Rydel RE, Rogers J (1999) Soluble amyloid beta peptide concentration as a predictor of synaptic change in Alzheimer's disease. Am J Pathol 155:853-862.

Luo Y, Bolon B, Kahn S, Bennett BD, Babu-Khan S, Denis P, Fan W, Kha H, Zhang J, Gong Y, Martin L, Louis JC, Yan Q, Richards WG, Citron M, Vassar R (2001) Mice deficient in BACE1, the Alzheimer's beta-secretase, have normal phenotype and abolished beta-amyloid generation. Nat Neurosci 4:231-232.

Lupien SJ, de LM, de SS, Convit A, Tarshish C, Nair NP, Thakur M, McEwen BS, Hauger RL, Meaney MJ (1998) Cortisol levels during human aging predict hippocampal atrophy and memory deficits. Nat Neurosci 1:69-73.

Lupien SJ, McEwen BS (1997) The acute effects of corticosteroids on cognition: integration of animal and human model studies. Brain Res Brain Res Rev 24:1-27.

Lyketsos CG, Lopez O, Jones B, Fitzpatrick AL, Breitner J, DeKosky S (2002) Prevalence of neuropsychiatric symptoms in dementia and mild cognitive impairment: results from the cardiovascular health study. JAMA 288:1475-1483.

Lyketsos CG, Olin J (2002) Depression in Alzheimer's disease: overview and treatment. Biol Psychiatry 52:243-252.

Marchetti C, Marie H (2011) Hippocampal synaptic plasticity in Alzheimer's disease: what have we learned so far from transgenic models? Rev Neurosci 22:373-402.

Marzolo MP, Bu G (2009) Lipoprotein receptors and cholesterol in APP trafficking and proteolytic processing, implications for Alzheimer's disease. Semin Cell Dev Biol 20:191-200.

Massey PV, Bhabra G, Cho K, Brown MW, Bashir ZI (2001) Activation of muscarinic receptors induces protein synthesis-dependent long-lasting depression in the perirhinal cortex. Eur J Neurosci 14:145-152.

Matsuoka Y, Picciano M, Malester B, LaFrancois J, Zehr C, Daeschner JM, Olschowka JA, Fonseca MI, O'Banion MK, Tenner AJ, Lemere CA, Duff K (2001) Inflammatory responses to amyloidosis in a transgenic mouse model of Alzheimer's disease. Am J Pathol 158:1345-1354.

Maviel T, Durkin TP (2003) Role of central cholinergic receptor sub-types in spatial working memory: a five-arm maze task in mice provides evidence for a functional role of nicotinic receptors in mediating trace access processes. Neuroscience 120:1049-1059.

McEwen BS (1998) Stress, adaptation, and disease. Allostasis and allostatic load. Ann N Y Acad Sci 840:33-44.

McIntyre CK, Marriott LK, Gold PE (2003a) Cooperation between memory systems: acetylcholine release in the amygdala correlates positively with performance on a hippocampus-dependent task. Behav Neurosci 117:320-326.

McIntyre CK, Marriott LK, Gold PE (2003b) Patterns of brain acetylcholine release predict individual differences in preferred learning strategies in rats. Neurobiol Learn Mem 79:177-183.

McLean CA, Cherny RA, Fraser FW, Fuller SJ, Smith MJ, Beyreuther K, Bush AI, Masters CL (1999) Soluble pool of Abeta amyloid as a determinant of severity of neurodegeneration in Alzheimer's disease. Ann Neurol 46:860-866.

Middei S, Geracitano R, Caprioli A, Mercuri N, mmassari-Teule M (2004) Preserved fronto-striatal plasticity and enhanced procedural learning in a transgenic mouse model of Alzheimer's disease overexpressing mutant hAPPswe. Learn Mem 11:447-452.

Middei S, Roberto A, Berretta N, Panico MB, Lista S, Bernardi G, Mercuri NB, mmassari-Teule M, Nistico R (2010) Learning discloses abnormal structural and functional plasticity at hippocampal synapses in the APP23 mouse model of Alzheimer's disease. Learn Mem 17:236-240.

Mizoguchi K, Ishige A, Takeda S, Aburada M, Tabira T (2004) Endogenous glucocorticoids are essential for maintaining prefrontal cortical cognitive function. J Neurosci 24:5492-5499.

Mizoguchi K, Yuzurihara M, Ishige A, Sasaki H, Chui DH, Tabira T (2000) Chronic stress induces impairment of spatial working memory because of prefrontal dopaminergic dysfunction. J Neurosci 20:1568-1574.

Modell S, Yassouridis A, Huber J, Holsboer F (1997) Corticosteroid receptor function is decreased in depressed patients. Neuroendocrinology 65:216-222.

Mohandas E, Rajmohan V, Raghunath B (2009) Neurobiology of Alzheimer's disease. Indian J Psychiatry 51:55-61.

Morimoto BH, Koshland DE, Jr. (1990) Induction and expression of long- and short-term neurosecretory potentiation in a neural cell line. Neuron 5:875-880.

Morris RG, Garrud P, Rawlins JN, O'Keefe J (1982) Place navigation impaired in rats with hippocampal lesions. Nature 297:681-683.

Muller MB, Landgraf R, Preil J, Sillaber I, Kresse AE, Keck ME, Zimmermann S, Holsboer F, Wurst W (2000) Selective activation of the hypothalamic vasopressinergic system in mice deficient for the corticotropin-releasing hormone receptor 1 is dependent on glucocorticoids. Endocrinology 141:4262-4269.

Muller MB, Zimmermann S, Sillaber I, Hagemeyer TP, Deussing JM, Timpl P, Kormann MS, Droste SK, Kuhn R, Reul JM, Holsboer F, Wurst W (2003) Limbic corticotropin-releasing hormone receptor 1 mediates anxiety-related behavior and hormonal adaptation to stress. Nat Neurosci 6:1100-1107.

Murray CJ, Lopez AD (1996) Evidence-based health policy--lessons from the Global Burden of Disease Study. Science 274:740-743.

Neve RL, McPhie DL, Chen Y (2001) Alzheimer's disease: dysfunction of a signalling pathway mediated by the amyloid precursor protein? Biochem Soc Symp37-50.

Nikolaev A, McLaughlin T, O'Leary DD, Tessier-Lavigne M (2009) APP binds DR6 to trigger axon pruning and neuron death via distinct caspases. Nature 457:981-989.

Nilsberth C, Westlind-Danielsson A, Eckman CB, Condron MM, Axelman K, Forsell C, Stenh C, Luthman J, Teplow DB, Younkin SG, Naslund J, Lannfelt L (2001) The 'Arctic' APP mutation (E693G) causes Alzheimer's disease by enhanced Abeta protofibril formation. Nat Neurosci 4:887-893.

Nitsch RM, Hock C (2008) Targeting beta-amyloid pathology in Alzheimer's disease with Abeta immunotherapy. Neurotherapeutics 5:415-420.

Nuntagij P, Oddo S, LaFerla FM, Kotchabhakdi N, Ottersen OP, Torp R (2009) Amyloid deposits show complexity and intimate spatial relationship with dendrosomatic plasma membranes: an electron microscopic 3D reconstruction analysis in 3xTg-AD mice and aged canines. J Alzheimers Dis 16:315-323.

Oddo S, Billings L, Kesslak JP, Cribbs DH, LaFerla FM (2004) Abeta immunotherapy leads to clearance of early, but not late, hyperphosphorylated tau aggregates via the proteasome. Neuron 43:321-332.

Oddo S, Caccamo A, Shepherd JD, Murphy MP, Golde TE, Kayed R, Metherate R, Mattson MP, Akbari Y, LaFerla FM (2003) Triple-transgenic model of Alzheimer's disease with plaques and tangles: intracellular Abeta and synaptic dysfunction. Neuron 39:409-421.

Packard MG, Hirsh R, White NM (1989) Differential effects of fornix and caudate nucleus lesions on two radial maze tasks: evidence for multiple memory systems. J Neurosci 9:1465-1472.

Packard MG, McGaugh JL (1996) Inactivation of hippocampus or caudate nucleus with lidocaine differentially affects expression of place and response learning. Neurobiol Learn Mem 65:65-72.

Page RM, Baumann K, Tomioka M, Perez-Revuelta BI, Fukumori A, Jacobsen H, Flohr A, Luebbers T, Ozmen L, Steiner H, Haass C (2008) Generation of Abeta38 and Abeta42 is independently and differentially affected by familial Alzheimer disease-associated presenilin mutations and gamma-secretase modulation. J Biol Chem 283:677-683.

Panchal M, Loeper J, Cossec JC, Perruchini C, Lazar A, Pompon D, Duyckaerts C (2010) Enrichment of cholesterol in microdissected Alzheimer's disease senile plaques as assessed by mass spectrometry. J Lipid Res 51:598-605.

Parvathenani LK, Tertyshnikova S, Greco CR, Roberts SB, Robertson B, Posmantur R (2003) P2X7 mediates superoxide production in primary microglia and is up-regulated in a transgenic mouse model of Alzheimer's disease. J Biol Chem 278:13309-13317.

Patten DA, Germain M, Kelly MA, Slack RS (2010) Reactive oxygen species: stuck in the middle of neurodegeneration. J Alzheimers Dis 20 Suppl 2:S357-S367.

Pedersen WA, Culmsee C, Ziegler D, Herman JP, Mattson MP (1999) Aberrant stress response associated with severe hypoglycemia in a transgenic mouse model of Alzheimer's disease. J Mol Neurosci 13:159-165.

Pedersen WA, McMillan PJ, Kulstad JJ, Leverenz JB, Craft S, Haynatzki GR (2006) Rosiglitazone attenuates learning and memory deficits in Tg2576 Alzheimer mice. Exp Neurol 199:265-273.

Pedersen WA, McCullers D, Culmsee C, Haughey NJ, Herman JP, Mattson MP (2001) Corticotropin-Releasing Hormone Protects Neurons against Insults Relevant to the Pathogenesis of Alzheimer's Disease. Neurobiology of Disease 8:492-503.

Pleckaityte M (2010) [Alzheimer's disease: a molecular mechanism, new hypotheses, and therapeutic strategies]. Medicina (Kaunas) 46:70-76.

Pocock JM, Kettenmann H (2007) Neurotransmitter receptors on microglia. Trends Neurosci 30:527-535.

Potkin SG, Guffanti G, Lakatos A, Turner JA, Kruggel F, Fallon JH, Saykin AJ, Orro A, Lupoli S, Salvi E, Weiner M, Macciardi F (2009) Hippocampal atrophy as a quantitative trait in a genome-wide association study identifying novel susceptibility genes for Alzheimer's disease. PLoS One 4:e6501.

Priller C, Bauer T, Mitteregger G, Krebs B, Kretzschmar HA, Herms J (2006) Synapse formation and function is modulated by the amyloid precursor protein. J Neurosci 26:7212-7221.

Pych JC, Chang Q, Colon-Rivera C, Gold PE (2005) Acetylcholine release in hippocampus and striatum during testing on a rewarded spontaneous alternation task. Neurobiol Learn Mem 84:93-101.

Quirarte GL, Roozendaal B, McGaugh JL (1997) Glucocorticoid enhancement of memory storage involves noradrenergic activation in the basolateral amygdala. Proc Natl Acad Sci U S A 94:14048-14053.

Raadsheer FC, Hoogendijk WJ, Stam FC, Tilders FJ, Swaab DF (1994a) Increased numbers of corticotropin-releasing hormone expressing neurons in the hypothalamic paraventricular nucleus of depressed patients. Neuroendocrinology 60:436-444.

Raadsheer FC, Oorschot DE, Verwer RW, Tilders FJ, Swaab DF (1994b) Age-related increase in the total number of corticotropin-releasing hormone neurons in the human paraventricular nucleus in controls and Alzheimer's disease: comparison of the disector with an unfolding method. J Comp Neurol 339:447-457.

Raadsheer FC, Tilders FJ, Swaab DF (1994c) Similar age related increase of vasopressin colocalization in paraventricular corticotropin-releasing hormone neurons in controls and Alzheimer patients. J Neuroendocrinol 6:131-133.

Raadsheer FC, van Heerikhuize JJ, Lucassen PJ, Hoogendijk WJ, Tilders FJ, Swaab DF (1995) Corticotropin-releasing hormone mRNA levels in the paraventricular nucleus of patients with Alzheimer's disease and depression. Am J Psychiatry 152:1372-1376.

Ragozzino ME, Choi D (2004) Dynamic changes in acetylcholine output in the medial striatum during place reversal learning. Learn Mem 11:70-77.

Ragozzino ME, Detrick S, Kesner RP (1999) Involvement of the prelimbic-infralimbic areas of the rodent prefrontal cortex in behavioral flexibility for place and response learning. J Neurosci 19:4585-4594.

Ragozzino ME, Ragozzino KE, Mizumori SJ, Kesner RP (2002) Role of the dorsomedial striatum in behavioral flexibility for response and visual cue discrimination learning. Behav Neurosci 116:105-115.

Rapoport M, Dawson HN, Binder LI, Vitek MP, Ferreira A (2002) Tau is essential to beta -amyloid-induced neurotoxicity. Proc Natl Acad Sci U S A 99:6364-6369.

Rapoport M, Ferreira A (2000) PD98059 prevents neurite degeneration induced by fibrillar beta-amyloid in mature hippocampal neurons. J Neurochem 74:125-133.

Rasmuson S, Andrew R, Nasman B, Seckl JR, Walker BR, Olsson T (2001) Increased glucocorticoid production and altered cortisol metabolism in women with mild to moderate Alzheimer's disease. Biol Psychiatry 49:547-552.

Ray B, Gaskins DL, Sajdyk TJ, Spence JP, Fitz SD, Shekhar A, Lahiri DK (2011) Restraint stress and repeated corticotrophin-releasing factor receptor activation in the amygdala both increase amyloid-beta precursor protein and amyloid-beta peptide but have divergent effects on brain-derived neurotrophic factor and pre-synaptic proteins in the prefrontal cortex of rats. Neuroscience 184:139-150.

Refojo D, Schweizer M, Kuehne C, Ehrenberg S, Thoeringer C, Vogl AM, Dedic N, Schumacher M, von WG, Avrabos C, Touma C, Engblom D, Schutz G, Nave KA, Eder M, Wotjak CT, Sillaber I, Holsboer F, Wurst W, Deussing JM (2011) Glutamatergic and dopaminergic neurons mediate anxiogenic and anxiolytic effects of CRHR1. Science 333:1903-1907.

Reul JM, de Kloet ER (1985) Two receptor systems for corticosterone in rat brain: microdistribution and differential occupation. Endocrinology 117:2505-2511.

Reul JM, Gesing A, Droste S, Stec IS, Weber A, Bachmann C, Bilang-Bleuel A, Holsboer F, Linthorst AC (2000) The brain mineralocorticoid receptor: greedy for ligand, mysterious in function. Eur J Pharmacol 405:235-249.

Rezvani AH, Levin ED (2001) Cognitive effects of nicotine. Biol Psychiatry 49:258-267.

Rich EL, Shapiro M (2009) Rat prefrontal cortical neurons selectively code strategy switches. J Neurosci 29:7208-7219.

Rich EL, Shapiro ML (2007) Prelimbic/infralimbic inactivation impairs memory for multiple task switches, but not flexible selection of familiar tasks. J Neurosci 27:4747-4755.

Rissman RA, Lee KF, Vale W, Sawchenko PE (2007) Corticotropin-releasing factor receptors differentially regulate stress-induced tau phosphorylation. J Neurosci 27:6552-6562.

Roberson ED, Scearce-Levie K, Palop JJ, Yan F, Cheng IH, Wu T, Gerstein H, Yu GQ, Mucke L (2007) Reducing endogenous tau ameliorates amyloid beta-induced deficits in an Alzheimer's disease mouse model. Science 316:750-754.

Rodriguez JJ, Witton J, Olabarria M, Noristani HN, Verkhratsky A (2010) Increase in the density of resting microglia precedes neuritic plaque formation and microglial activation in a transgenic model of Alzheimer's disease. Cell Death Dis 1:e1.

Roozendaal B (2002) Stress and memory: opposing effects of glucocorticoids on memory consolidation and memory retrieval. Neurobiol Learn Mem 78:578-595.

Roozendaal B, Phillips RG, Power AE, Brooke SM, Sapolsky RM, McGaugh JL (2001) Memory retrieval impairment induced by hippocampal CA3 lesions is blocked by adrenocortical suppression. Nat Neurosci 4:1169-1171.

Rossato JI, Zinn CG, Furini C, Bevilaqua LR, Medina JH, Cammarota M, Izquierdo I (2006) A link between the hippocampal and the striatal memory systems of the brain. An Acad Bras Cienc 78:515-523.

Rothman SM, Mattson MP (2010) Adverse stress, hippocampal networks, and Alzheimer's disease. Neuromolecular Med 12:56-70.

Rowan MJ, Klyubin I, Wang Q, Anwyl R (2005) Synaptic plasticity disruption by amyloid beta protein: modulation by potential Alzheimer's disease modifying therapies. Biochem Soc Trans 33:563-567.

Sandi C (2011) Glucocorticoids act on glutamatergic pathways to affect memory processes. Trends Neurosci 34:165-176.

Sapolsky RM, Krey LC, McEwen BS (1986) The neuroendocrinology of stress and aging: the glucocorticoid cascade hypothesis. Endocr Rev 7:284-301.

Schroeder JP, Wingard JC, Packard MG (2002) Post-training reversible inactivation of hippocampus reveals interference between memory systems. Hippocampus 12:280-284.

Selkoe DJ (2001) Alzheimer's disease: genes, proteins, and therapy. Physiol Rev 81:741-766.

Selkoe DJ (2002) Alzheimer's disease is a synaptic failure. Science 298:789-791.

Selkoe DJ (2008) Biochemistry and molecular biology of amyloid beta-protein and the mechanism of Alzheimer's disease. Handb Clin Neurol 89:245-260.

Sheline YI, Wang PW, Gado MH, Csernansky JG, Vannier MW (1996) Hippocampal atrophy in recurrent major depression. Proc Natl Acad Sci U S A 93:3908-3913.

Smith GW, Aubry JM, Dellu F, Contarino A, Bilezikjian LM, Gold LH, Chen R, Marchuk Y, Hauser C, Bentley CA, Sawchenko PE, Koob GF, Vale W, Lee KF (1998) Corticotropin Releasing Factor Receptor 1-Deficient Mice Display Decreased Anxiety, Impaired Stress Response, and Aberrant Neuroendocrine Development. Neuron 20:1093-1102.

Smith PK, Krohn RI, Hermanson GT, Mallia AK, Gartner FH, Provenzano MD, Fujimoto EK, Goeke NM, Olson BJ, Klenk DC (1985) Measurement of protein using bicinchoninic acid. Anal Biochem 150:76-85.

Sotiropoulos I, Catania C, Pinto LG, Silva R, Pollerberg GE, Takashima A, Sousa N, Almeida OF (2011) Stress acts cumulatively to precipitate Alzheimer's disease-like tau pathology and cognitive deficits. J Neurosci 31:7840-7847.

Sotiropoulos I, Catania C, Riedemann T, Fry JP, Breen KC, Michaelidis TM, Almeida OF (2008a) Glucocorticoids trigger Alzheimer disease-like pathobiochemistry in rat neuronal cells expressing human tau. J Neurochem 107:385-397.

Sotiropoulos I, Cerqueira JJ, Catania C, Takashima A, Sousa N, Almeida OF (2008b) Stress and glucocorticoid footprints in the brain-the path from depression to Alzheimer's disease. Neurosci Biobehav Rev 32:1161-1173.

Squire LR, Zola SM (1996) Structure and function of declarative and nondeclarative memory systems. Proc Natl Acad Sci U S A 93:13515-13522.

Stalder M, Phinney A, Probst A, Sommer B, Staufenbiel M, Jucker M (1999) Association of microglia with amyloid plaques in brains of APP23 transgenic mice. Am J Pathol 154:1673-1684.

Starkman MN, Giordani B, Berent S, Schork MA, Schteingart DE (2001) Elevated cortisol levels in Cushing's disease are associated with cognitive decrements. Psychosom Med 63:985-993.

Starkman MN, Giordani B, Gebarski SS, Schteingart DE (2003) Improvement in learning associated with increase in hippocampal formation volume. Biol Psychiatry 53:233-238.

Starkstein SE, Jorge R, Mizrahi R, Robinson RG (2005) The construct of minor and major depression in Alzheimer's disease. Am J Psychiatry 162:2086-2093.

Steckler T, Holsboer F (2001) Interaction between the cholinergic system and CRH in the modulation of spatial discrimination learning in mice. Brain Res 906:46-59.

Steffens DC, Potter GG (2008) Geriatric depression and cognitive impairment. Psychol Med 38:163-175.

Stenzel-Poore MP, Cameron VA, Vaughan J, Sawchenko PE, Vale W (1992) Development of Cushing's syndrome in corticotropin-releasing factor transgenic mice. Endocrinology 130:3378-3386.

Sturchler-Pierrat C, Abramowski D, Duke M, Wiederhold KH, Mistl C, Rothacher S, Ledermann B, Burki K, Frey P, Paganetti PA, Waridel C, Calhoun ME, Jucker M, Probst A, Staufenbiel M, Sommer B (1997) Two amyloid precursor protein transgenic mouse models with Alzheimer disease-like pathology. Proc Natl Acad Sci U S A 94:13287-13292.

Swaab DF, Chung WC, Kruijver FP, Hofman MA, Hestiantoro A (2003) Sex differences in the hypothalamus in the different stages of human life. Neurobiol Aging 24 Suppl 1:S1-16.

Swaab DF, Bao AM, Lucassen PJ (2005) The stress system in the human brain in depression and neurodegeneration. Ageing Research Reviews 4:141-194.

Tampellini D, Gouras GK (2010) Synapses, synaptic activity and intraneuronal abeta in Alzheimer's disease. Front Aging Neurosci 2.

Timpl P, Spanagel R, Sillaber I, Kresse A, Reul JM, Stalla GK, Blanquet V, Steckler T, Holsboer F, Wurst W (1998) Impaired stress response and reduced anxiety in mice lacking a functional corticotropin-releasing hormone receptor 1. Nat Genet 19:162-166.

Tol J, Roks G, Slooter AJ, van Duijn CM (1999) Genetic and environmental factors in Alzheimer's disease. Rev Neurol (Paris) 155 Suppl 4:S10-S16.

Tolman EC, RITCHIE BF, KALISH D (1946) Studies in spatial learning: Orientation and the short-cut. J Exp Psychol 36:13-24.

Touma C, Ambree O, Gortz N, Keyvani K, Lewejohann L, Palme R, Paulus W, Schwarze-Eicker K, Sachser N (2004) Age- and sex-dependent development of adrenocortical hyperactivity in a transgenic mouse model of Alzheimer's disease. Neurobiol Aging 25:893-904.

Tronche F, Kellendonk C, Kretz O, Gass P, Anlag K, Orban PC, Bock R, Klein R, Schutz G (1999) Disruption of the glucocorticoid receptor gene in the nervous system results in reduced anxiety. Nat Genet 23:99-103.

Tseng BP, Green KN, Chan JL, Blurton-Jones M, LaFerla FM (2008) Abeta inhibits the proteasome and enhances amyloid and tau accumulation. Neurobiol Aging 29:1607-1618.

Vale W, Spiess J, Rivier C, Rivier J (1981) Characterization of a 41-residue ovine hypothalamic peptide that stimulates secretion of corticotropin and beta-endorphin. Science 213:1394-1397.

Van Pett K, Viau V, Bittencourt JC, Chan RK, Li HY, Arias C, Prins GS, Perrin M, Vale W, Sawchenko PE (2000) Distribution of mRNAs encoding CRF receptors in brain and pituitary of rat and mouse. J Comp Neurol 428:191-212.

Vardy ER, Catto AJ, Hooper NM (2005) Proteolytic mechanisms in amyloid-beta metabolism: therapeutic implications for Alzheimer's disease. Trends Mol Med 11:464-472.

Walker FO (2007) Huntington's Disease. Semin Neurol 27:143-150.

Wang HW, Pasternak JF, Kuo H, Ristic H, Lambert MP, Chromy B, Viola KL, Klein WL, Stine WB, Krafft GA, Trommer BL (2002) Soluble oligomers of beta amyloid (1-42) inhibit long-term potentiation but not long-term depression in rat dentate gyrus. Brain Res 924:133-140.

Warburton EC, Koder T, Cho K, Massey PV, Duguid G, Barker GR, Aggleton JP, Bashir ZI, Brown MW (2003) Cholinergic neurotransmission is essential for perirhinal cortical plasticity and recognition memory. Neuron 38:987-996.

Wei G, Jewett AI, Shea JE (2010a) Structural diversity of dimers of the Alzheimer amyloid-beta(25-35) peptide and polymorphism of the resulting fibrils. Phys Chem Chem Phys 12:3622-3629.

Wei W, Nguyen LN, Kessels HW, Hagiwara H, Sisodia S, Malinow R (2010b) Amyloid beta from axons and dendrites reduces local spine number and plasticity. Nat Neurosci 13:190-196.

Willem M, Garratt AN, Novak B, Citron M, Kaufmann S, Rittger A, DeStrooper B, Saftig P, Birchmeier C, Haass C (2006) Control of peripheral nerve myelination by the beta-secretase BACE1. Science 314:664-666.

Winkler I, Cowan N (2005) From sensory to long-term memory: evidence from auditory memory reactivation studies. Exp Psychol 52:3-20.

Winters BD, Forwood SE, Cowell RA, Saksida LM, Bussey TJ (2004) Double dissociation between the effects of peri-postrhinal cortex and hippocampal lesions on tests of object recognition and spatial memory: heterogeneity of function within the temporal lobe. J Neurosci 24:5901-5908.

Winters BD, Saksida LM, Bussey TJ (2008) Object recognition memory: neurobiological mechanisms of encoding, consolidation and retrieval. Neurosci Biobehav Rev 32:1055-1070.

Yirmiya R, Goshen I (2011) Immune modulation of learning, memory, neural plasticity and neurogenesis. Brain Behav Immun 25:181-213.

Yu YW, Chen TJ, Hong CJ, Chen HM, Tsai SJ (2003) Association study of the interleukin-1 beta (C-511T) genetic polymorphism with major depressive disorder, associated symptomatology, and antidepressant response. Neuropsychopharmacology 28:1182-1185.

Zhu CW, Sano M (2006) Economic considerations in the management of Alzheimer's disease. Clin Interv Aging 1:143-154.

Zobel AW, Nickel T, Kunzel HE, Ackl N, Sonntag A, Ising M, Holsboer F (2000) Effects of the high-affinity corticotropin-releasing hormone receptor 1 antagonist R121919 in major depression: the first 20 patients treated. J Psychiatr Res 34:171-181.

8. Acknowledgements

First of all, I am deeply grateful to Prof. Dr. Wolfgang Wurst for giving me the opportunity to work on this interesting and meaningful topic.
Next, I sincerely want to thank Dr. Jan Deussing for providing the scope of conducting this project within his group, for his constant faith in me, his great analytical and also creative mindset and thorough proofreading of my thesis. Together, these terms added to the development of my own scientific thinking and abilities.
I am very grateful to Prof. Dr. Dr. Dr. h.c. Florian Holsboer for providing an excellent scientific environment at the MPI for Psychiatry.
I sincerely want to thank the examination board, Prof. Dr. Wolfgang Wurst, Prof. Dr. Kay Schneitz and Prof. Dr. Angelika Schnieke, for spending time and effort with the evaluation of my thesis.
My gratitude is expressed to Dr. Michael Willem, whose contribution was decisive for all biochemeical analyses. His optimistic nature was enormously encouraging and I really enjoyed working with him.
Sincere thanks goes to all members of my Thesis Committee, Dr. Sabine Hölter-Koch, Dr. Michael Willem, Dr. Jan Deussing and Prof. Dr. Wolfgang Wurst, for conspirative discussions, inspiring ideas and enthusiasm concerning my project.
Moreover, I want to thank all colleagues who accompanied my way during the last three years: thank you for creating a great working atmosphere and also for your scientific input. In the RG Deussing I am especially thankful to Nina Dedic, who was always interested and eager to give advice concerning behavioral testings and statistics, Claudia Kühne for helping in any thinkable concern, Marcel Schieven for the corticosterone assessment and Sabrina Bauer for preparing tail lysates. Furthermore, I thank Dr. Carsten Wotjak and Karl Kleinknecht (RG Wotjak) for enabling the use of the water cross maze, Dr. Carola Romberg (RG Almeida) in terms of the OR task, Prof. Dr. Gerhard Rammes (guest) for electrophysiological measurements, Heike Hampel and Brigitte Nuscher (Adolf-Butenandt-Institute) for helping pipetting the multitudinous samples and the animal care takers for constant surveillance of my mice.
Finally, I owe sincere gratitude to my friends for creating an expedient balance to the research environment and encouraging me throughout laboured times. Ultimate deep thankfulness appertains to my parents as without their education and being nothing of all that would have ever been possible.

9. Curriculum vitae

Personal information

Kristin Lerche
Date of birth: 28.12.1984
Place of birth: Torgau, Germany
Citizenship: german

Education

Since 06/2012	**Medical Advisor, Clinical Research**, Novartis Pharma GmbH
02/2009 – 05/2012	**PhD, RG Deussing**, **MPI of Psychiatry**, Munich Topic: “Dissecting the role of CRH and CRH-R1 in Alzheimer´s disease”
10/2003 - 10/2007	Studies of **Pharmacy**, Johann Wolfgang Goethe-University, Frankfurt am Main
12/2008	Approbation **Apothekerin** (3. Staatsexamen), Frankfurt am Main
1991 - 2003	School, Osnabrück; 2003 **Abitur,** Ratsgymnasium Osnabrück

Work experience

05/2008 – 10/2008	Internship **Europa-Apotheke**, Düsseldorf
11/2007 - 04/2008	Internship **Novartis Pharma Production GmbH**, Wehr Department: Quality assurance
09/2004	**Famulatur** Atlas-Apotheke, Osnabrück
03/2004	**Famulatur** Titus-Apotheke, Frankfurt am Main

Publications

Lerche K, Willem M, Romberg C, Krummhaar M, Wotjak CT, Kleinknecht K, Nitsch RM, Holsboer F, Wurst W, Deussing JM. CRH-R1 knockout alleviates amyloid beta burden and promotes response learning in arcAß mice (working title) - manuscript in preparation

Attendance of conferences and symposia (selected)

10/2011	27. AGNP symposium, Ludwig-Maximilians-University, Munich: *"CRH-R1KO promotes learning shift and attenuates Aß burden in an Alzheimer´s disease mouse model"* (poster)
07/2011	Institute symposium, Max-Planck-Institute of Psychiatry, Munich: *"Alzheimer´s disease and the CRH system – Is there a link between mood and neurodegenerative disorders?"* (talk)
05/2011	Molecular Mechanisms of Neurodegeneration, Mailand, Italy
02/2011	Helmholtz Alliance for mental health in an aging society (Helma-Evaluation), Munich: *"Dissecting the role of CRH and CRH-R1 in Alzheimer´s disease"* (poster)
07/2010	Institute symposium, Max-Planck-Institute of Psychiatry, Munich: *"Dissecting the role of CRH and CRH-R1 in Alzheimer´s disease"* (poster)
10/2009	26. AGNP symposium, Ludwig-Maximilians-University, Munich
07/2007	Fertigarzneimittelseminar, Johann Wolfgang Goethe-University, Frankfurt am Main: *"H_2-Rezeptorantagonisten*" (talk)

Additional information

Interests	Mountaineering, travelling
Organisations	Deutsche Pharmazeutische Gesellschaft (DPhG) Minnerva-femmenet Mentoring Programm